SYNERGISTIC INTERACTION OF BONE MORPHOGENETIC PROTEIN AND TRANSFORMING GROWTH FACTOR-ß IN BONE INDUCTION AND REGENERATION

Nicolaas Duneas

A thesis submitted to the Faculty of Medicine, University of the Witwatersrand, Johannesburg, in fulfilment of the requirements for the degree of Doctor of Philosophy.

Johannesburg, 1998

DECLARATION

I, Nicolaas Duneas declare that this thesis is my own work. It is being submitted for the degree of Doctor of Philosophy in the University of the Witwatersrand, Johannesburg. It has not been submitted before for any degree or examination at this or other University.

.....

20th day of AUGUST, 1998

'That the knowledge they seek is not knowledge of something which comes into being for a moment and then perishes, but knowledge of what always is.'

Plato, The Republic, Book VII, 526E-528C.

To my parents.

PUBLICATIONS ARISEN FROM MATERIAL PRESENTED IN THIS THESIS

Duneas, N., Crooks, J., and Ripamonti, U. 1998. Transforming growth factor-ß1: Induction of bone morphogenetic protein genes expression during endochondral bone formation in the baboon, and synergistic interaction with osteogenic protein-1 (BMP-7), *Growth Factors.* In press.

Ripamonti, U., and **Duneas, N.** 1998. Tissue morphogenesis and regeneration by bone morphogenetic proteins *Plast. Reconst. Surg.* **101**, 227-239.

Ripamonti, U., **Duneas, N.**, van den Heever, B., Bosch, C., and Crooks, J. 1997. Recombinant transforming growth factor-ß1 induces endochondral bone in the baboon, and synergizes with recombinant osteogenic protein-1 (BMP-7) to initiate rapid bone formation. *J. Bone Min. Res.* **12**, 1584-1595.

Ripamonti, U., and **Duneas, N.** 1996. Tissue engineering of bone by osteoinductive biomaterials *Mat. Res. Soc. Bull.* **21**, 36-39.

Ripamonti, U., Bosch, C., van den Heever, B., **Duneas, N.**, Melsen, B., and Ebner, R. 1996. Limited chondro-osteogenesis by recombinant human transforming growth factor-ß1 in calvarial defects of adult baboon (*Papio ursinus*). *J. Bone Min. Res.* **11**, 938-945.

ABSTRACT

Several members of the bone morphogenetic protein and osteogenic protein (BMP/OP) and transforming growth factor-ß (TGF-ß) families are molecular regulators of cartilage and bone regeneration, although their precise mode of signal transduction and combined interactions are poorly understood. The presence of several molecular forms suggests multiple functions *in vivo* as well as synergistic interactions during both embryonic bone development and regeneration of cartilage and bone in postfoetal life. Heterotopic and orthotopic implantation of BMPs/OPs elicit the local differentiation of new bone in a number of animal models studied, whereas reports to date show that implantation of TGF-ßs in heterotopic sites of the rat results in fibrovascular tissue formation, without evidence of bone formation. Instead, TGF-ßs show limited osteo-chondrogenic activity only when applied orthotopically in some, and not all of the animal models studied. Here, data are presented that show for the first time that, in contrast to previously described animal models, implantation of TGF-$ß_1$ with a collagenous matrix carrier in the rectus abdominis of the baboon (*Papio ursinus*) results in *de novo* bone formation, as evidenced radiographically, histologically and biochemically. TGF-$ß_1$ induced endochondral bone at heterotopic sites of the baboon at doses of 5 µg/100 mg collagenous matrix as carrier, with an inductive efficiency comparable to single applications of 5 and 25 µg recombinant human osteogenic protein-1 (rhOP-1), a morphogen whose osteoinductive activity has previously been demonstrated in a number of animal models. It was shown further, that rhOP-1 and TGF-$ß_1$ (of porcine

or recombinant source), interact synergistically to induce massive ossicles in extraskeletal sites of the primate as early as 14 or 15 days after implantation. Binary combinations of the morphogens induced ossicles with indeces of bone formation which were greater than the sum of indeces of single application of each respective morphogen. By applying isobolographic analysis, a well established pharmacological mathematical model previously developed for the study of interactions between pharmacologic agents, it was shown that the interaction between rhOP-1 and TGF-$ß_1$ in bone induction was of the type defined as synergism. The level of tissue induced by single applications of rhOP-1 (5, 25 and 125 µg/100 mg collagenous matrix) was raised several-fold by the simultaneous addition of comparatively low doses of TGF-$ß_1$ (0.5, 1.5 and 5 µg), which by itself induced bone formation at doses of 5µg/100 mg collagenous matrix. Combinations of rhOP-1 and TGF-$ß_1$ yielded a 2- to 3-fold increase in cross-sectional area of the newly generated ossicles, with markedly elevated parameters of bone formation, and corticalisation of the newly formed bone by day 15, culminating in marrow generation by day 30. The tissue generated by the combined application of rhOP-1 and TGF-$ß_1$ showed distinct morphological differences when compared with rhOP-1-treated specimens, with large zones of endochondral development and extensive bone marrow formation. Heterotopic tissue generated on day 30 by single application of rhOP-1 or TGF-$ß_1$ expressed comparable levels of OP-1, BMP-3 and type IV collagen mRNA transcripts, whereas TGF-$ß_1$ and type II collagen mRNA expression was 2- to 3-fold higher in TGF-$ß_1$–treated impants, as determined by Northern analysis. In ossicles generated by rhOP-1 in combination with TGF-$ß_1$, mRNA for type II collagen, a marker of chondrogenesis, was increased

in a TGF-ß dose-dependent manner. Type IV collagen mRNA, a marker of angiogenesis, was synergistically upregulated with a 3- to 4-fold increase compared to ossicles generated by single application of rhOP-1 or TGF-$ß_1$. Since angiogenesis is a prerequisite for osteogenesis, increased angiogenesis may be at least part of the mechanism whereby morphogen combinations interact synergistically in endochondral bone formation. Single application of pTGF-$ß_1$ induced ossicles expressing mRNA for OP-1, BMP-3 and TGF-$ß_1$, showing that osteogenesis elicited by pTGF-$ß_1$ proceeds, at least in part, *via* the expression of genes of the BMP/OP family. Single applications of rhOP-1 and pTGF-$ß_1$ induced ossicles expressing high levels of their own mRNA, suggesting an autoinductive effect of these morphogens in the initiation of the bone differentiation cascade. At the doses tested, synergy was optimal at a ratio of 1:20 by weight of TGF-$ß_1$ and rhOP-1 respectively.

Morphogen combinations (5 µg pTGF-$ß_1$ with 20 µg rhOP-1, and 5 and 15 µg pTGF-$ß_1$ with 100 with 100 µg rhOP-1 per gram of collagenous matrix as carrier) induced exuberant tissue formation and greater amounts of osteoid than rhOP-1 alone when implanted in calvarial defects of the baboon as evaluated on day 30 and 90, with displacement of the temporalis muscle above the defects. Since single application of TGF-$ß_1$ in the primate did not induce bone formation in calvarial defects, whilst it induces endochondral bone differentiation in heterotopic sites, the data indicate that that the bone inductive activity of TGF-$ß_1$ is site and tissue specific. The findings presented may provide the basis for synergistic molecular therapeutics for cartilage and bone regeneration in clinical contexts.

ACKNOWLEDGEMENTS

I would like to thank my supervisor, Professor Ugo Ripamonti (MD, PhD), Director of the Bone Research Laboratory of the South African Medical Research Council and the University of the Witwatersrand, Johannesburg, for endless teaching, coaching, mentorship and inspiration, especially during critical moments in the creation of this work. The many nights spent together in the lab catalysed an intense energy that manifested itself in the following pages.

I thank the Department of Orthopaedic Surgery, University of the Witwatersrand, Johannesburg, where I was registered student during the execution of this work.

I thank Jean Crooks and Barbara Löken, Chief Research Technologists at the Bone Research Laboratory, for the excellent processing of the undecalcified tissue specimens of bone, surely the best in the world.

I thank sisters Marina Engelbrecht and Marianne Hendrikse, Central Animal Services, University of the Witwatersrand, for assistance during animal work.

I am most grateful to Dave Amm of the School of Biology, whose excellent skills at the lathe, enabled the crafting of an outstanding support column for the construction of the chromatographic apparatus, which played a key role in the purification of the ever so scarce TGF-β_1.

I thank Angela Klein for expert typing skills in references.

I am grateful to Professor Wouter de Wet and Corni Strydom, of the Department of Medical Biochemistry of the university, for valuable help given towards designing of molecular biology experiments.

I thank my close friends, Dr. Ilario Dal Mas and Dr. Nathaniel Lentsha Ramoshebi for their support and critical input to experimental strategies.

All surgical procedures were performed by Professor Ripamonti.

This work was supported by grants of the South African Medical Research Council, the University of the Witwatersrand, Johannesburg, and of the Slome Orthopaedic Research and Development Fund, Department of Orthopaedic Surgery of the University of the Witwatersrand, Johannesburg.

TABLE OF CONTENTS

3.2 Materials and methods

LIST OF FIGURES

LIST OF TABLES

Preface

As is often the case in science, discoveries are frequently made by accident. As the name suggests, to discover is to un-cover. It was always there, lying hidden, waiting to be exposed. Once exposed, it becomes knowledge, and it is the privilege and pleasure of the un-coverer to disseminate it throughout the world.

One such accident, is the subject of this thesis. The protein transforming growth factor-ß, a morphogen whose perceived role in bone regeneration is torn between two opposing schools of thought, has had many argue over its true status as an osteoinductive factor. It promotes bone formation at bony sites, but, unlike its superfamily relatives, the bone morphogenetic proteins, it fails the acid test for true osteoinductivity: bone induction at extraskeletal sites. Well, that is, at least until now. A simple experiment, conjured by us at the Bone Research Laboratory and the then zealous members of the school that supports that TGF-ßs are not osteoinductive, devised an extraskeletal implantation in the rectus abdominis of the baboon: implants of collagenous matrix loaded with TGF-$ß_1$, interposed by implants of collagen loaded with its superfamily relative, the osteoinductive osteogenic protein-1 (OP-1, bone morphogenetic protein-7). The forecast outcome was osteoinduction by OP-1, but not by TGF-$ß_1$, as has been the case in reports by others using rabbits and rats. The unexpected outcome: large masses of ossified tissue, transversing all implants including the controls. The first conclusion: diffusion of TGF-$ß_1$ and OP-1 led to a local formation of a combination that resulted in superior bone formation, a 'synergistic combination osteogenesis' as we dubbed it. Yes, we concluded, TGF-$ß_1$ is indeed a promoter of bone formation as others have suggested, but more that that, it is a powerful synergist, owing to the dramatic rapidity and massive size of the newly induced tissue. Additional experiments yielded the big surprise: TGF-$ß_1$ is inductive on its own right, when implanted singly into the rectus abdominis of the baboon, and leads to ossified tissues expressing mRNA for BMPs.

A major point for consideration was the observation that TGF-$ß_1$, in our experiments, was not osteo-inductive in calvarial defects of the baboon, capable only of limited chondro-osteogenesis confined to defect margins. As is often the case, discoveries frequently raise yet more questions. The big one in this case is that of the site specific morphogenetic action of TGF-$ß_1$, that is, osteoinduction at extraskeletal sites but not orthotopic sites. That is yet one other discovery that needs to be un-covered.

The race is on.

Abbreviations used in this thesis

BMP	bone morphogenetic protein
bp	base pairs
BSA	bovine serum albumin
cDNA	complementary deoxyribonucleic acid
DTT	dithiothreitol
EDTA	ethylenediamine tetraacetic acid
h	human
kDa	kilodalton
mRNA	messenger ribonucleic acid
OP	osteogenic protein
p	porcine
PBS	phosphate-buffered saline
r	recombinant
RNA	ribonucleic acid
SSC	saline sodium citrate
TGF-ß	transforming growth factor-ß

1. CHAPTER 1

1.1 FORMULATION OF THE HYPOTHESIS

1.1.1 INTRODUCTION

The work presented in this thesis is the result of pursued inquiry following unexpected observations arising out of experiments in four primates, in which we sought to determine the *in vivo* response of a factor whose osteoinductive function is in dispute: that of transforming growth factor-ß, a morphogen belonging to a superfamily which bears its name. The TGF-ß superfamily consists of a large group of morphogens which are among the most versatile carriers of morphogenetic and differentiation signals. To date, more than 30 homologous proteins have been described that constitute members of the TGF-ß superfamily. Members of this superfamily participate in setting up the basic body plan during embryogenesis in diverse groups such as insects, amphibians and mammals, controlling the formation of the neural tube, limb, cartilage, bone and sexual organs. The TGF-ß superfamily includes the bone morphogenetic proteins (BMPs) and osteogenic proteins (OPs) (Wozney *et al.*, 1988, Ozkaynak *et al.*, 1990; Celeste *et al.*, 1990), activins and inhibins (Schwall *et al.*, 1988), the 60A (Wharton *et al.*, 1991) and decapentaplegic gene product of *Drosophila melanogaster* (Padgett *et al.*, 1987; Ferguson and Anderson, 1992), the Vg-1 gene product of *Xenopus laevis* (Weeks and Melton, 1987), the *Vg-1*-related murine analogue of murine Vgr-1 (Lyons *et al.*, 1989), the more distantly related growth and differentiating factors (GDFs) (Lee, 1991;

McPherron and Lee, 1993) of which the cartilage derived morphogenetic proteins (CDMPs) (Chang *et al.*, 1994) are family members, and finally the five TGF-ß isoforms themselves (Sporn, 1990).

A remarkable feature of BMPs and of TGF-ßs, and one which is of central importance to this work, is their postfoetal activities, particularly of repair and regeneration of bone. These features are discussed in depth in section *1.2.* Although both TGF-ßs and BMPs are regarded as major players in bone homeostasis, repair and regeneration of the adult skeleton, to date BMPs/OPs, and more recently CDMPs, are set apart from TGF-ßs by virtue of their ability to induce the *de novo* formation of bone in extraskeletal sites in a number of animal models studied. Implantation of naturally purified BMP (Urist *et al.*, 1984; Sampath *et al.*, 1987; Luyten *et al.*, 1989) or of recombinantly expressed BMPs in the heterotopic sites of animals (Wang *et al.*, 1990, Hammonds *et al.*, 1991, Sampath *et al.*, 1992) leads to new bone formation by induction as early as 12 days post implantation in rats. Osteoinduction by BMPs/OPs and CDMPs is not unique to themselves: recombinant Drosophila decapentaplegic and 60A also have the capacity to induce endochondral bone formation in mammals (Sampath *et al.*, 1993), indicating that these genes have been conserved for at least 600 million years.

Observations made whilst the writer was employed as biochemist at the Bone Research Laboratory, suggested a synergistic interaction during heterotopic osteoinduction between two members of the TGF-ß superfamily, osteogenic protein-1

(OP-1/BMP-7) and TGF-$ß_1$. This led to subsequent experimentation, presented in this thesis, in search of the nature of this interaction. Following these initial observations, a number of startling discoveries were made: for the first time, it was shown that TGF-$ß_1$, either recombinantly produced or purified from platelets, induced the *de novo* formation of cartilage and bone at heterotopic sites of the adult baboon. This is in contrast to our previous work showing, paradoxically, that TGF-$ß_1$ fails to heal calvarial defects in the same animal model, resulting instead in limited chondro-osteogenesis confined to the defect margins by day 30 (Ripamonti *et al.*, 1996a). In addition, it was shown that TGF-$ß_1$ interacts synergistically with OP-1 in rats and baboons to induce large ossicles with increased parameters of bone formation, a phenomenon we dubbed 'combination osteogenesis', a term extended from terminologies developed by pharmacologists in defining drug interactions (Greco *et al.*, 1995).

The following section serves as an historical perspective for the formulation of the hypothesis, whose investigation follows in the main body of the thesis.

1.1.2 EXPERIMENTS LEADING TO FORMULATION OF THE HYPOTHESIS

1.1.2.1 The orthotopic study in the baboon

Details of the orthotopic model in the baboon are to be found in section *3.2.7.* Details as to morphogens used, preparation of collagenous matrix as carrier, and analytical methods are to be found in Chapter 3. In order to test biologic actions of rhTGF-$ß_1$ at orthotopic sites, four adult male Chacma baboons (*Papio ursinus*) were utilised, each treated at four calvarial sites with doses of rhTGF-$ß_1$ of 5, 30 and 100 μg of the morphogen per gram of allogeneic insoluble collagenous bone matrix as carrier. Two full-thickness calvarial defects of 25 mm were created on each side of the calvaria with a craniotome. The defects were treated with each of the three doses of rhTGF-$ß_1$ delivered with 1 gram of insoluble collagenous matrix. The fourth defect was treated with insoluble collagenous matrix lacking rhTGF-$ß_1$, representing the control.

1.1.2.2 The heterotopic study in the baboon.

To test osteoinductivity of rhTGF-$ß_1$ in the rectus abdominis of the baboon, implants were prepared that contained 5 μg of rhTGF-$ß_1$ per of 100 mg of insoluble collagenous bone matrix. For the purpose of positive controls, implants containing rhOP-1 were also prepared. It was decided to design a dose response curve for rhOP-1, and consequently, implants were prepared that contained 0 (control), 5, 25 and 125 μg of rhOP-1 per 100 mg of insoluble collagenous matrix. Lyophilised preparations

containing doses of morphogens were implanted bilaterally in a series of longitudinal pouches prepared in the rectus abdominis muscle. Specimens were harvested simultaneously on day 30, and processed for histology and histomorphometry.

1.1.3 Observations

Orthotopic specimens

Representative histological sections of control and rhTGF-$ß_1$-treated specimens are shown in Figure 1. Histological analysis showed that rhTGF-$ß_1$ failed to induce bone formation across the defects with any of the doses tested. Noteworthy were the islands of cartilage, observed in close proximity to the calvarial margins in rhTGF-$ß_1$-treated defects. There was no correlation between rhTGF-$ß_1$ dose and amount of cartilage present at these sites. In one defect treated with 100 µg of rhTGF-$ß_1$, bone and cartilage were found at some distance from the margins of the defect, in a pericranial site. In all other specimens, bone was found only at the margins of the defects. In rhTGF-$ß_1$-treated specimens, there was an apparent dose-related increase in the formation of granulation tissue with both fibrotic and angiogenic features. This tissue was localised pericranially, between the implanted collagenous matrix and the temporalis muscle (Fig. 1).

Figure 1 (opposite page). *Low power photomicrographs of calvarial specimens harvested on day 30. Undecalcified sections cut at 7 µm were stained with Goldner's trichrome (original magnification x3).*
A: Collagenous matrix without rhTGF-$ß_1$ (control)
B, C and D: Specimens of collagenous matrix treated with 5, 30 and 100 µg rhTGF-$ß_1$, respectively showing limited osteogenesis, confined to the margins of the defects only.

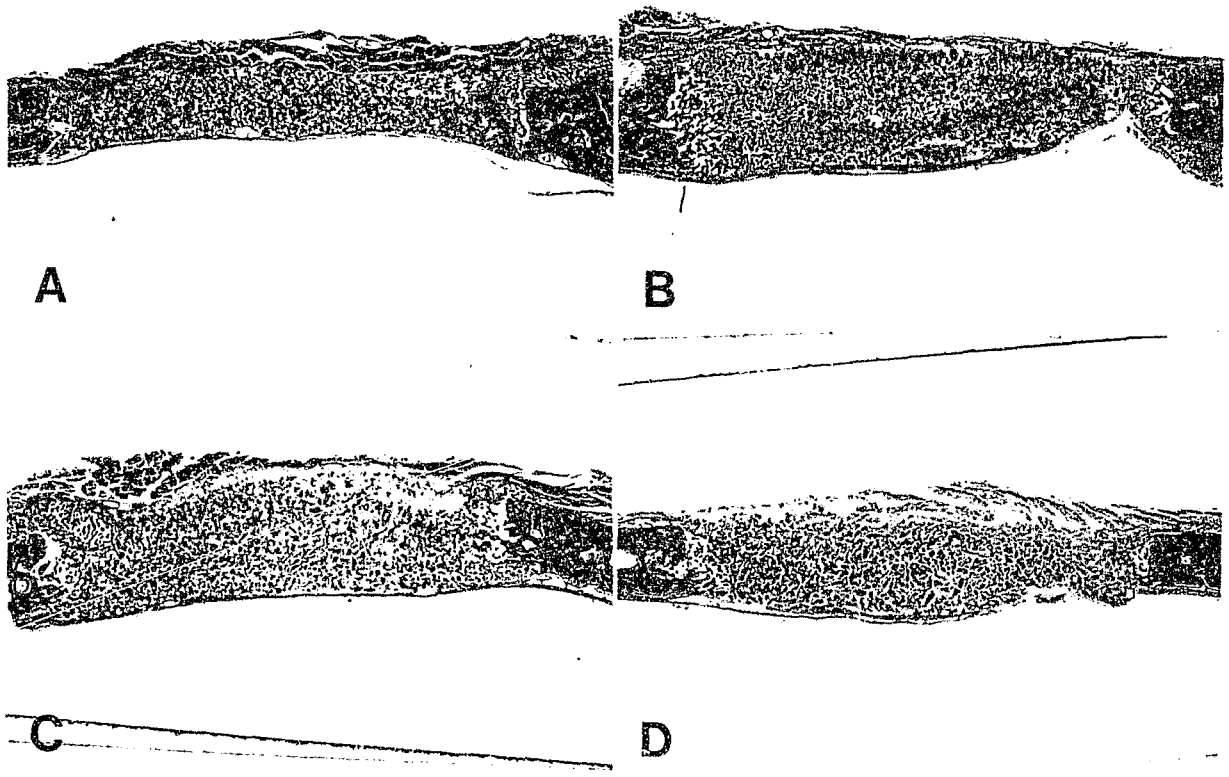
A
B
C
D

Histomorphometric analysis showed no significant differences between control and rhTGF-β_1-treated specimens with regard to mineralised bone and osteoid volumes, when considering the entire area across the defect. Limited chondro-osteogenesis was induced by rhTGF-β_1, which was confined to the interfacial regions. This suggested that the implanted rhTGF-β_1 exerted an effect on osteoprogenitor and osteoblastic cells originating from the severed calvarial margins and periosteum. The presence of cartilage in rhTGF-β_1-treated specimens indicated that TGF-β_1 promotes bone formation *via* an endochondral route in defects of membranous bone. The increased fibrogenesis and angiogenesis generated by the implanted rhTGF-β_1 was consistent with the biological activity of the morphogen when tested in extraskeletal sites of rodents (Roberts *et al.*, 1986; Rosen *et al.*, 1990). The orthotopic results in primates, however, contrasted markedly with previous reports showing that a single application of rhTGF-β_1 promoted a dose-dependent increase in 12-mm defects in the rabbit 28 days after treatment (Beck *et al.*, 1991).

Heterotopic specimens

Histological results of implantation of individual pellets with rhOP-1 and rhTGF-$ß_1$ in the rectus abdominis on day 30, are shown in Figure 2.

Figure 2. *Tissue morphogenesis in 4 baboons by interposed recombinant morphogens .*

rhOP-1 and rhTGF-$ß_1$, delivered with 100 mg collagenous carrier, were implanted singly in the rectus abdominis of the baboon and generated tissue harvested on day 30 and subjected to histological analysis on undecalcified sections cut at 4 µm.

A: Low power photomicrograph of a large specimen block showing extensive ossification of the space between the rectus muscle fibres and the fascia, with prominent fibrosis and vascular invasion between ossicles (original magnification x2.2)

B and C: Photomicrographs of massive ossicles that had formed between the muscle fibres and the posterior fascia of the rectus abdominis. Corticalisation of the ossicles and extensive bone marrow formation (C), permeating trabeculae of newly formed bone. Arrow in C indicates a large zone of chondrogenesis protruding within the rectus abdominis, displaced by the ossicle growth (original magnification x3.2).

D: Maturational gradients of tissue morphogenesis at the periphery of newly formed ossicles. There is a gradient of morphological structures highly suggestive of a rudimentary growth plate (toluidine blue, original magnification x 20).

E: Photomicrograph of another ossicle showing classic features of chondrogenesis and osteogenesis as seen in the embryonic growth plate. Subjacent to cartilage zones with columns of progressively maturing chondroblasts (D and E), there is vascular invasion, chondrolysis and generation of trabeculae of bone with marrow (modified Goldner's trichrome, original magnification x 30). The formation of ossified blocks meant that it was impossible to discern which tissues arose from which implants.

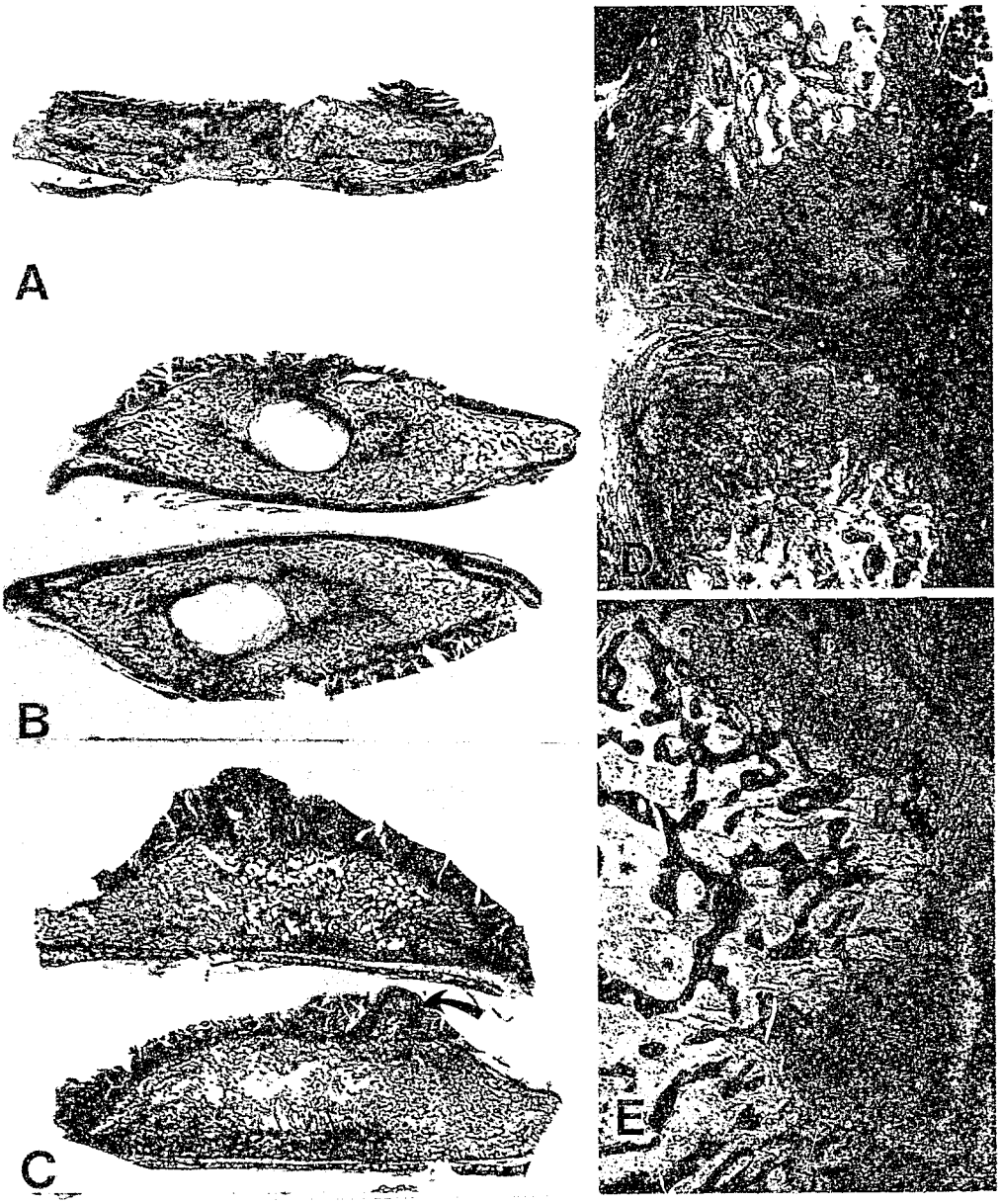
A
B
C
D
E

Newly generated tissue had grown to form large ossicles with a planar-convex geometry, and extending for several centimetres, preferentially along the longitudinal plane of the fascia (Fig. 2). Ossicles showed peripheral corticalisation while newly formed trabeculae, interspersed with newly generated bone marrow, occupied the centre of the specimens (Figs. 1C-1E). In one specimen, two juxtaposed ossicles had grown toward each other and, while separated by a layer of intervening fibrous tissue, each ossicle showed a gradient of morphological structures highly suggestive of a rudimentary embryonic growth plate (Figs. 2D and 2E).

A number of conclusions were drawn. Firstly, the generation of such large ossicles on day 30 pointed to a possible desorption and diffusion effect of the two recombinant morphogens and an inductive wave of differentiation along responding cells of the fasciae and muscular tissue (Fig. 2). Secondly, the large amounts of newly generated tissue pointed to a possible synergistic interaction of rhOP-1 and rhTGF-β_1 in bone induction.

1.1.4 Hypothesis

It was hypothesised that if these levels of induction could be generated by placing separately the two morphogens as described in section *1.1.3*, then a combination of both OP-1 and rhTGF-$ß_1$ in the same implant would result in a potent and localised synergistic induction of endochondral bone differentiation. The rapid induction of large amounts of chondro-osteogenic tissue, with morphogenetic fates which can be determined and controlled by careful manipulation of implanted morphogen combinations to achieve a desired response eg. predominantly osteogenic versus predominantly chondrogenic, would have important implications for future therapeutic approaches.

1.1.5 Aims of the study

Against this background, this work was set to accomplish a number of aims:

1. To characterise the nature of the interaction of TGF-ß and BMP during combination osteogenesis

    a) of both recombinant (rhOP-1; rhTGF-$ß_1$) and native forms of the morphogens (porcine TGF-$ß_1$; bovine BMP)
        i) in primate and rodent heterotopic sites.
        ii) in primate orthotopic sites.

2. To determine dose rersponse curves for bone induced by rhOP-1 at heterotopic sites, both in the rodent and the primate.

3. To gain insights into the mechanism of synergistic induction of bone formation using analytical methods including histomorphometry, biochemistry and Northern analysis.

4. To develop a process for the large scale purification of native TGF-$ß_1$ from lyophilised porcine platelets for experimental use in primate studies requiring large amounts of this scarce and expensive morphogen.

1.1.6 Preview of the organisation of the Thesis

The bone differentiation cascade elicited by heterotopic implantation of BMPs/OPs in adult animals bears remarkable similarity to embryogenic bone development, and to post-foetal repair and regeneration of bone. It is pertinent therefore, to expound a brief literature review of embryonic and post-foetal actions of these morphogens, to describe their receptor systems and insights into their signal transduction mechanisms, in order to gain perspectives into possible mechanisms of the observed interaction, and finally to describe work accomplished to date that pertains to pre-clinical applications of these morphogens.

Following the literature review (section *1.2*), Chapter 2 describes the purification of porcine TGF-$ß_1$ and bovine BMP. Chapter 3 describes the work performed in rodents and primates, with single and combined applications of the two morphogens, at orthotopic and heterotopic sites, and biochemical, histological and Northern analyses of generated tissues.

1.2 LITERATURE REVIEW

1.2.1 Introduction

Approximately 500 million years ago, the Paleozoic era heralded an evolutionary marvel: the skeleton, an evolutionary hallmark marking the birth of the vertebrates. In the struggle against gravity, the skeleton was a means to rise to greater dimensions, an ' to conquer the continents. A feature of this evolutionary development was the capacity for the repair of the bony skeleton. The ancient Greeks were aware of the remarkable repair capacity of bone. In the past decade, the elucidation of the transforming growth factor superfamily of proteins, and in particular of the bone morphogenetic proteins, has marked a new era in which the tissue engineering and morphogenesis of bone are now coming under the dominion of man. This knowledge may serve as a starting point at which this technology may in future become applicable laterally to tissues and organs beyond bone.

1.2.2 Embryonic osteogenesis

The individual constituents of the skeleton begin as mesenchymal condensations during the embryonic period (reviewed by Matthews, 1980). These mesenchymal cells are thought to be derived from the primary germ layers under the mechanical or chemotactic influence of other tissue structures such as the notochord and neural tube. Some of these cellular condensations ossify directly to form the membrane-derived or membranous bone as is observed for the craniofacial skeleton and the clavicle. This is

termed intramembrancus ossification and is marked by the direct condensation of mesenchymal tissue, differentiation of osteoblasts, matrix synthesis and eventual ossification of the newly generated extracellular matrix (Matthews, 1980). The remaining skeleton, both axial and appendicular, is derived from the differentiation of the mesenchymal cells firstly into a cartilage phase and subsequently into bone tissue, a process known as endochondral ossification. Endochondral bone formation is typically observed during long bone development. This occurs *via* two discrete processes: firstly the transformation of the cartilage anlage into the primary osseous collar and subsequent vascular invasion to form the primary ossification center, which will become the diaphysis and metaphyses, and secondly a usually postnatal vascular-mediated ossification in the cartilaginous epiphysis to form the secondary ossification center (Matthews, 1980). Selected areas of cartilage, the growth plates or physes develop between the primary and secondary growth plates. These are capable of growth both longitudinally and latitudinally. Cartilage tissue is hence replaced by bone, an event characteristic of endochondral ossification (reviewed by Matthews, 1980). The two types of bone formation, namely endochondral and membranous, refer only to the primary pattern of development. Subsequent growth after this initial differentiation may involve juxtaposed areas of both patterns. In this respect, endochondrally derived bones have intramembranous ossification with appositional growth from the periosteum. Similarly, membrane-derived bones may undergo subsequent growth by a modified endochondral process as happens in the proximal region of the clavicle (Matthews, 1980).

Embryonic events give rise to the five cell types responsible for the production of the five skeletal tissues in the body: the osteoblast producing bone, the chondroblast producing cartilage, the odontoblast producing dentine, the cementoblast producing cementum and the ameloblast producing enamel (Urist, 1980). A first sign that indicates imminent skeletogenesis, both during embryonic development and post-foetal bone regeneration is the condensation of mesodermal and mesenchymal cells to form the anlage or primordium of the bone. These condensing cells either arise locally in the position the bone will occupy subsequently, as in the formation of the embryonic vertebrae and the formation of a fracture callus, or they migrate from elsewhere in the body to the site at which skeletogenesis is to occur, as in the migration of ectomesenchymal cells into the embryonic mandible (Urist, 1980).

It is now known that nature exploits embryonic-like mechanisms in post-foetal life for the repair and maintenance of tissues. The repair of a bone fracture is a typical example. A bone fracture induces the formation of new bone that remodels into the healing callus, a process following the route of endochondral ossification. This postfoetal osteogenesis may be considered to recapitulate events that occur in the normal course of embryonic bone development as described above. The new bone results from local mesenchymal condensations, a cartilage phase and extracellular matrix production, vascular invasion and mineralisation, and finally the formation of new bone *via* the differentiation of osteoprogenitor cell lines (Urist, 1980). Central to the elucidation of mechanisms whereby fracture healing might deploy embryonic processes to achieve its end, was the observation that implantation of demineralised

bone matrix was able to do the same: to initiate new bone formation *via* a process that was remarkably similar to events occurring during embryogenic bone development (Urist, 1965).

1.2.3 Bone formation by induction

Perhaps no other concept has fascinated bone biologists more than the phenomenon of bone formation by induction. The observation by Lacroix (1945) that bone alloimplants are capable of inducing new bone in the recipient led him first to hypothesize the existence of bone inducing factors which he dubbed 'osteogenins'. The existence of such factors was strongly supported by the discovery that demineralised bone matrix is capable of inducing the *de novo* formation of bone when implanted extraskelletally in rats (Urist, 1965). Endochondral bone was induced *via* a process that was reminiscent of events occurring during embryonic osteogenesis. This work initiated efforts by others that led eventually to the cloning and characterisation of morphogens responsible for osteogenic activity.

Reddi and Huggins (1972) characterised the sequence of events that take place upon implantation of demineralised bone matrix into the subcutaneous space of the rat. Briefly, there is the chemoattraction of fibroblasts to the implanted demineralised bone matrix, chondrogenesis, calcification and chondrolysis followed by vascularisation and formation of bone. On day one, the implant had formed an

encapsulated conglomerate of fibroblastic cells that had invaded the implanted matrix. On day three there appeared transiently some leukocytes, followed by a compact mass of fibroblasts on day five, with associated immature cartilage progenitors and chondroblasts. On days seven and eight cartilage was present, and many chondrocytes displayed cell division. A noteworthy feature was the strongly metachromatic extracellular matrix in toluidine blue stained sections, pointing to an abundance of cartilage matrix. Day seven marked the calcification of this matrix. Cartilage was found exclusively in the centre of the plaque, whereas the rim was fibroblastic. On day 9, there was an incursion of capillaries into the newly formed tissue, followed by the appearance of osteoblasts, marking the start of chondrolysis. Cartilage had disappeared in most cases by day 14, and completely by day 18. Day ten marked the first time appearance of bone, increasing to large quantities by day 14, associated with cartilage. On days 18-21, the tissue consisted of large masses of bone, and erythropoiesis was evident in the centres of the ossicles. Alkaline phosphatase activity rose sharply on day seven, reaching a maximum threshold on day ten, then declined to basal levels. Incorporation of radiolabeled sulphate, a marker for cartilage matrix synthesis, was considerable by day three, rising steadily until day eight whence it declined markedly thereafter. The incorporation of phosphate was lowest at day seven, rose considerably on days eight to ten and plateaued at high values through days ten to 21. Calcium followed a similar incorporation pattern as that of phosphate. Ossification was limited to the centre of the newly formed tissue. On day 700, the newly formed tissue comprised vital bone with haematopoietic bone marrow, and fibrotic tissue was absent (Reddi and Huggins, 1972).

Clues that the factor responsible for the osteoinductivity of demineralised bone matrix was soluble, came from the classic experiments showing that guanidinium chloride extraction of demineralised bone matrix resulted in inactive insoluble collagenous bone matrix, and that reconstitution of the solubilised component with the insoluble collagenous bone matrix led to the revival of osteoinductive activity in the rat heterotopic bioassay (Sampath and Reddi, 1981). This discovery laid the foundation for the development of the heterotopic bioassay in rodents for the identification of osteogenic molecules. The implantation of osteogenic activity in the rat subcutis leads to new bone formation typically by day 12 (Sampath and Reddi, 1981). The heterotopic bioassay is today regarded by many as the acid test for true osteoinductivity. A factor that is capable of inducing new bone formation extraskeletal sites, is said to epitomise osteoinductive principles.

Identification of osteoinductive proteins in mammalian bone proved to be difficult due to the relative inaccessibility of small quantities of the putative proteins tightly bound to the organic and inorganic components of the extracellular matrix of bone. By using partially purified osteogenic fractions derived from bones of various species, Sampath and Reddi (1983) showed that the osteogenic activity was not species specific, i.e. an osteogenic fraction from bovine bone matrix was able to induce bone in the rat when reconstituted with guanidine-inactivated rat collagenous matrix. Similarly, the implantation of bovine-derived osteogenic fractions into intramuscular

sites of the baboon and subcutaneous space of rats was capable of initiating new bone formation (Ripamonti *et al.*, 1991). The heterotopic bioassay in rats, coupled with the use of readily available starting material such as bovine bone, and the application of increasingly refined purification schemes, provided the starting point for the purification of native BMPs (Wang *et al.*, 1988; Luyten *et al.*, 1989; Sampath *et al.*, 1990). Partial amino acid sequence identity of the first factors was eventually accomplished (Wozney *et al.*, 1988; Luyten *et al.*, 1989) leading to the elucidation of the genetic code and expression for an entirely new family of protein initiators called bone morphogenetic proteins (BMPs), a family related to the transforming growth factor-ß superfamily of morphogens (Wozney *et al.*, 1988). Of the first of these to be described were bone morphogenetic protein-2, -3 -4, (Wozney *et al.*, 1988). Other BMP family members were then described: BMP -5, -6, -7 (osteogenic protein-1/OP-1) and -8 (OP-2) (Celeste *et al.*, 1990; Ozkaynak *et al.*, 1990; Ozkaynak *et al.*, 1992). Other related members were later identified, including growth/differentiation factor-1 (GDF-1) (Lee, 1990), GDF-3 and GDF-9 (Alexandra *et al.*, 1993), GDF-10 a BMP-3-related protein (Cunningham *et al.*, 1995) and the cartilage derived morphogenetic proteins (CDMP-1 and -2, Chang *et al.*, 1994), of which CDMP-1 is a GDF-5 equivalent (Hotten *et al.*, 1994).

1.2.4 The TGF-ß Superfamily

1.2.4.1 Overview

The TGF-ß superfamily includes the bone morphogenetic proteins (Wozney *et al.*, 1988, Ozkaynak *et al.*, 1990; Celeste *et al.*, 1990), activins and inhibins (Schwall *et al.*, 1988), the 60A (Wharton *et al.*, 1991) and decapentaplegic (DPP) gene products of *Drosophila melanogaster* (Padgett *et al.*, 1987; Ferguson and Anderson, 1992), the Vg-1 gene product of *Xenopus laevis* (Weeks and Melton, 1987), the *Vg-1*-related analogue of murine Vgr-1 (Lyons *et al.*, 1989), the more distantly related growth and differentiating factors (Lee, 1991; McPherron and Lee, 1993) of which the cartilage derived morphogenetic proteins (CDMPs) (Chang *et al.*, 1994) are family members, and finally the TGF-ßs themselves (Roberts and Sporn, 1990).

TGF-ßs themselves were first identified as 25 kDa homodimers that stimulate the growth of normal rat fibroblasts in soft agar culture (Assoian *et al.*, 1983). The TGF-ß family is currently known to comprise five closely related proteins termed TGF-$ß_1$ through TGF-$ß_5$ (Roberts and Sporn, 1990). In addition, the existence of a TGF-$ß_{2.3}$ heterodimer has been reported by Ogawa *et al.* (1992). TGF-$ß_1$ through TGF-$ß_3$ have been identified in mammalian cells, TGF-$ß_4$ in chicken and TGF-$ß_5$ in *Xenopus laevis*. These different TGF-ßs are highly conserved between species. TGF-$ß_1$ is identical in man, monkey, pig, cow and chicken. TGF-$ß_2$ is 71% homologous to TGF-$ß_1$, and the remaining TGF-ßs share between 64% and 83% homology with TGF-$ß_1$ (Roberts *et al.*, 1991).

Members of the TGF-ß family have diverse biological activities and play critical roles in the migration, proliferation and differentiation of a variety of cells during embryogenesis (Heine *et al.*, 1987; Pelton *et al.*, 1990) and in the repair, regeneration and maintenance of tissues during postfoetal life (Roberts and Sporn, 1990; Derynck, 1994; Kingsley, 1994). The many differences in the *in vitro* biological activities of TGF-$ß_1$, TGF-$ß_2$ and TGF-$ß_3$ which have been reported have led to many conflicting and contradictory views on the functions of this morphogen. For example, the growth of endothelial cells (Jennings *et al.* 1988, Cheifetz *et al.* 1990) and certain haematopoietic cells (Ottman and Pelus, 1989, Ohta, 1987) are strongly inhibited by TGF-$ß_1$ and TGF-$ß_3$ whereas a substantially greater concentration of TGF-$ß_2$ is required to achieve the same degree of inhibition (Ottman and Pelus, 1989, Ohta, 1987). In addition, TGF-ß exhibits biphasic effects on some systems, inhibiting some cell function in one system whereas stimulating the same function in another system. An interesting aspect of TGF-ß's biphasic nature relates to granulocytes and macrophages. TGF-ß exerts both inhibitory and stimulatory effects on macrophages, often depending on the species of the population of the macrophages and the conditions of their stimulation (Bogdan and Nathan, 1993). Exogenously added TGF-$ß_1$ or TGF-$ß_2$ in the presence of interleukin-1 or granulocyte-macrophage colony stimulating factor inhibited formation of colonies by early erythroid and immature granulocyte-macrophage progenitor cells (Keller *et al.*, 1988). In contrast, TGF-$ß_1$ enhanced the growth of the more mature progenitor cells after stimulation with granulocyte-macrophage colony stimulating factor (Keller *et al.*, 1991).

The antiproliferative activity of TGF-ß is well documented in epithelial cells grown *in vitro,* whereas growth stimulatory effect occurs mainly in cells of mesenchymal origin such as fibroblasts. TGF-ß has been shown to have profound effects on nearly all cell types, and its action is particularly evident on mesenchymal cells, influencing their chemotactic (Postlethwaite *et al.* 1987) proliferative (Moses *et al.* 1987; Centrella *et al.* 1987; Hill *et al.* 1986) and differentiating functions (Ignotz and Massague 1986; Seyedin *et al.* 1985; Massague *et al.,* 1986).

Results obtained by Kulkarni *et al.* (1993) indicate that TGF-ß plays a prominent role in the homeostatic regulation of immune cell proliferation and extravasation into tissues. The generation of TGF-ß null mice resulted in excessive inflammatory response and early death. The organs most heavily affected were the heart and lungs. The authors maintain that the absence of TGF-$ß_1$ in these mice may facilitate a generalised activation of the immune system by stimuli that are unable to promote disease in normal littermates. Since TGF-$ß_1$ is known to antagonise a number of pro-inflammatory molecules such as interleukin-1, -6, tumour necrosis factor and interferon gamma, TGF-$ß_1$ null mice can be expected to have increased activity of pro-inflammatory cytokines. This may result in an uncontrollable pro-inflammatory cytokine cascade (Kulkarni *et al.,* 1993). TGF-ß secreted within an inflammatory site or injected locally, induces leukocyte migration, chemotaxis and accumulation (Wahl *et al.,* 1993). TGF-ß promotes in a dose and time dependent fashion, monocyte

adhesion to type IV collagen, laminin and fibronectin. TGF-ß may potentially facilitate the movement of monocytes through the extracellular matrix by triggering the expression of collagenase type IV and the 92 and 72 kDa gelatinases (Wahl *et al.,* 1993).

The high content of TGF-$ß_1$ in platelets is believed to play a critical role in events of injury (Border and Ruoslahti, 1992). Upon degranulation of the platelets at the site of injury, TGF-ß is released into the surrounding tissue (Assoian and Sporn, 1986). TGF-ß then initiates a complex sequence of events that promotes healing including: chemoattraction of monocytes and leukocytes (Wahl *et al.* 1987), induction of angiogenesis (Roberts *et al.,* 1986) and control of the production of cytokines and other inflammatory mediators (Kulkarni *et al.*, 1993). Repair may be facilitated by TGF-ß in numerous different ways: TGF-ß stimulates the synthesis of individual matrix components including fibronectin, tenascin, collagens and proteoglycans in fibroblastic cells (Border and Ruoslahti, 1992). It simultaneously blocks matrix degradation by decreasing the synthesis of proteases and increasing the levels of protease inhibitors (Edwards *et al.,* 1987). TGF-ß also increases the expression of integrins and changes their relative proportions on the surface of cells in a manner that could facilitate adhesion to the matrix (Ignotz and Massague, 1987).

TGF-$ß_1$ increases steady-state levels of its own message in a number of normal and transformed cells in culture. The positive autocrine feedback was reported for foetal

murine fibroblasts, where exogenous TGF-ß$_1$ rapidly induced expression of its own mRNA (Bascom *et al.*, 1989). TGF-ß$_1$ was capable of increasing its own message 2-3 fold within 3 hours in human lung carcinoma, human lung fibroblasts, human fibrosarcoma and rat osteosarcoma cell lines (Purchio *et al.*, 1988). The ability of TGF-ß$_1$ to stimulate its own synthesis may provide a way to amplify and sustain the physiological processes elicited by this factor.

An upregulation of TGF-ß$_1$ transcription has been reported for several *in vivo* systems involving injury and repair, such as phorbol ester treatment of skin (Cheifetz *et al.*, 1987) and bone fracture healing (Danielpour *et al.*, 1989). In the case of phorbol ester treatment, the increase in TGF-ß$_1$ mRNA levels is transient and can occur as early as two to three hours after treatment, suggesting a relatively short effect. In contrast, the increase in TGF-ß$_1$ mRNA occurs later in the bone fracture model: at day five and again at day 15 following fracture of the femur in rats, coinciding with the onset of membranous and endochondral ossification, respectively (Danielpour *et al.*, 1989). Van Obberghen-Schilling *et al.* (1988) reported that increased TGF-ß$_1$ mRNA expression appears to be a general response to TGF-ß$_1$ treatment in several normal and transformed cell lines including human lung fibroblasts, human fibrosarcoma cells, rat kidney cells and rat osteosarcoma cells. Accumulation of TGF-ß$_1$ mRNA was detected within three hours of addition of the polypeptide to cells, and enhanced message levels persisted as long as TGF-ß$_1$ was present in the medium. This autoinduction was half-maximal at approximately 10 pM TGF-ß$_1$ and maximal

stimulation corresponded to a two to three fold increase in transcript levels. In normal rat kidney cells, the rise in TGF-$ß_1$ mRNA was actinomycin-D sensitive and was accompanied by a three-fold increase in secretion of the protein into the culture medium. Treatment of rat kidney cells with PDGF and EGF also resulted in a two to three fold increase in TGF-$ß_1$ mRNA.

TGF-ß superfamily members and epithelial-mesenchymal interactions

Classic studies in experimental embryology have demonstrated that vertebrate organ development depends on sequential and reciprocal interactions between tissue layers, synthesising paracrine and autocrine factors that serve to regulate patterning and tissue formation. (Spemann and Mangold, 1924). The position of the condensed mesoderm or ectomesenchyme, and the shape, size and rate of growth of the condensed cells are determined by the inductive interaction with adjacent ectoderm (prospective epithelium). These inductive epithelial-mesenchymal interactions, also called secondary induction, lead to cell differentiation and to the organisation of cells into tissues and organs.

Although the importance of epithelial-mesenchymal interactions for the development of most organs is well established, the actual mechanisms involved in the mediation of inductive signals are not fully understood. However, it is now established that epithelial-mesenchymal interactions rely, at least in part, on the synthesis of members of the TGF-ß superfamily, suggesting that differentiation of these cell types may be

orchestrated by the interplay of TGF-ß-related factors (Heine *et al.*, 1987; Vainio *et al.*, 1993; Kingsley, 1994; Thesleff and Nieminen, 1996; Vukicevic *et al.*, 1996). TGF-ß is often detected in both epithelial and mesenchymal cells (Heine *et al.*, 1987). Expression data of TGF-$ß_{1-3}$ isoforms show these morphogens to be expressed temporally and spatially in various developing tissues undergoing epithelial-mesenchymal interactions, including the kidney, heart, skin, palate, hair, whisker follicles, lung, mammary gland and teeth (Lehnert and Akhurst, 1988; Pelton *et al.*, 1989, 1990; Millan *et al.*, 1991; Schmidt *et al.*, 1991). TGF-$ß_1$ protein is predominantly found in mesenchymal tissues such as connective tissue, cartilage and bone, and in tissues derived from neural crest mesenchyme, including the palate of teeth (Heine *et al.*, 1987). TGF-$ß_2$ mRNA has been detected in early facial mesenchyme, and widely in various epithelia, suggesting that this morphogen may regulate epithelial cell growth and differentiation of developing tissues, including the skin and palate (Pelton *et al.*, 1989). Miettinen *et al.* (1994) has shown that mouse mammary epithelial cells undergo a reversible transition to a mesenchymal phenotype upon TGF-ß treatment. This occurred in parallel with increased expression of the mesenchymal marker fibronectin and a reorganisation of actin stress fibres from an epithelial to a fibroblastic pattern. This suggests that TGF-ß can induce epithelial to mesenchymal transdifferention (Miettinen *et al.*, 1994). The transdifferentiation appears to involve a protein kinase C, and this transdifferentiation cannot by mimicked by activin. The authors implicate the involvement of a TGF-ß type I receptor for the transdifferentiation (Miettinen *et al.*, 1994).

Numerous experiments indicate that in vertebrates, BMPs play key roles in mesoderm formation and differentiation, nervous system development and skeletogenesis as well as limb bud patterning. *In situ* hybridisation analysis has shown that in addition to developing cartilage and bone, BMPs are also expressed at sites of epithelial-mesenchymal interactions in several organs in the embryo (Lyons *et al.*, 1989; 1990; Jones *et al.*, 1991; Vainio *et al.*, 1993; Harland, 1994; Kingsley, 1994; Vukicevic *et al.*, 1996). High levels of OP-1 (BMP-7) mRNA expression were detected in murine kidney (Ozkaynak *et al.*, 1991). BMP-3 protein was detected in human lung in addition to human kidney (Vukicevic *et al.*, 1994). OP-1 (BMP-7) protein was found to have high-affinity binding to basement membranes (Vukicevic *et al.*, 1994). In developing human embryos and human foetuses, the expression of OP-1 mRNA was found to be highest in human foetal kidney and heart between 12-14 weeks of gestation, followed by other tissues including brain and lung, but not liver (Helder *et al.*, 1995). The authors suggested that OP-1 (BMP-7) plays important roles in the initiation and/or progression of limb formation. In addition, it was suggested that OP-1 may be involved in the terminal differentiation of chondrocytes and subsequent bone formation (Helder *et al.*, 1995).

BMP-2 and BMP-4 are expressed during limb bud formation (Lyons et al., 1990, Jones *et al.*, 1991, Francis *et al.*, 1994). BMP-7/OP-1 is expressed at high levels in both the limb bud and branchial arches in mouse embryos (Lyons *et al.*, 1995) and in the chick (Wall *et al.*, 1995). BMP-8b mutant mice were shown to exhibit germ-cell

deficiencies and degrees of infertility (Zhao *et al.*, 1996). BMP-4 plays a role in mouse embryonic lung development (Bellusci *et al.*, 1996). BMP-4 was found to be expressed in the branching points of embryonic lung epithelium, placing this morphogen at a control point in branching morphogenesis of lung (Urase, 1996). BMP-4 and BMP-7 were found to be the signal produced by the dorsal aorta that direct sympathetic nervous differentiation (Reissmann, 1996). A classic example of epithelial-mesenchymal interaction is clearly evidenced in tooth development and morphogenesis (Vainio *et al.*, 1993). BMP-4 is expressed in the presumptive dental epithelium at the initiation of embryonic tooth development. Subsequently, epithelial signalling leads to mesenchymal induction of *BMP-4* expression (Vainio *et al.*, 1993).

The embryonic development of the vertebrate kidney proceeds along the interaction of the epithelial ureteric bud and the metanephric mesenchyme (Saxen, 1987). Following the invasion of the metanephric mesenchyme by the ureteric bud, nephrogenesis involves essentially the reciprocal inductive interaction between these two tissues. OP-1 (BMP-7) deficient mice die shortly after birth as a result of poor kidney development (Luo *et al.*, 1995; Dudley *et al.*, 1995). *In situ* hybridisation showed that the absence of OP-1 in the mutant mice resulted in the absence of key molecular markers of nephrogenesis, implicating that OP-1 is an inducer of nephrogenesis (Luo *et al.*, 1995; Vukicevic *et al.*, 1996). Additional abnormalities in the mutant mice included skeletal patterning defects of the rib cage, skull and of polydactily in the hindlimbs. Also, eye defects of anophthalmia and microphthalmia,

appearing to originate in the stages of lens induction, were noted (Luo *et al.*, 1995; Dudley *et al.*, 1995; Solursh *et al.*, 1996). Interestingly, the early inductive tissue interactions responsible for establishing the kidney and the eye appeared unaffected, and moreover, axis formation, neural patterning and gut development all appeared to occur normally in OP-1 deficient mice. The authors hypothesised that, in view of the early pattern of OP-1 expression in normal developing mouse embryos, overlapping expression of closely related TGF-ß superfamily members may rescue gastrulating embryos (Dudley *et al.*, 1995; Dudley *et al.*, 1997). OP-1 was found to be expressed in the ureteric epithelium before mesenchymal condensation, and was subsequently seen in the condensing mesenchyme and during glomerulogenesis (Vukicevic *et al.*, 1996), indicating a requirement for this morphogen during metanephric mesenchyme differentiation and a functional role during kidney development.

Rat embryos cultured in the presence of OP-1 blocking antibodies consistently exhibited over-all reduced size and absence of eyes. Histological sections revealed a greater reduction in neural retinal development. The authors concluded that OP-1 is required for vertebrate eye development (Solursh *et al.*, 1996). In contrast, a large proportion of TGF-$ß_1$ deficient mice managed to grow normally for the first two weeks after birth (Kulkarni *et al.*, 1993). These mice, which produce no detectable amounts of TGF-$ß_1$ mRNA or protein, developed a rapid wasting syndrome, and died 3 to 4 weeks of age. Pathological examination revealed an excessive inflammatory response with massive infiltration of lymphocytes and macrophages in many organs,

mainly in the heart and lungs. The lesions resembled those found in autoimmune disorders. The authors suggested a prominent role for TGF-$ß_1$ in homeostatic regulation of immune cell proliferation and extravasation into tissues. The absence of TGF-$ß_1$ may facilitate a generalised activation of the immune system by stimuli that are unable to provoke disease in normal littermates. This is consistent with the reported role of TGF-$ß_1$ as potent immunosuppressor (Wahl, 1992), by way of antagonising the activity of interleukin 1, tumour necrosis factor alpha, interferon gamma and interleukin 6.

Experimental embryology has shown that the ground state for the mesoderm is ventral, and special signal from the dorsal vegetal region, specifically the Niewkoop center, and then the Spemann organizer of the dorsal mesoderm cause dorsal development to occur (reviewed by Harland, 1994). BMP-4 is expressed in the embryo at the time of ectodermal fate determination, functioning as a potent epidermal inducer and as a neural inhibitor (Wilson and Hemmati-Brivanlou, 1995). In animal cap experiments, BMP-4 led to neural differentiation, whilst neuralising activity was inhibited (Sasai *et al.*, 1995). BMP signalling is essential for ventralising activity during normal interaction of animal pole tissue with prospective ventral mesodermal cells (Maeno *et al.*, 1994).

BMPs/OPs and related TGF-ß superfamily members are deployed both during embryonic development, and in post-natal life in repair and regeneration processes.

Of particular relevance to this work are the functions of these morphogens which pertain to cartilage and bone biology.

1.2 Role of BMPs and TGF-ßs in the biology of bone

Together with BMPs/OPs, TGF-$ß_1$ and TGF-$ß_2$ are most abundant in the extracellular matrix of bone, indicating that TGF-ß isoforms play important roles in bone physiology and homeostasis (Roberts and Sporn, 1990; Centrella *et al.*, 1994). Demineralisation of bone results in the predominantly collagenous extracellular matrix to which remain bound both the TGF-ßs and BMPs. Implantation of demineralised bone matrix in the subcutaneous space of the rat induces new bone formation *via* a cartilage phase (Urist, 1965; Reddi and Huggins, 1972). This model has been the subject of numerous studies. Carrington *et al.* (1988) used it to monitor the accumulation, localisation and compartmentation of TGF-ß during the bone formation cascade elicited by demineralised bone matrix. TGF-ß was present in highest concentrations at the time when the transition from calcified cartilage to bone was taking place and consequently, when osteoblasts, known to produce and be responsive to TGF-ß in culture, were present (Carrington *et al.*, 1988). Immunohistochemical analysis of the developing bone indicated that the TGF-ß was tightly bound to mineralised matrix of calcified cartilage and bone. This compartmentation of TGF-ß may be a mechanism for storing latent or processed TGF-ß. The amount of TGF-ß increased four-fold during the stage of bone formation. Whilst TGF-ß mRNA was found to be constant during the stages of expression, TGF-ß immunochemical detection increased in an uncoordinated fashion, leading to the conclusion that either TGF-ß is under translational rather that transcriptional control or else it accumulates as a result of its high affinity for the mineral component of the matrix (Carrington *et al.*, 1988).

Implantation of recombinantly produced BMPs/OPs in conjunction with a suitable carrier leads to a multistep differentiation cascade with culmination in endochondral bone formation. The precise cellular targets that respond to BMPs/OPs however, remain unknown. Cunningham *et al.* (1992) characterised cellular infiltrates arising from implanted collagenous matrix reconstituted with osteogenin (BMP-3) in rats, and found numerous cells of the monocyte lineage. *In vitro* studies showed that OP-1 was 3-4 orders of magnitude more potent a chemoattractant for neutrophils and monocytes than for fibroblasts (Postlethwaite *et al.*, 1994). This suggests that neutrophils and monocytes are the first cells *in vivo* to be recruited to the site of OP-1 implantation, their arrival preceding the accumulation of fibroblasts (Cunningham *et al.*, 1992). The order in which cells infiltrate sites of OP-1 implantation in experimental animals i.e. neutrophils followed by monocytes then fibroblasts, could be related to the different chemotactic potency that OP-1 has for each these cell types. The early accumulation of neutrophils and monocytes and later migration of fibroblast-like mesenchymal cells are seen at implantation sites of both OP-1 and TGF-$ß_1$ suggesting that these cells are critical for both fibrogenesis and osteogenesis, and that both OP-1 and TGF-ß can call forth the same cell types (Cunningham *et al.*, 1992). It is subsequent action on these cells by OP-1 and TGF-ß that results in the phenotypic transformations observed *in vivo*. Although OP-1 and TGF-$ß_1$ share 34% amino acid sequence identity in the highly conserved 7 cysteine domain, the disparity in their biological effects on cells of mesenchymal origin is of considerable interest

and calls for future studies to explore structure-function relationships between these two molecules (Cunningham *et al.*, 1992).

There have been in the past conflicting views on the osteoinductive status of TGF-ß. These stem perhaps from disagreement on the definition of the term 'osteoinductive'. Some authors for example, choose to describe TGF-ß as osteoinductive based upon the ability to induce closure of skull defects in rodents (Beck *et al.*, 1991), in lieu of evidence for *heterotopic* osteoinductivity, considered by others as the acid test for bona fide osteogenic proteins. It is noteworthy, that injection or implantation of either TGF-$ß_1$ or TGF-$ß_2$ at subcutaneous sites of rats (Roberts *et al.*, 1986; Sampath *et al.*, 1987; Hammond *et al.*, 1991) results in induction of fibrovascular tissue with no evidence of cartilage or bone. TGF-$ß_2$ was also not active in the *in vivo* bioassay (Sampath *et al.*, 1987; Bentz *et al.*, 1991). In the present work, the demonstration of osteoinductivity in intramuscular sites of the baboon is the first demonstration of endochondral bone formation induced by TGF-ß. However, the lack of osteoinductive capacity in orthotopic sites of the baboon (Chapter III) gives rise to yet more questions as to the apparent site specific action of TGF-ß.

During endochondral bone formation, the chondrocytes of the cartilage phase intermediate undergo distinct steps of differentiation (Bohme *et al.*, 1995). The resting chondrocytes first proliferate, then they hypertrophy producing collagen X and alkaline phosphatase, mineralisation is followed by vascular invasion, culminating in

endochondral ossification. In contrast, in adult articular cartilage, chondrocytes are arrested in the resting stage, producing collagen II, IX and XI. The mechanism whereby this occurs was of interest to Bohme *et al.* (1995) who used a chick sternum model to study resting chondrocyte populations versus hypertrophying chondrocyte populations. In the chicken, the cranial part of the sternum is known to be fated to ossify in adolescence, whereas the caudal part remains cartilaginous until adulthood. In effect, the developing chick sternum comprises a heterogeneous population of cells resembling those of growth plates at various stages of late differentiation. Bohme *et al.* (1995) found that caudal cells were able to suppress, in coculture, the maturation of cranial cells, leading them to postulate that the caudal cells produce diffusible inhibitors of chondrocyte hypertrophy and maturation. They tested TGF-ß and bFGF as candidate inhibitors of cartilage cell hypertrophy and maturation. TGF-ß is produced by chondrocytes and gradients of TGF-ß concentrations exist in growth plates with larger amounts of the factor produced in the hypertrophic zone. In cartilage undergoing endochondral ossification, gradients of basic fibroblast growth factor are formed with an orientation that is inverse to that of TGF-ß concentration gradients. They proposed that TGF-ß and bFGF interact synergistically to suppress maturation of cranial cells in culture, leading them to postulate that these factors are important in regulating cartilage homeostasis (Bohme *et al.*, 1995).

The development of the heterotopic bioassay for bone inducing factors has been crucial for the design of experiments aimed to glean insights into the mechanisms and

nature of bone induction. Sampath *et al.* (1992) studied parameters of bone generated in heterotopic sites of the rat by implants of rhOP-1 of different doses delivered with insoluble collagenous bone matrix as carrier, and led them to conclude the following:

> OP-1 induces bone in a **dose dependent** manner as determined by calcium content and specific alkaline phosphatase activity
>
> The response to dose reaches a **plateau** beyond which the calcium content per milligram newly induced tissue does not change
>
> the **size** of the newly formed bone is dependent upon the volume of the initial implant
>
> higher doses of OP-1 increase the **rate** and **temporal** sequence of the bone induction cascade
>
> higher doses of OP-1 lead to increased rate of bone **remodelling** and to earlier **resorption** of the carrier insoluble collagenous matrix

These concepts are critical when therapeutic osteogenic devices are to be designed. Considerations as to the speed of osteogenesis, amount of regenerated tissue that is required and the doses of morphogen to use are all of critical importance. In work performed by Volek-Smith and Urist (1996) using rhBMP-2 implanted intramuscularly in rats, they and showed dose dependent changes in regenerated bone area, alkaline phosphatase activity and histomorphometric parameters of cartilage, osteoid and bone. Wang *et al.* (1990) also showed that rhBMP-2 loaded onto bone matrix as carrier induces bone formation in the rat ectopic assay. Higher doses of the morphogen yielded earlier cartilage and bone formation. Yu *et al.* (1991) followed the temporal pattern of gene expression of typical markers of newly induced bone, and

reported an increase in steady-state levels of the chondrogenic marker type II collagen on day 5 and peaking on day 7, which then decreased rapidly to undetectable levels on day 9, at a time coinciding with the calcification of the cartilage as a prelude to osteoblastic differentiation. Type IX collagen, also a marker of cartilage, appeared at high levels on day 7, and diminished by day 9, leading to the conclusion that type IX collagen is a late marker for chondrogenesis. Fibronectin mRNA, coding for the important cell attachment factor, was most highly expressed during mesenchymal cell proliferation and attachment to the implanted matrix. Peaks occurred during early chondrogenesis, and during haematopoeisis. Integrin mRNA was continuously expressed throughout the 21-day study period. Type I collagen mRNA expression was detectable as early as day 1, and rose steadily throughout the 21-day period of the study (Yu *et al.*, 1991). In primate models, the chromatographic adsorption of native BMPs onto porous hydroxyapatite generated new bone in intramuscular sites of *Papio ursinus* (Ripamonti *et al.*, 1993). Bone also formed when collagenous matrix was used (Ripamonti *et al.*, 1992). Notably, porous hydroxyapatites were capable of spontaneous bone induction without exogenous BMPs, pointing to a possible endogenous adsorption of circulating BMPs to the hydroxyapatite, eliciting bone formation by day 60 (Ripamonti *et al.*, 1993).

An aspect of paramount importance relates to the development of suitable carrier materials for delivery of BMPs. There are disadvantages related to currently available delivery systems, primarily due to unsuitable physical characteristics. An

ideal biomaterial for tissue engineering of bone should be non-immunogenic, carvable, and amenable to contouring for optimal adaptation to the various shapes of bone defects, providing mechanical support when needed. Most importantly, it should initiate optimal osteogenic activity with relatively low doses of BMPs/OPs, and it should also promote rapid vascular and mesenchymal cell invasion. In addition it should remodel and resorb once the regenerative processes are under way. The geometrical configuration of the substratum is also of critical importance. In rodent subcutaneous experiments using hydroxyapatites pretreated with BMPs, bone did not form with granular forms of hydroxyapatite (Ripamonti *et al.*, 1992), but was observed only in porous hydroxyapatites of block configuration. The critical role of the geometry of the substratum in the regulation of cell growth and endochondral bone differentiation has been reported previously using different geometric configurations of collagenous matrix, indicating that the endochondral sequence can be greatly altered by the geometry of the inductor (Reddi, 1974; Sampath and Reddi, 1984).

During development and adult life, osteoblasts and osteoclasts continuously replace old bone with new bone through the process of bone remodelling (reviewed by Parfitt, 1994). The cycles of resorption and bone deposition are believed to be tightly linked, thereby maintaining skeletal integrity, bone mass and shape. Evidence accumulated to date suggests that secreted TGF-ß could be involved in the local regulation of skeletal development and turnover (Centrella *et al.*, 1994). Generally, TGF-ß has been shown to inhibit the growth and phenotypic expression of osteoblasts grown *in vitro* (Noda

and Rodan, 1986; Harris *et al.,* 1994), but can act as a potent chemoattractant for osteoblasts (Pfeilschifter *et al.,* 1990). Injection of TGF-ß periosteally has been shown to stimulate cartilage and bone formation (Noda and Camilliere 1989; Joyce *et al.*, 1990). A single application of TGF-ß results in complete healing of critical size skull defects in rabbits (Beck *et al.,* 1991). The authors postulated that TGF-ß stimulates the recruitment and proliferation of osteoblasts to the defect site, and that an increased number of osteoblasts were responsible for new bone formation. Matrix secretion, however, was not affected by exogenous application of TGF-ß (Beck *et al.*, 1991).

In vitro, TGF-$ß_1$ significantly enhanced DNA synthesis in cultured articular chondrocytes at levels 3-fold higher than that of BMP-4. TGF-$ß_1$ was also more potent than BMP-4 in enhancing proteoglycan synthesis in these cultures (Luyten *et al.,* 1994). *In vitro*, TGF-ß induces extracellular matrix secretion by osteoblasts, inhibits matrix mineralisation and modulates osteoprogenitor cell proliferation and the expression of osteoblastic differentiation markers (Centrella *et al.*, 1994). In embryonic bone organ cultures of mouse metatarsal long bones, OP-1 stimulated cartilage growth of bone ends, caused partly by differentiation of perichondrial cells into chondrocytes, resulting in increased appositional growth (Dieudonne *et al.,* 1994). In contrast, TGF-$ß_1$ and TGF-$ß_2$ inhibited cartilage growth and reduced the length of whole bone rudiments compared with controls. In the ossifying centre of the bone collar, both OP-1 and TGF-ß inhibited cartilage hypertrophy, growth of the bone collar and matrix mineralisation. The interpretation was that OP-1 and TGF-ß exhibit

opposite effects on cartilage growth but similar effects on osteogenesis in the model used (Dieudonne *et al.,* 1994). TGF-$ß_1$ was shown to enhance chondrogenesis in periosteal explants cultured in agarose medium in a dose dependent manner. Higher doses induce chondrogenesis in control fascia lata explants. It was concluded that TGF-$ß_1$ can induce differentiation towards cartilage production as well as enhance it once it has been initiated (Miura *et al.*, 1994). Generally, results have varied substantially, depending on the cell system used. The precise role of TGF-ß has been hard to infer from these studies. Besides its complex and variable effects on bone cell populations *in vivo* and *in vitro*, a given experimental result with TGF-ß may be potentially relevant to many different aspects of skeletal morphogenesis, including the generation of bone shape, bone growth or bone remodelling.

Systemic injection of TGF-$ß_2$ leads to generalised increase in osteoblastic activity (Rosen *et al.,* 1994). Systemic administration of TGF-$ß_2$ also prevented the impaired bone formation and osteopenia induced by unloading in rats (Machwate *et al.,* 1995). Unloading, or the process of removing of weight bearing on the skeleton or parts thereof, has been associated with inhibition of bone formation (Globus *et al.,* 1986). Machwate *et al.* (1995) induced osteopenia in rats and then administered TGF-$ß_2$ by systemic infusion. This resulted in the prevention of the decrease in metaphyseal bone and osteoid volume, of metaphyseal bone weight and calcium content and bone protein content. In control rats that were not subjected to unloading, no changes in the above parameters were measured.

Additional insights into *in vivo* roles of TGF-ß came from experiments conducted by Erlebacher and Derynck (1996). Their model of a TGF-$ß_2$ overexpressing transgenic mouse showed that the animal suffered a dramatic age-dependent loss of bone mass. They attributed this effect to a primary defect in bone remodelling, associated with increased activities of both the osteoblastic and osteoclastic cells. It was suggested that the increase in bone turnover caused age dependent bone loss as a result of a net imbalance between bone resorption and formation. This indicated that TGF-ß2 may co-ordinate simultaneously osteoblastic and osteoclastic activities (Erlebacher and Derynck, 1996). The mineralisation defect observed in the transgenic animals suggests that TGF-$ß_2$ may negatively regulate bone matrix mineralisation *in vivo*. These conflicting results suggest that the target cells of TGF-ß might not be differentiated osteoblasts (Mizuno and Kuboki, 1995). Interestingly, the TGF-$ß_2$ gene was inserted under the control of the osteocalcin promoter. Since osteocalcin is of the most abundant non-collagenous extracellular protein in the bone matrix, the strategy leads to the overexpression of the TGF-$ß_2$ protein. Osteocalcin was previously thought to be positively correlated with mineralisation events of bone. Recently however, osteocalcin was instead shown to be an inhibitor of bone formation *in vivo* (Ducy *et al.*, 1996). Previously, TGF-$ß_1$ was shown to inhibit osteocalcin synthesis. The finding that exogenous application of TGF-$ß_2$ leads to increased bone deposition, and the prevention of the osteoporotic phenotype in unloaded rats (Machwate *et al.*, 1995), whilst the endogenous product leads to an osteoporotic phenotype is interesting indeed. If osteocalcin is an inhibitor of bone formation, then driving the

TGF-β_2 gene under the osteocalcin promoter may not be a good idea, since the expression of osteocalcin may coincide temporally with the inhibition of bone formation *in vivo*. Either TGF-β_2 is unable to overcome this inhibition, or else it increases bone remodelling in the direction of mineral loss.

Van Vlasselaer *et al.* (1994) suggested that TGF-ß might promote "uncommitted" cells to osteogenic cells, implying that the target cells of TGF-ß might be undifferentiated cells. Data of Mizuno and Kuboki (1994) support this, and further indicate that collagen and TGF-ß might be implicated in the recruitment of osteoblasts during embryogenesis and repair of bone. Hasegawa *et al.* (1994) demonstrated that a type I collagen matrix induced the differentiation of bone marrow cells to osteoblasts *in vitro*. Mizuno and Kuboki (1995) demonstrated that this activity was enhanced by TGF-β_1. Bone marrow cells cultured on collagen matrix including 2 ng/ml TGF-ß were temporally stimulated in their formation of mineralised nodules. Osteocalcin levels were increased four-fold as compared to control cultures lacking TGF-β_1. This indicated that differentiation of the marrow cells to osteoblasts was accelerated by the presence of TGF-β_1. Calcium contents of the matrix had also increased two-fold higher when compared to control cultures lacking TGF-β_1. This indicated a more intense mineralisation, and that the marrow cells cultured in TGF-β_1 containing matrix, differentiated to osteoblasts faster than those on the collagen matrix alone. Alkaline phosphatase activity peaked on day 10 for TGF-β_1 containing cultures as opposed to day 15 for control cultures, again implying that TGF-β_1

accelerated the effect of the collagen matrix on bone marrow cells (Mizuno and Kuboki, 1995).

1.2.4.3 Molecular characteristics of TGF-ß

The TGF-ßs occur as disulphide-linked dimers of 12 500 dalton subunits. Both homodimers and heterodimers can occur (Centrella *et al.*, 1994). Active TGF-ß is a 25 kDa dimer, which contains 9 cysteine residues. Seven of these are conserved within members of the TGF-ß superfamily. Overall, the mature region of TGF-$ß_3$ has approximately 80% identity to the mature regions of TGF-$ß_1$ and TGF-$ß_2$. The precursor regions of these three molecules share only 27% sequence identity (ten Dijke *et al.* 1988; Derynck *et al.* 1988). These proteins are synthesised as large precursor proteins that undergo proteolytic processing at RXXR sites to yield mature active dimers of disulphide-linked monomers. Each monomer contains a conserved C-terminal 7-cysteine domain with 20% to 92% sequence identity amongst superfamily members (Kingsley, 1994).

The molecular structure of TGF-$ß_2$ has been determined at high resolution by x-ray crystallography (Daopin *et al.*, 1992, Schlunegger and Grutter, 1992). These studies reveal several unique features: the dimer has an extended rather that a compact, globular conformation. Eight of the nine cysteine residues in each monomer chain are involved in an unusual, compact pattern of intrachain disulphide bridges dubbed the "TGF-ß knot". There is only one interchain disulphide bridge, suggesting that hydrophobic interactions between the two chains are of major importance in stabilising the dimer. Furthermore, there are two cavities, accessible to water, between the hydrophobic cores in the interface area. The functional implications of

this unusual hydrophilic area in the interior of the molecule are not clear at present. Nuclear magnetic resonance studies of TGF-ß in solution may suggest that the factor may exist in several conformations.

TGF-ß is mostly synthesised in an inactive form as a pre-pro monomeric protein and is cleaved to yield a 112 amino acid polypeptide that remains associated with a latent (pro) portion of the molecule (Lyons and Moses, 1990). In most cell types, the latent TGF-ß complex also contains a protein named the TGF-ß binding protein which is covalently bound to the latency associated peptide *via* a disluphide bridge. Bone cells are unique in that they produce two latent forms of TGF-ß, one which contains TGF-ß binding protein and one which does not. The precise function of the TGF-ß binding protein is unknown, but it has been reported to form long fibrillar strands in cultures of mineralising foetal rat bone cells. The authors postulate that in these cultures, the fibrillar strands may play a role in initiating and directing new nodule formation (Bonewald and Dallas, 1994). Biologically active TGF-ß results from dimerisation of the monomers (most abundant are homodimers) and release of the latent peptide portion. Activation of latent TGF-ß has been demonstrated for macrophages, osteoclast and osteoblast-like cells. The matrix proteoglycan, decorin, can bind TGF-ß thereby inactivating the molecule (Border and Ruoslahti, 1992).

1.2.4.4 Molecular characteristics of BMPs/OPs

On the basis of characteristics that include amino acid similarity and tertiary structure characteristics, the BMPs/OPs are grouped as a family within the TGF-ß superfamily. The BMPs comprise a growing family of more than 14 proteins, 9 of which have been shown when expressed recombinantly, to singly induce heterotopic bone formation *in vivo*. All but BMP-1 are members of the TGF-ß superfamily. BMP-1 is in fact a misnamed protease (Reddi, 1996). Its real function is that of a procollagenase (Kessler *et al.*, 1996), and is more correctly called procollagen C-proteinase, functioning *in vivo* for the proper assembly of collagen within the extracellular matrix. The supramolecular self assembly of triple-helical collagen is triggered by the processing of COOH-terminal procollagen peptide by the newly discovered function of BMP-1, placing BMP-1 in an essential control point in morphogenesis (Reddi, 1996).

The elucidation of the OP-1 structure (Griffith *et al.*, 1996) confirmed the proposal that the TGF-ß fold is prototypical for the conserved C-terminal region of the TGF-ß superfamily, and that moreover, all TGF-ß superfamily members share the BMP/OP/TGF-ß structural motif. Interestingly, by aligning the conserved C-terminal 7-cysteine domain of a number of TGF-ß superfamily proteins, they concluded that the conformation of the OP-1 omega loop is more characteristic of the superfamily as a whole. The omega loop is a structural feature of a specific secondary structure-forming segment of TGF-ß-superfamily members. Moreover, scrutiny of the

structure/function relationship of amongst these factors leads to the conclusion that BMPs are phylogenetically more ancient than TGF-ßs. This gives one reason to suggest that the TGF-ß superfamily should be renamed to BMP-superfamily.

On the basis of their primary amino acid sequences, BMP-2 through BMP-8 may be grouped into 3 separate sets. BMP-3 is the sole member of its subset, sharing 43% to 49% identity with each of the other subsets (Luyten *et al.*, 1989). BMP-5, -6 and –7 (OP-1) possess an average of 89% amino acid identity with respect to each other, constituting together a separate subset. BMP-2 and BMP-4 are the most closely related, to the order of 92 % amino acid identity in their carboxy-terminal regions. In similarity with TGF-ß superfamily members, the BMPs are synthesised with an amino-terminal propeptide region that is later cleaved off. Mature BMP, lacking this propeptide region, is secreted in an active form. Dimerisation and molecular maturation seem to occur intracellularly, or on secretion (Israel *et al.*, 1992).

1.2.4.5 A case for a structural superfamily

Knowledge of the three dimensional structure of proteins can provide important insights into their evolutionary relationship. Proteins may evolve from a common ancestor to a point at which they no longer share significant overall sequence homology, but their evolutionary relatedness may still be evident from a structural comparison. Hence nerve growth factor, TGF-$ß_1$ and platelet derived growth factor all share the common feature of dimeric forms linked by a cluster of disulphide bridges, named as the cysteine knot motif by McDonald and Hendrickson (1993). Recently *lefty*, a new divergent form of the TGF-ß superfamily was identified which encodes a morphogen for left-right determination during development. It possesses a cysteine knot motif characteristic of the TGF-ß superfamily and is secreted in a processed form of approximately 25-31 kDa (Meno *et al.*, 1996).

Crystallographic studies have revealed a novel three-dimensional fold comprising a unique clustering of three cysteine bridges in the three-dimensional space of nerve growth factor (McDonald *et al.*, 1991). Similar folds were observed for TGF-$ß_2$ (Daopin *et al.*, 1992) and for platelet derived growth factor-BB (Oefner *et al.*, 1992). The three cysteine bridges of nerve growth factor have been shown to have topological equivalents in TGF-ß and platelet derived growth factor-BB: both TGF-$ß_2$ and platelet derived growth factor-BB form 8-membered cysteine rings through which the third disulphide bridge penetrates. Superposing the conserved half-cysteines of nerve growth factor and TGF-$ß_2$ indicates very similar arrangement for the two

molecules (McDonald and Hendrickson, 1993). Another common feature is the four extended segments of twisted antiparallel ß strand that result in an elongated, asymmetrical shaped protomer. The common ß-strand structure and conserved cysteine knot motif within each protomer argue that these growth factors have undergone a divergent evolutionary process from a common ancestral molecule. From a functional viewpoint, these three molecules appear to have little in common beyond their ability to induce a biological response by binding to a specific cell surface receptor kinase. These factors belong to distinct families, which were not previously thought to be functionally or structurally related, as their biological roles are distinct and no significant sequence similarity was evident. NGF is a member of the neurotrophin family, playing a key role in the survival of certain neuronal populations in the peripheral and central nervous system (Bradshaw *et al.*, 1993). PDGF is the major serum mitogen for cells of mesenchymal origin (Heldin *et al.*, 1992). Given their distant relatedness based on structural similarity of their protomers, it is intriguing when comparing the respective regions responsible for receptor binding. Mutagenesis of NGF, TGF-ß and PDGF-BB has localised key receptor binding determinants on each (Ibanez *et al.*, 1992, 1993; Qian *et al.*, 1992). These studies suggest that the structurally non-conserved, variable regions of each molecule contain the receptor-binding determinants for each ligand. The determinants are therefore specific for each ligand. However, scrutiny of the positional location of the receptor binding determinants seems to indicate that they are topologically conserved between the three molecules. It would be interesting to see the outcome of similar studies involving members of the BMP family.

The dimeric nature of these molecules may play a key role in the mode of signal transduction. Ligand-induced receptor oligomerisation is thought to initiate signal transduction, leading to phosphorylation of the active receptor (Ullrich and Schlessinger, 1991). Receptor dimerisation has been observed for NGF receptors (Grob and Bothwell, 1983; Meakin and Shooter, 1991), for TGF-ß (Wrana *et al.*, 1992), for the PDGF receptors (Heldin *et al.*, 1992) and for the BMP receptors (Rozenweig *et al.*, 1995; Nohno *et al.*, 1995; Liu *et al.*, 1995).

In conclusion, structural considerations of NGF, TGF-ß and PDGF and BMP have revealed that the prototypical members of supposedly different families adopt a similar protomeric fold. On this basis they form a structural superfamily (McDonald and Hendrickson, 1993).

1.2.4.6 Receptors of the transforming growth factor-ß superfamily

A number of TGF-$ß_1$ binding proteins have been identified, mainly through crosslinking studies involving radioactively labeled TGF-$ß_1$ (ligand) and a variety of *in vitro* membrane receptor labeling assays. With binding constants in the nanomolar range, all these proteins seem to be important intermediaries between cells and TGF-ßs. However, only some of these binding proteins have to date been shown to act as true receptors, acting to convey the signal across the cell membrane resulting in the elicitation of a gene response. The most widely distributed of these are proteins of 53 kDa and 70 kDa, named TGF-ß type I and II receptors, and designated TßR-I and TßR-II respectively, according to their size. Sets of specific type I and II receptors have also been identified for the BMPs and the activins, and it is now recognised that TGF-ßs, BMPs and activins each bind to type I and type II receptors of approximately 55 kDa and 70 kDa (Liu *et al.*, 1994). Generally speaking, type I and type II receptors are glycoproteins that appear to cooperate in the mediation of multiple TGF-ß responses. The overall structures of TßR-I and TßR-II are similar and each consist of a relatively short cysteine-rich extracellular domain, followed by a single transmembrane domain and a protein kinase domain with a specificity towards serine/threonine residues. The type I receptor kinase domains of the respective TGF-ß superfamily members show greater similarity amongst themselves when compared to the type II receptor kinase domains, with which they show less than 10% amino acid sequence identity. The type I receptors share various other structural features not found in the type II receptors, including the spacing of cysteines in the extracellular region and a highly conserved serine- and glycine-rich segment adjacent to the amino-

terminal boundary of the kinase domain. The serine/threonine kinase domains of TßR-I and TßR-II have 41% amino acid sequence similarity and within the kinase domains two short inserts without similarity to other kinases can be found. TßR-I has a short C-terminal tail of five amino acid residues, whereas that of TßR-II is longer and consists of 24 amino acid residues. TßR-I and TßR-II can also be distinguished by the presence of a region rich in serine and threonine residues preceding the kinase domain in TßR-I but not TßR-II. This 30 amino acid region, termed the GS domain, contains the core sequence SGSGSG in the middle, and it is highly conserved among type I receptors for proteins in the TGF-ß superfamily (Kingsley, 1994; Wrana *et al*, 1994; ten Dijke, 1994). The currently favoured model for mechanism of signal transduction through the receptor system is one of ligand induced receptor dimerisation, leading to the association of ligand with a receptor type I-type II complex which then becomes activated leading to downstream signal transduction.

A third TGF-ß binding protein, betaglycan, is a membrane proteoglycan with a core protein of approximately 110 kDa that carries chondroitin sulphate and heparan sulphate glycosaminoglycan chains. Betaglycan has been found to bind TGF-$ß_1$ *via* its core protein and to basic fibroblast growth factor *via* its heparan sulphate chain. Betaglycan also exists in a released form that can be found in the extracellular matrix and serum, binding TGF-ß with similar affinities as the membrane-associated form (Massague, 1990). The integral core protein is comprised of 853 amino acids having a large extracellular domain and a relatively short, 43 amino acid cytoplasmic tail.

There is a 70 % identity between the cytoplasmic and transmembrane domain of betaglycan and endoglin, a protein expressed at highest levels in endothelial cells, and implicated in cell-cell interactions. The extracellular domains of betaglycan and endoglin have little resemblance. The cytoplasmic domain of betaglycan is rich in serines and threonines, some of which might act as regulating phosphorylation sites (Lopez-Cassilas, 1991).

A number of hypotheses have been put forward as to the action of betaglycan. Betaglycan could act as a component of the two-receptor system, presenting TGF-ß and FGF to their respective signalling receptors (Massague *et al.*, 1992). Betaglycan could also act as a reservoir for TGF-ß, releasing TGF-ß to type I and type II receptors, which have a significantly higher affinity for TGF-ß than does betaglycan. The precise function of betaglycan is however not known, and signalling activity has so far not been shown.

In addition, some cells express a set of membrane proteins that exclusively either bind TGF-$ß_1$ or TGF-$ß_2$ (Cheifetz and Massague, 1991). Bovine heart endothelial cells express TGF-$ß_1$ binding proteins of 90 kDa and 170 kDa that have high affinity for TGF-$ß_1$ but not TGF-$ß_2$, as well as binding proteins of 140 kDa and 60 kDa that bind TGF-$ß_2$ but not TGF-$ß_1$. Three of the isoform restricted binding proteins, those of 60, 140 and 170 kDa, are bound to the membrane by means of a phosphatidylinositol glycan anchor, as suggested by the ability of a PI-specific phospholipase C to release

them from the cell surface. The 90 kDa complex is part of a disulphide-linked 180-kDa complex that is resistant to phospholipase C. Bovine heart endothelial cells lack betaglycan. The possibility therefore arises that betaglycan and the isoform restricted binding proteins may function as regulators of cell access to TGF-ß (Cheifetz and Massague, 1991).

Mechanism of activation of the TGF-ß receptor system

Genetic evidence from cell mutants suggests that TGF-$ß_1$ binding to receptor I requires the presence of receptor II, and furthermore that both receptors are required for signalling in any response (Laiho *et al.,* 1991). This mechanism of ligand induced dimerisation appears to be shared by receptors of other TGF-ß superfamily members (Carcamo *et al.,* 1994). Studies with TGF-ß and cloned type I receptors have consistently demonstrated their inability to bind ligand in the absence of type II receptors (Ebner *et al.,* 1993, Attisano *et al.,* 1993, Wrana *et al.* 1994) and the failure of the latter to signal in the absence of type I receptors (Wrana *et al.,* 1992). Another feature of this system is the ability of type II receptor to interact with different type I receptor isoforms. Thus, the TGF-ß type II receptor, TßR-II, can interact with at least 2 type I receptors, called TßR-I or ALK-5 (Franzen *et al.,* 1993) or R4 (Bassing *et al.,* 1994), and TSR-I (Attisano *et al.*, 1993). The activin type II receptors ActR-II and ActR-IIB can interact with at least three distinct activin type I receptors (ten Dijke *et al.,* 1994). It has been suggested that the specificity of the biological response to

ligand in a given cell type appears to be defined by the particular type I receptor engaged in the complex, thus providing a basis for the multifunctional nature of these morphogens (Carcamo *et al.*, 1994).

The early signalling events triggered by TGF-ß involve TßR-II, a constitutively active kinase which uses the ligand, TGF-ß, to recruit, phosphorylate and signal through TßR-I, thus generating the first step of a TGF-ß signalling pathway (Wrana *et al.*, 1994). The TGF-ß type II receptor is constitutively autophosphorylated and ligand plays no appreciable change in this activity, suggesting that this is a general feature of type II serine/threonine kinase receptors. Type I receptor phosphorylation occurs on serine and threonine residues and is mediated by receptor II. Hence receptor type II can be thought of as a type I receptor kinase, and receptor I as the propagator of the signal to substrates downstream of the TGF-ß receptor complex. Consistent with this model, the nature of the biological response to ligand in both TGF-ß and activin systems is specified primarily by the type I receptor isoform that is engaged in the complex. Type I receptors are unable to bind ligand free in the medium. However, receptor type I can recognise ligand bound to type II receptor to form a stable ternary complex. The formation of this complex is tightly correlated with signalling (Wrana *et al.*, 1994).

Proteolytic studies of radiolabeled receptor complexes revealed that only the GS domain, a region highly conserved in type I receptors from Drosophila through to

humans was phosphorylated *in vivo* (Wrana *et al.,* 1994). Mutations in the GS domain which prevented phosphorylation of critical threonine and serine residues resulted in a mutant type I receptor able to form complexes with type II receptor, and to bind TGF-ß, but which did not induce gene expression. Thus, phosphorylation of receptor type I by type II is an essential step in the TGF-$ß_1$ signalling pathway (Wrana *et al.,* 1994). In particular, it was found that the signalling activity of TßR-I does not depend on any particular serine residue in the GS domain, but rather on how many of the serine residues in the region are intact (Franzen *et al.,* 1995). Mutation of two or more of the GS domain residues impairs signalling and phosphorylation activity (Wieser *et al*,1995). Replacement of a threonine residue, one of two located near the canonical kinase domain with aspartic acid, yields a product with elevated *in vitro* kinase activity and signals anti-proliferative and transcriptional responses in the absence of ligand and TßR-II (Wieser *et al*, 1995).

Receptors for BMPs/OPs

Essentially, the same principles pertaining to TGF-ß receptors apply to BMP receptors. BMPs exert their effects through interaction with type I and type II receptors of approximately 53 kDa and 70 kDa respectively. A series of serine/threonine kinase receptors, the activin receptor-like kinase series designated ALK-1 through -6, (Franzen *et al.* 1993; ten Dijke *et al.* 1994) have been shown to serve as type I receptors for members of the TGF-ß superfamily. ALK-5 is a TGF-ß

type I receptor also designated TßR-I (Franzen *et al.,* 1993) and ALK-2 (ActR-I) and ALK-4 (Act R-IB) are activin type I receptors (Ebner *et al.*,1993A, 1993B; Attisano *et al.*, 1993). ALK-3 and ALK-6 have been shown to be to be type I receptors for members of the BMP family, and are named BMPR-I and BMPR-IB respectively (ten Dijke *et al.,* 1994). BMPR-I and BMPR-IB can bind OP-1 and BMP-4 in the presence of Daf-4, a protein from *Caenorhabditis elegans* which serves as a type II receptor in hybrid experimental receptor complex systems (ten Dijke *et al.*, 1994). Other components of the receptor system, namely the type II receptors were cloned by Liu *et al.* (1995) and Rosenzweig *et al.* (1995) and named BMPR-II. BMPR-II is a transmembrane serine/threonine kinase that binds BMP-2 and OP-1 (BMP-7) and, though weakly, BMP-4 (Rosenzweig *et al.*, 1995). Binding is observed in association with multiple type I receptors, including BMPR-IA, BMPR-IB and ActR-I, which is also an activin type I receptor. The combinatorial nature of these receptors and their capacity to crosstalk with the activin receptor system may explain, at least in part, the multifunctional nature of their ligands. The BMP type II receptor appears to be distantly related to the DAF-4 type II receptor from *Caenorhabditis elegans.* In mammalian cells, the interaction of BMPR-II is restricted to BMP type I receptors and is ligand dependent. Although BMPR-II can bind ligand on its own, binding is enhanced by type I receptors, and is a requirement to effect optimal signal transduction. A type II receptor for the BMP-4 transduction system was cloned by Nohno *et al* (1995). BRK-3 which is expressed in a variety of adult tissues, optimally binds BMP-4 only in the presence of BMP type I receptors, much like the BMPR-II and OP-1/BMP-2 system.

Insights as to the function of BMP receptors in early embryogenesis were made by utilising functionally defective mutants of the BMP-4 type II receptor (Maeno *et al.*, 1994; Suzuki *et al.*, 1994). These defective receptors, when expressed as dominant-negatives in the *Xenopus* embryos effectively block the signalling pathway of BMP-4 and BMP-2. Expression of the defective receptor in ventral blastomeres caused their respecification to dorsal mesoderm, suggesting that BMP-4 and -2 are involved in dorsal-ventral specification, and that ventral fate in the embryo requires induction rather than resulting from the absence of dorsal specification (Suzuki *et al.*, 1994). Similarly, expression of the defective receptor in the ventral marginal cells at the two-cell stage in *Xenopus* embryos caused the respecification to a dorsal phenotype of a tissue that is fated to be a "mesenchyme" ball containing blood cells.

Downstream substrates of BMPs/OPs' and TGF-ßs' receptors

More recently, the understanding of the intracellular pathways by which signals of the TGF-ß superfamily members are mediated, has been spurred by studies of the SMAD family of signal transducers (reviewed by Whitman, 1997). Discovered through genetic screens in Drosophila melanogaster and Caenorhabditis elegans, the biochemistry and cell biology of vertebrate SMADs has implicated them as regulators of the cell-specific transcriptional responses that are induced by TGF-ß superfamily members. The *Mad* (mothers against decapentaplegic) gene in Drosophila and the related *Sma* genes from *Caenorhabditis elegans* have been genetically implicated in signalling by members of the BMP subfamily (Sekelsky *et al.*, 1995; Savage *et al.*, 1996). Liu *et al.* (1996) used information from the *Mad* and *Sma* genes to clone a human homologue designated *Smad1*. Subsequently, a growing family of vertebrate homologues has been identified, designated, to date, as Smad1 to Smad7. Smad1 and, probably, Smad5 mainly act downstream of receptors of the BMPs/OPs. Smad2, and possibly, Smad3 act downstream of receptors binding several other ligands, including TGF-ß itself. Smad proteins are phosphorylated by their cognate type I upstream receptors. Phosphorylated Smads can each form stable complexes with Smad4, which is found in the signalling pathways of all the different classes of TGF-ß superfamily ligands. This complex then translocates to the nucleus, where it regulates transcriptional responses to ligands (Kretzschmar *et al.*, 1997). A good example is Smad1 which moves into the nucleus in response to BMP-4 signal (Liu *et al.*, 1996).

Microinjection of *Smad1* messenger RNA into Xenopus embryo animal caps mimics the mesoderm ventralising effects of BMP-4 (Liu *et al.*, 1996). It was shown further that Smad1 encodes transcriptional activators, and this activity which is located in the C-terminal domain is unmasked upon removal of the N-terminal domain, and is stimulated by BMP-receptor-mediated signals. BMP-4 stimulates Smad1 phosphorylation, but how this regulates transcriptional activity of Smad1 is not clear (Liu *et al.*, 1996).

Recently, an inhibitory class of SMADs were reported, Smad6 and Smad7 (Imamura *et al.*, 1997; Nakao *et al.*, 1997; Hayashi *et al.*, 1997). These Smads inhibit the SMAD-based signalling pathway described above. Smad6 and Smad7 can inhibit both TGF-ß and BMP signalling in cultured cells or in frog embryos (Imamura *et al.*, 1997; Nakao *et al.*, 1997; Hayashi *et al.*, 1997). The product of the *Daughters against decapentaplegic (Dad)* gene is also an inhibitory Smad, acting in the homologous signalling pathway in Drosophila (Tsuneizumi *et al.*, 1997). The *Dad* gene inhibits patterning by decapentaplegic, a Drosophila BMP homologue, in the Drosophila imaginal wing disk (Tsuneizumi *et al.*, 1997).

The *in vitro* gene responses elicited by TGF-ß are numerous, and include the suppression of c-*myc* correlating to growth suppression and inhibition (Moses *et al.* 1990), and inhibition of cyclin dependent kinases (Koff *et al.*, 1993; Ewen *et al.*, 1993; Polyak *et al* , 1994). The steps between receptor binding and these nuclear

events are yet to be fully elucidated. Halstead *et al.* (1995) used a TGF-ß -responsive promoter linked to a reporter gene in a human lung carcinoma cell model to provide evidence that phosphatidylcholine-specific phospholipase C and protein kinase C may be early intermediates in the TGF-ß signalling pathways. Luo *et al.* (1995) have given insights into the specificity of the TGF-ß receptor kinases by experimenting with a spatially addressable combinatorial peptide library, immobilised on a hydrophilic matrix. The identification of the element peptide motif being recognised by a kinase is an essential first step in understanding the mechanism of its signal transduction, as it provides insights into its biological target or targets. Using the above system, the optimal substrate peptide was found to be identical for both TßR-I and TßR-II, its amino acid motif being KKKKKK(S/T)XXX. This is surprising as it is currently supported that the two kinases may play different roles in intracellular signal transduction. The optimal peptide substrate sequence for TßR-I and TßR-II is very similar to the nuclear localisation sequences found in many proteins that migrate from the cytoplasm to the nucleus, such as the STAT proteins (Darnell *et al.*, 1994).

To further the investigation of signalling by TGF-ß, Kawabata *et al.* (1995) have sought to isolate proteins that interact with the cytoplasmic region of TßR-I. One of the proteins identified was the alpha subunit of farnesyl-protein transferase (FT) that modifies a series of proteins including Ras. TßR-I specifically interacts with FT alpha in a yeast two-hybrid model system (Kawabata *et al.*, 1995). Glutathione S-transferase-TßR-*in vitro* fusion proteins were found to bind FT alpha translated *in*

vitro. TßR-I was also found to phosphorylate FT alpha. They further showed that the constitutively active form of the TßR-I receptor was able to make a strong interaction with FT alpha, whereas the inactive form of TßR-I was unable to. The current model of phosphorylation of TßR-I by TßR-II, suggesting that TßR-I is the effector subunit of the receptor complex, which transduces signals to intracellular targets has in effect been confirmed, and shows that a constitutively active TßR-I is able to mediate TGF-$ß_1$ specific cellular responses, in the absence of ligand and TßR-II (Kawabata *et al.*, 1995)

1.2.4.7 Pre-clinical and clinical studies of BMPs/OPs as molecular therapeutics.

Naturally sourced BMPs were first to be tested in applications of osteoinduction for the repair of bony defects in primate models, including humans. The first experiments were reported by the group of Johnson *et al.* (1988, 1988b, 1990). These described their results in treating 47 refractory tibial and femoral nonunions with the use of naturally derived human BMPs. Results showed union with BMP supplementation in patients who had undergone unsuccessful multiple surgical grafting attempts. In the calvarial model of *Papio ursinus*, the efficacy of native BMPs was demonstrated both with porous hydroxyapatite substrata (Ripamonti *et al.*, 1992) and collagenous substrata (Ripamonti *et al.*, 1992, 1993). Naturally derived BMPs were also effective in regenerating cementum, periodontal ligament and alveolar bone in surgically created periodontal defects in the baboon (Ripamonti *et al.*, 1994).

Tissue transformation is another method whereby bone tissue can be formed in combination with a suitable signal. In an experiment by Khouri *et al.* (1991), it was shown that tissue transformation of muscle into bone can be mediated by injection of naturally- derived BMP. This was achieved using vascularised muscle flaps compartmentalised into polymer moulds in the shape of a femur. The result was viable bone tissue in the shape of a rat femur. In a later experiment, calvarial defects in rats were successfully repaired with muscle flap tissue injected with bovine BMP

fractions (Khouri *et al.*, 1996). Again, the injection of BMPs into muscle caused transformation of the tissue into new bone, leading to closure of the defect.

The cloning and expression of recombinant BMPs/OPs made available potentially unlimited quantities of otherwise scarce morphogens. The most obvious proposal for clinical applications of recombinant BMPs/OPs *in vivo* is as molecular initiators of bone and bone marrow regeneration. Ample evidence is accruing on the efficacy and safety of two members of the BMP/OP family now available in recombinant form: hOP-1 and hBMP-2, currently the subject of intensive pre-clinical and clinical research for craniofacial and orthopaedic applications. The craniofacial skeleton develops mostly *via* the intramembranous route of bone formation. Sites investigated for hBMP/OP applications have included the calvaria, mandible and palate, where nonhealing bone defects were surgically created in different animal models, including primates. Carrier biomaterials for delivery of BMPs/OPs have ranged from guanidinium-inactivated insoluble collagenous bone matrix, the synthetic polymer poly (D,L-lactide-*co*-glycolide, PLGA), to sintered porous hydroxyapatite ceramics. hBMP-2 delivered at doses of 5 μg by porous blocks of sintered hydroxyapatite placed subperiosteally on the rabbit cranium resulted in bone formation within the porous spaces of the hydroxyapatite as evaluated histologically by 3 weeks (Ono *et al.*, 1995). hBMP-2 combined with PLGA regenerated critical size defects in the rat calvaria at doses of 10 and 30 μg (Kenley *et al.*, 1994).The PLGA carrier was resorbed by 3 weeks, resulting in restoration of the defects with normal contouring. In

similar experiments, 6.5 μg hBMP-2 delivered by 25 mg of insoluble collagenous matrix, regenerated rat calvarial defects time- and dose-dependently, in a manner which was superior to demineralised bone matrix (Marden, 1994). In the more appropriate primate calvarial model, doses of hOP-1 were used to study the temporal sequence of tissue morphogenesis and the induction of bone in large calvarial defects of adult baboons (Ripamonti *et al.*, 1996), primates which share a remarkable degree of similarity with respect to bone remodelling with man (Schnitzler *et al.*, 1993). Histological and histomorphometric analysis showed that doses of 100 and 500 μg hOP-1 per g of baboon or bovine collagenous matrix as carrier induced complete regeneration of the defects by day 90 (Ripamonti *et al.*, 1996). Osteoblast differentiation, osteoid matrix secretion and mineralization occurred initially at the pericranial aspect of the specimens, followed by endocranial bone differentiation. Whilst chondrogenesis was limited, newly formed bone contained fully differentiated bone marrow elements as early as day 15, even with the 100 μg dose of hOP-1. One year after implantation of hOP-1 there was architectural restoration of the internal and external cortices of the calvaria.

Full thickness critical size defects in the ramus of rat mandibles were treated with hBMP-2 delivered by a PLGA/blood clot composite at doses of 10 μg per 100 μl of delivery vehicle (Linde and Hedner, 1995). Bridging of the defect was achieved by day 12, with voluminous amounts of bone outside the boundary of the defect as seen histologically. Treated sites which were covered with an expanded polytetrafluoroethylene membrane (Gore-Tex) were also bridged with new bone, but

with optimal contouring of the regenerate, indicating that the shape of the newly formed bone may be controlled by suitable segregative devices (Linde and Hedner, 1995). In 2.5 cm full-thickness canine bone defects prepared in the body of edentulous mandibles, hBMP-2 at doses of 250 μg per 500 mg of collagenous matrix, induced bone regenerates which showed 27% relative strength to control hemimandibles at 6 months. Histomorphometric analysis showed that 68% of the defect area treated with hBMP-2 was replaced by new bone (Toriumi *et al.*, 1991). Additional novel applications of interest to craniomaxillofacial surgeons are maxillary sinus augmentations and cleft palate repair. In a goat maxillary sinus floor augmentation model, sites treated with hBMP-2 delivered by a resorbable collagenous sponge showed increased radiopacity when compared to negative controls (Nevins *et al.*, 1996). When applied to surgically created canine maxillary alveolar clefts, however, a dose of 200 μg hBMP-2 delivered by PLGA as carrier was inferior to autogenous bone grafts on day 60, reaching comparable levels on day 120, though hBMP-2 treated defects displayed the least amount of bone formation (Mayer *et al.*, 1996).

Orthopaedic applications of hOP-1 and hBMP-2 have been pursued vigorously in pre-clinical studies. In rodent segmental femoral defects, hBMP-2 at doses of 11 μg delivered by collagenous matrix showed radiographic, histological and mechanical evidence of union by 4.5 weeks (Yasko *et al.*, 1992). In an identical model seeking to determine utility of PLGA as carrier, different particle sizes of the carrier and doses of hBMP-2 were tested in segmental femoral defects of the rat and evaluated at 9 weeks

(Lee *et al.*, 1994). Union incidence and torque failure parameters were dose dependently increased by hBMP-2, achieving bone stiffness comparable to unoperated controls when 247 μm particle size of PLGA were used. In the larger sheep model, segmental osteoperiosteal femoral defects of 2.5 cm were successfully treated with hBMP-2 at doses of 500 μg per g of collagenous matrix, achieving union by day 90 as determined radiographically. Bending strength against contralateral unoperated femurs was found to be superior to autogenous bone graft-treated defects (Gerhart *et al.*, 1994). In subsequent long term studies in the sheep, recanalisation of the medullary cavity with neocortex formation was found to be nearly complete by 52 weeks (Kirker-head *et al.*, 1995).

In a rabbit ulnar defect model, 1.5 cm segmental osteoperiosteal defects were treated with a wide dosage range of hOP-1 delivered by collagenous matrix. Doses in the range of 6 to 400 μg hOP-1 per 125 mg collagenous matrix induced healing within 8 weeks (Cook *et al.*, 1994). In an analogous 8 week model, 2 cm rabbit ulnar defects were treated with different doses of hBMP-2 delivered with PLGA as carrier. There was a dose-dependent response in bone regeneration, with 100% union achieved with 40 μg hBMP-2 per 100 μl of delivery vehicle. The newly formed bone was biomechanically of comparable strength to unoperated control ulnae (Bostrom *et al.*, 1996).

In a similar canine long bone model, 2.5 cm segmental defects were treated with hOP-1 at doses up to 2 500 μg, delivered by 500 mg of collagenous matrix (Cook *et al.*,

1994). hOP-1 induced complete bridging of defects by 8 weeks as determined radiographically, and torsional strength at 12 weeks was, on average, 72% of untreated contralateral sites. Additional parameters of angular deformation to failure and energy absorption to failure were 92% and 67% of controls, respectively, demonstrating the efficacy of hOP-1 (Cook *et al.*, 1994). In African green monkeys, hOP-1 at doses in the range of 250 to 2000 μg per 400 mg of collagenous matrix was implanted into surgically-created 2 cm osteoperiosteal defects in the distal tibiae, and at doses of 1000 μg per 400 mg of collagenous matrix into ulnae (Cook *et al.*, 1995). Radiographic and histological evaluation at 20 weeks revealed that all hOP-1 treated sites underwent new bone formation. Mechanical testing of hOP-1 treated sites showed an average torsional strength to failure of 92 and 69% when compared to contralateral unoperated ulnae and tibiae, respectively. Autogenous bone-treated tibiae showed an average torsional strength of 23% when compared to untreated tibiae, whilst none of the ulnae treated with autogenous bone healed sufficiently for mechanical testing.

In a canine posterior segmental spinal fusion model, hBMP-2 delivered by PLGA/blood clot composite at a dose of 400 μg per 2 cm^2 of delivery system per implant site resulted in equivalent spinal fusion rates as determined by biomechanical testing when compared to autogenous grafts (Muschler *et al.*, 1994). In a canine posterolateral transverse process model, hBMP-2 delivered by an open-cell polylactic acid polymer resulted in 100% fusion rates at 3 months, and was superior to autogenous cortico-cancellous iliac bone grafts (Sandhu *et al.*, 1995). The efficacy of

rhOP-1, delivered by collagenous matrix in a canine spinal fusion model, was evaluated at multiple time periods (Cook *et al.*, 1994). rhOP-1 resulted in stable fusions by 6 weeks post-implantation, reaching complete fusion at 12 weeks, as determined radiographically and histologically. The effective dose was 200 μg per 800 mg of collagenous matrix, allowing a significantly increased development rate of structural and functional stability when compared to autogenous bone grafts.

In a rabbit lumbar intertransverse process arthrodesis model, hBMP-2 resulted in 100% fusion rates by 5 weeks, with superior efficacy to sites treated with autogenous bone grafts as assessed radiographically, histologically, and biomechanically (Schimandler *et al.*, 1995).

Additional *in vivo* roles of hBMPs/OPs for function other than cartilage and bone induction have recently been demonstrated by the induction of dentinogenesis (Rutherford *et al.*, 1993; Nakashima, 1994) and of cementogenesis during regeneration of periodontal wounds in primates (Ripamonti *et al.*, 1996). The accrued data from these extensive pre-clinical studies have enabled both hBMP-2 and hOP-1 to proceed into the arena of clinical trials for both craniofacial and orthopaedic applications. This has followed the pioneering work of Urist and co-workers, who first used bone-derived BMPs for the treatment of refractory femoral and tibial nonunions in humans (Johnson *et al.*, 1988, 1988b, 1990).

The efficacy of recombinant BMPs/OPs in the generation of new bone in numerous animal models bodes well for the future of this route of treatment. There still remain questions however, as to the apparent redundancy of multiple morphogen homologues, all of which are capable of singly initiating new bone formation. The experiments described in this thesis may shed some light on the subject. In addition to a novel function for TGF-$ß_1$, i.e. as inducer of heterotopic endochondral bone formation in the baboon, combinations of rhOP-1 and TGF-$ß_1$ are shown to interact synergistically both in heterotopic and orthotopic sites of the baboon, and to induce large tissue constructs which are temporally and spatially enhanced.

CHAPTER II

2. PURIFICATION OF PORCINE TRANSFORMING GROWTH FACTOR-β_1 AND BOVINE BONE MORPHOGENETIC PROTEIN

2.1 PURIFICATION OF pTGF-β_1

2.1.1 Introduction

For the purpose of *in vivo* experiments in rats, and more specifically in primates, TGF-β_1 is mostly required in milligram quantities. The scarcity of willing donors of this morphogen, together with the unaffordable prices with which this factor is commercially offered at, necessitated that TGF-β_1 be additionally secured *via* purification from natural sources.

The purification of the mammalian TGF-ßs, namely TGF-β_1 , TGF-β_2, TGF-β_3 and the heterodimers TGF-$\beta_{1.2}$ and TGF-$\beta_{2.3}$, from natural sources has been reported (Seyedin, *et al.*, 1985; Assoian, *et al.*, 1983; Roberts, *et al.*, 1990; Yasushi, *et al.*, 1992). With the exception of the report of Assoian *et al.* (1983), all procedures give yields of TGF-ß in the range of µg TGF-ß per kg of tissue, making these procedures unsuitable for this project. Assoian *et al.* (1983) has shown that human platelets are rich in TGF-β_1, to the order of mg TGF-β_1 per kg tissue. Still later, Assoian (1987) improved his purification protocol which involves the extraction of crude TGF-β_1 from fresh human platelets with acidic ethanol. Crude TGF-β_1 is precipitated of

crude, resolubilised in acetic acid, and chromatographed through acrylamide based gel filtration media, firstly under non-denaturing conditions, then under denaturing conditions (Assoian, 1987). This procedure exploits the different apparent molecular weights that TGF-β_1 displays when chromatographed in the presence of solvents differing in their denaturing properties. Chromatography of TGF-β_1 in non-denaturing solvents such as 1M acetic acid results in the aberrant elution of TGF-β_1 at a position corresponding to 15 kDa (Assoian, 1987). Addition of a denaturant to the eluant, such as urea, prevents retarded elution of the TGF-β_1, and it elutes at a position corresponding to 25 kDa (Assoian, 1987). Performing the sequential gel filtration chromatography of TGF-β_1, first under non-denaturing conditions and then under denaturing conditions, effects the purification of TGF-β_1. The first step results in the elution of TGF-β_1 within the low molecular weight range, together with low molecular weight contaminants. In the second step, TGF-β_1 elutes at the higher molecular weight position, allowing for the separation of TGF-β_1 from the lower molecular weight contaminants. The final purification step involves reverse phase high performance liquid chromatography (HPLC) of the morphogen, in yields of 500 µg to 750 µg from 250 units of clinically outdated human platelets (Assoian, 1987).

Van den Eijnen-van Raaij *et al.* (1988) obtained similar quantities of TGF-β_1 from 40 units of clinically outdated platelets. Their procedure is a modification of that of Assoian (1987), and involves the gel chromatography of the resolubilised extract on acrylamide media of higher exclusion limits of 100 kDa as opposed to that of 60 kDa (Assoian, 1983) under non-denaturing conditions. This step is followed by HPLC on

cation-exchange resin, and finally of HPLC on a C18 column. The procedure yielded pure TGF-β_1 as determined by polyacrylamide gel electrophoresis, Western blot analysis, and quantitation using an *in vitro* growth inhibition assay of mink lung epithelial cells (van den Eijnen-van Raaij *et al.*, 1988).

Due to technical constraints in our laboratory, it was decided to adopt, with modifications, the more suitable strategy of Assoian (1987), for the purification of TGF-β_1 from commercially supplied lyophilised porcine platelets (Zymbio a.s., Norway). Modifications included the use of an agarose-acrylamide composite gel filtration matrix (Sephacryl S-100, Pharmacia Biotech, Uppsala, Sweden) of nominal molecular exclusion of 100 kDa. Previous workers have employed the acrylamide based matrices (Bio-Rad, Richmond, California) of exclusion limits of 60 kDa (Assoian, 1987) and 100 kDa (van den Eijnden-van Raaij *et al.*, 1988). These gels however, possess inherent weaknesses in their bead structures, deforming under higher pressures, and flow rates, and thus compromising the performance of the gel matrix. It is imperative for beads to maintain their spherical shape if adequate flow rates are to be achieved, and if resolving power is to be maintained, hence conforming to the criteria of ideal chromatographic media (Pharmacia hand-book, Gel filtration, theory and practice, Uppsala, Sweden, 1993). To alleviate some of these problems, Assoian (1987) describes the use of a coarser, more robust grade of polyacrylamide gel for packing the bottom one-third of the column, and of a finer grade for packing the remaining two-thirds of the column. Coarser grade gels however, have lower

resolving powers than finer grade gels. This column preparation technique is tedious, and prone to error in preparation. Moreover, one is allowing two grades of the material to come into contact with each other with unavoidable mixing, and this excludes any possibilities of repacking of the column should it become necessary.

The composite Sephacryl gel of Pharmacia is a cross-linked copolymer of allyl dextran and N,N-methylenebisacrylamide, and is more robust than its polyacrylamide counterpart. A 100 cm x 6.8 cm column was packed using the fine S-100 material of 100 kDa exclusion limit, and employing a perspex support column designed and manufactured as part of this project. This column exhibited adequate flow rates and resolving power, allowing for the purification of TGF-β_1.

The following describes the isolation of pTGF-β_1 from 50 g of lyophilised porcine platelets which represents, according to the suppliers (Zymbio a.s., Snara, Norway), the equivalent of 250 units of platelets.

2.1.2 MATERIALS AND METHODS

Design and construction of support column

The column and associated components was designed as part of this project, and manufactured in-house by the School of Biology of the university. It comprises the support column of perspex material of 130 cm length, 68 mm internal diameter and 4 mm wall thickness, designed to fit perspex end support plungers of 10 cm in thickness. The support plungers are of two components, designed to be forced together by interconnecting stainless steel bolts, causing the expansion of the 65 mm ring seal of 3.5 mm thickness which serves to press against the column walls creating a watertight seal. The column outlet is surfaced with a 10 μm pore diameter nylon screen, effectively preventing loss of gel matrix material in the eluate. Packing of the gel material is achieved by the temporary fitting of a column reservoir of 120 cm length, one end fitted with a polypropylene adapter housing double ring seals, and capable of a water-tight fit to the support column. Assembled, the packing column and support column together create a packing environment of 2.3 metres in height. At the conclusion of the packing step, the reservoir column is removed and the upper support plunger fitted in place, and connected to the outlet of a peristaltic pump. All components were treated with dichloro-silane to create a water repulsive layer, and to minimise adsorption of proteins.

The column performance was tested by the chromatography of a mixture of BSA fraction 5, trypsinogen and cytochrome c through the column. The column successfully resolved all components. The chromatographic plate number was measured using the following formula (Pharmacia product information guide):

$$N = 5.54 \times (V_e/W_{0.5h})^2 \times 1000/L$$

where N = plate number per metre

V_e = peak elution volume (ml)

$W_{0.5h}$ = peak width at half peak height (ml)

L = length of chromatographic bed (mm)

The value was in the order of 3 800 plates per metre, less than half of that claimed by the manufacturer. Reasons for this may possibly be attributable to sub-optimal chromatographic conditions caused by the denaturing properties of urea which may adversely affect agarose structure. In any case, it was found that the resolution could be significantly improved by recirculating the eluate for an additional round of chromatography through the column.

Extraction solution (acid/ethanol). 490 ml 95% ethanol (EtOH), 10 ml 32% w/v HCl, 43 mg of the protease inhibitor phenylmethylsulphonyl fluoride (PMSF).

Eluant for gel filtration procedure 1. 1 M acetic acid

Eluant for gel filtration procedure 2. 1 M acetic acid, 8 M urea

Eluant for HPLC.	A 20%-50% gradient of acetonitrile in water containing 1% trifluoroacetic acid.

Extraction of platelets with acid/ethanol.

Lyophilised porcine platelets (50 g) were added to 10 volumes (500 ml) of acid/ethanol solution containing PMSF and extracted in a blender until homogeneous (approximately 3 minutes) at 4 °C. An addition of half a volume (250 ml) double distilled water was made and the homogenate was stirred at medium speed overnight (16 h). The homogenate was centrifuged in a Beckman centrifuge at 3500x g for 45 min. and the resulting pellet was re-extracted with 500 ml of acid ethanol. The recovered supernatants from extract 1 and extract 2 were processed independently, and pooled prior to the diafiltration step described below. The extract in each case was adjusted to pH 3.0 with the dropwise addition of concentrated (25%) ammonia solution under constant stirring. This was followed by the addition of 2 volumes cold ethanol (95%) and 4 volumes cold ethyl ether (4 °C), which caused the precipitation of crude TGF-$ß_1$. Precipitation was allowed to proceed for overnight at 4 °C. Much of the solvent was decanted, and the remaining precipitate slurry was centrifuged at 2000x g for 30 min. The remaining solvent was decanted and the pellet dried extensively *in vacuo*. The pellet was then resuspended in 1 M acetic acid (75 ml) by gentle stirring overnight at 4 °C. The resulting solution was clarified by centrifugation (2500x g, 30 min). At this stage, the resulting supernatants from extract 1 and extract 2 were pooled and dialysed against 1 M acetic acid using an Amicon ultrafiltration apparatus (Amicon, USA) loaded with a 73 mm 5 000 Da cut-off membrane

(product# YM -5). The volume was adjusted to 25 ml and the solution applied to the first chromatographic step.

Gel filtration on Sephacryl S-100 column in 1 M acetic acid

The gel filtration matrix Sephacryl S-100 (Pharmacia, Uppsala, Sweden) is a co-polymer of agarose and acrylic polymers with an exclusion limit of 100 kDa. The mean bead diameter of the matrix is 25 to 45 μm. The gel matrix material was packed as per manufacturer's instructions, and it was calibrated with a protein mixture consisting of 5 mg of each of bovine serum albumin (M_r 66 000), trypsinogen (M_r 24 000) and cytochrome c (M_r 12 500).

As a crude first step purification, the entire protein load was applied to the column, and the column was eluted at a speed of 8 cm/hr. At the predetermined eluant volume and corresponding to the expected elution position of the TGF-$ß_1$, the fraction was collected, and represented approximately half of the total protein. This procedure removed a large proportion of the high molecular weight contaminants as determined by SDS PAGE analysis and ELISA assay.

The resultant fraction was reconcentrated on a 5000 Da cut-off Amicon ultrafiltration membrane. It was decided to chromatograph the entire remaining TGF-$ß_1$ sample, but using a modification aimed to improve the resolution by effectively increasing the column length. This was achieved by connecting the eluant outlet port via the peristaltic pump directly to the top of the column, so that eluting proteins would be

subjected to another column length of gel filtration chromatography. The process was monitored by continuous UV absorbance recording at 280 nm wavelength. Eluting proteins after travelling two column volumes were collected as 50 ml fractions by manual collection. Fractions were analysed by ELISA assay to determine the presence of TGF-$ß_1$. Fractions were pooled and concentrated on a 5000 Da cut-off membrane (Amicon), exchanged into a solution of 1 M acetic acid, 8 M urea, and subjected to the second chromatographic procedure in the presence of the denaturating agent urea.

Gel filtration on Sephacryl S-100 column in 1 M acetic acid, 8 M urea. The same column of 100 cm x 6.8 cm was employed for this step. The column was equilibrated in 10 column volumes of 1 M acetic acid, 8 M urea. The TGF-$ß_1$ sample from the previous step in 17 ml of 1 M acetic acid, 8 M urea was loaded onto the column and chromatographed for two column passes at 8 cm/hr. Eluting fractions (50 ml) were collected manually. ELISA assay was used to determine fractions containing TGF-$ß_1$. These fractions were pooled, concentrated to 50 ml on a 5000 Da cutoff membrane (Amicon) and loaded directly onto a reverse phase HPLC C18 column.

Reverse phase HPLC of pTGF-$ß_1$. The TGF-$ß_1$ sample from the previous step was loaded onto a Vydac C18 HPLC column (The Separations Group, Hesperia, CA USA), 10 mm internal diameter and 250 mm in length. The column was washed with 0.1 % trifluoroacetic acid to remove unbound urea and acetic acid. Proteins were eluted with a gradient of 20 to 50 % acetonitrile in 0.1 % TFA. Fractions were collected according to eluting peaks. Individual peaks were tested and quantitated by

ELISA assay to determine fractions containing pTGF-$ß_1$. The purity of the pTGF-$ß_1$ was determined by densitometric analysis using a densitometer and associated software (Biomed Instruments Inc., CA). The pTGF-$ß_1$ was then aliquoted, lyophilised and stored dry at -20 °C.

ELISA Assay

Reagents

phosphate buffered saline (PBS)	80 mM Na_2HPO_4
	20 mM NaH_2PO_4
	100 mM NaCl, pH 7.4

Sodium acetate buffer, 100 mM, pH 5.6

pTGF-$ß_1$	stock solution 1.0 ng/µl in sodium acetate buffer pH 5.6 (R&D Systems, MN, USA)
Blocking solution:	5 % bovine serum albumin in PBS, 0.05 % Tween 20.
Primary antibody: The	chicken anti-pTGF-$ß_1$ IgG (R&D Systems, MN USA). stock of 1 mg/ml was diluted 1:1000 in PBS containing 0.05% Tween.
Secondary antibody:	biotinylated rabbit anti-chicken IGg (Amersham, UK) stock was diluted 1:1000 in PBS containing 0.05% Tween

detection:	streptavidin alkaline phosphatase (Amersham, Buckinghamshire, UK) diluted 250 fold in PBS.
substrate for alkaline phosphatase:	paranitrophenyl phosphate in 0.1 M triethanolamine buffer pH 9.2, 5mM $MgCl_2$

Procedure

pTGF-$ß_1$ samples collected from all manipulations during the course of the purification, were assayed by a direct ELISA technique in which the antigen i.e. pTGF-$ß_1$ is directly bound to the microtitre plate. Volumes assayed generally ranged from 5 to 10 µl, and duplicate determinations were performed. These were made to 100 µl with 20 mM sodium acetate buffer pH 5.6, loaded into microplate wells (Amersham, Polysorp plates) and incubated overnight at 37 °C. A standard curve was constructed in duplicate, ranging from 0 to 10 ng per well in a total volume of 100 µl sodium acetate buffer pH 5.6. Blocking solution was used at volumes of 250 µl per well. All other reagents were used at 100 µl per well. Antibody dilutions were done in PBS containing 0.05 % Tween. Streptavidin alkaline phosphatase was used according to the manufacturer's recommendations. Incubations were for 1 h at 37 °C. Detection was with 100 µl of 3 mM paranitrophenyl phosphate (pNPP) in 0.1 M triethanolamine buffer pH 9.2, 5 mM $MgCl_2$. The reaction was terminated with the addition of 100 µl 0.1 M NaOH. Measurements were done in a microtitre plate reader

at 414 nm. A standard curve was constructed using the software utility produced for this purpose (Prism, Graphpad Software Inc. CA USA).

Western blot analysis

Reagents

Blocking solution:	PBS, 0.1% Tween 20, 5 % skim milk powder
Primary antibody:	chicken anti-pTGF-$ß_1$ IGg (R&D Systems, MN USA). The stock of 1 mg/ml was diluted 1:100 in PBS containing 0.05% Tween.
Secondary antibody:	biotinylated rabbit anti-chicken IgG (Amersham, UK) stock was diluted 1:500 in PBS containing 0.05% Tween
detection: (Amersham, substrate for	streptavidin alkaline phosphatase Buckinghamshire, UK) diluted 250 fold in PBS.
alkaline phosphatase:	0.1 M diethanolamine buffer pH 9.0, 5 mM $MgCl_2$, 3.3 %4-nitro blue tetrazolium chloride, 1.65 % 5-bromo-4-chloro-3-indolyl-phosphate (Boehringer Mannheim GmbH, Germany).

Polyacrylamide SDS gel electrophoresis (12.5 % gel) was performed. The gel was removed from the electrophoresis sandwich and placed against a PVDF blotting membrane (Amersham, Buckinghamshire, and UK). A Western blot sandwich (Hoeffer, CA USA) was assembled according to manufacturer's instructions, and electroblotting was allowed to proceed overnight (16 hours) at 30 volts, followed by a

run at 100 volts for 2 hours. Transfer buffer was 15 % methanol, 25 mM Tris pH 8.2, 192 mM glycine, 0.1 % SDS. Membrane procedures were performed in an hybridisation oven (Hybaid Mini 10, Hybaid Ltd. UK). Probing of pTGF-$ß_1$ was performed with the sequential addition of primary antibody, secondary antibody and streptavidin-alkaline phosphatase complex, all at 37 °C for 1 hour. Washing of the membrane between additions of reagents was with PBS containing 0.05% Tween 20. Detection was with substrate solution for approximately 20 minutes. The reaction was stopped with an excess addition of water.

2.1.3 RESULTS AND DISCUSSION

Table 1. *Purification table for pTGF-β_1, showing purification parameters for each procedure.*

Procedure	Mg protein	% recovery	% purity	μg pTGF-β_1
acid ethanol extract #1 and #2 of 50 g lyophilised platelets	3 262	100	.0307	1 000
1 M acetic acid resolubilisation #1 and #2	1 514	104	.0688	1 042
diafiltration with 5 kDa membrane	1111	62	.0561	623
gel filtration chromatography in 1 M acetic acid	211	55	.261	551
gel filtration chromatography in 1 M acetic acid and 8 M urea	45.18	43	.95	431
HPLC chromatography	---	28	80	280

pTGF-β_1 was successfully purified to near homogeneity in a yield of 5.6 μg pTGF-β_1 per gram of lyophilised porcine platelets, in a total yield of 280 μg.

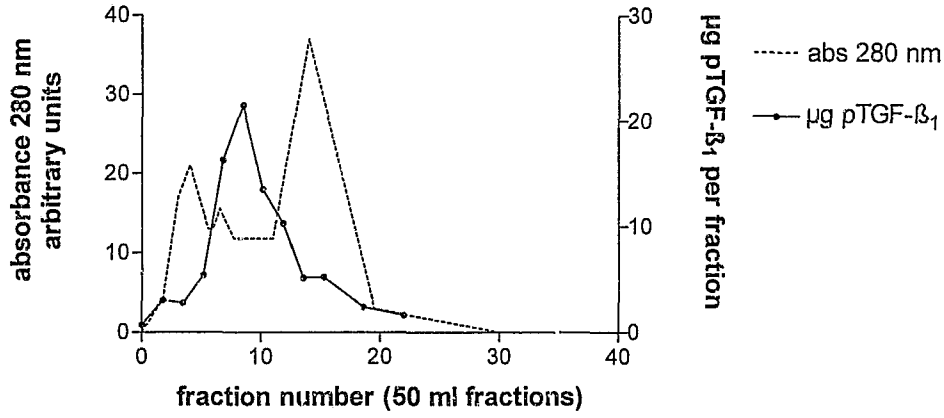

Figure 3. *Gel filtration chromatography of the platelet extract (20 ml), using the technique of rechromatography to double the effective column length. The column (100cm x 6.8 cm) was packed with Sephacryl S-100 (Pharmacia Biotech, USA). The eluant was 1 M acetic acid. Chromatography was at a rate of 8 cm/hr. The absorbance of the eluent was monitored continuously at 280 nm. 50 ml fractions were collected, and assayed for pTGF-β_1 by ELISA as described in Methods.*

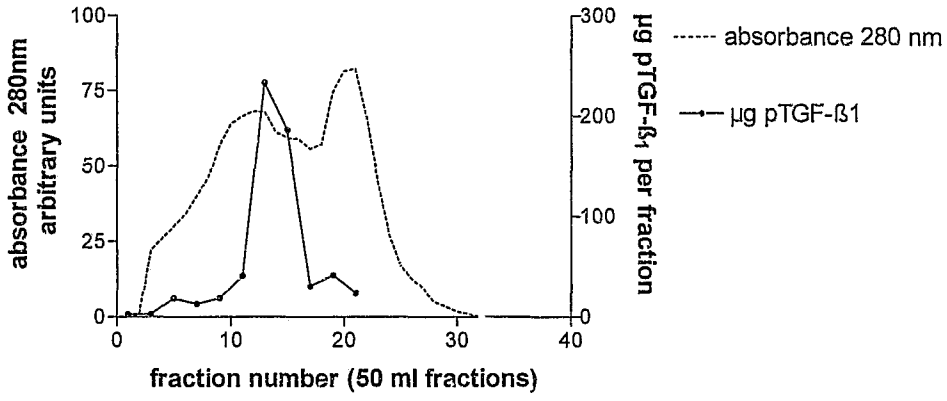

Figure 4. *Gel filtration chromatography of the crude pTGF-β_1 recovered from the first chromatographic step described in Figure 3. The eluant was 1 M acetic acid, 8 M urea. The crude pTGF-β_1 was loaded in the same medium in a volume of 17 ml. The technique of rechromatography was employed to double the effective column length. Chromatography was at a rate of 8 cm/hr. 50 ml fractions were collected, and assayed for pTGF-β_1 as described in Methods.*

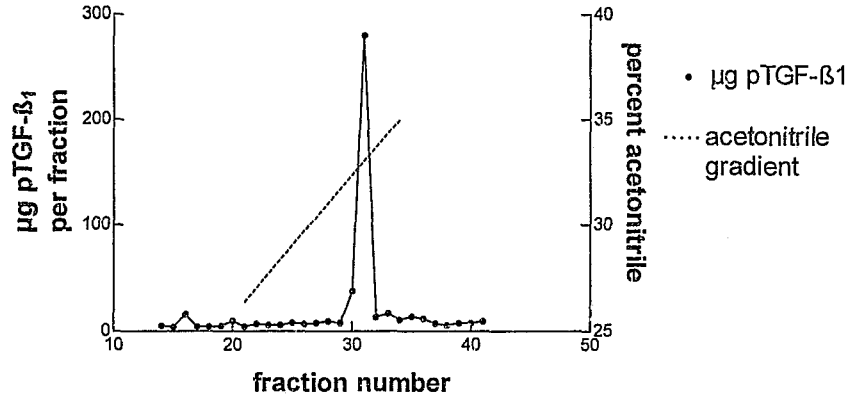

Figure 5. *Reverse phase HPLC of pTGF-β_1 recovered from the previous step described in Figure 4 . The column was equilibrated with 0.1 % TFA, and the crude pTGF-β_1 loaded onto the column at a rate of 1.2 ml/min. The column was washed with 0.1% TFA to remove non-binding urea and acetic acid. Proteins were eluted in peak fractions (not shown) with a gradient of acetonitrile in 0.1% TFA, from 0 % to 50 %. pTGF-β_1 eluted at a concentration of acetonitrile of 36.5 %. pTGF-β_1 was detected with an ELISA assay as described in Methods.*

Figure 6 (opposite). *Purification of pTGF-β_1.*

A. Silver-stained SDS PAGE gel (15 %, 1.5 mm thick) of HPLC purified pTGF-β_1, non-reducing conditions (lane b). The morphogen factor migrated to a position corresponding to approximately 25 kDa on the gel (lane b). Lanes c, d and e represent samples taken from various stages of purification, these being column 2, column 1 and resolubilisation of diethyl ether precipitate, respectively (see Methods). Molecular weight markers (lane a) are aldolase, triose phosphate isomerase, trypsin-inhibitor and lysozyme, in order of decreasing size.

B. Silver-stained SDS PAGE gel (15 %, 1.5 mm thick) of HPLC purified pTGF-β1, under reducing conditions of dithiothreitol. The morphogen factor migrated to a position of 12-13 kDa, in agreement with the dimer structure of this protein. Molecular weight markers are as shown in (A) above.

C. Western blot analysis of HPLC purified pTGF-β_1 (lane b) and commercial standard pTGF-β_1 (R&D Systems, MN, USA). Samples were resolved on a 12.5 % SDS PAGE gel, transferred to PVDF membrane and detected as described in Methods. Bands appeared at a position corresponding to 25 kDa, the molecular weight of native pTGF-β_1.

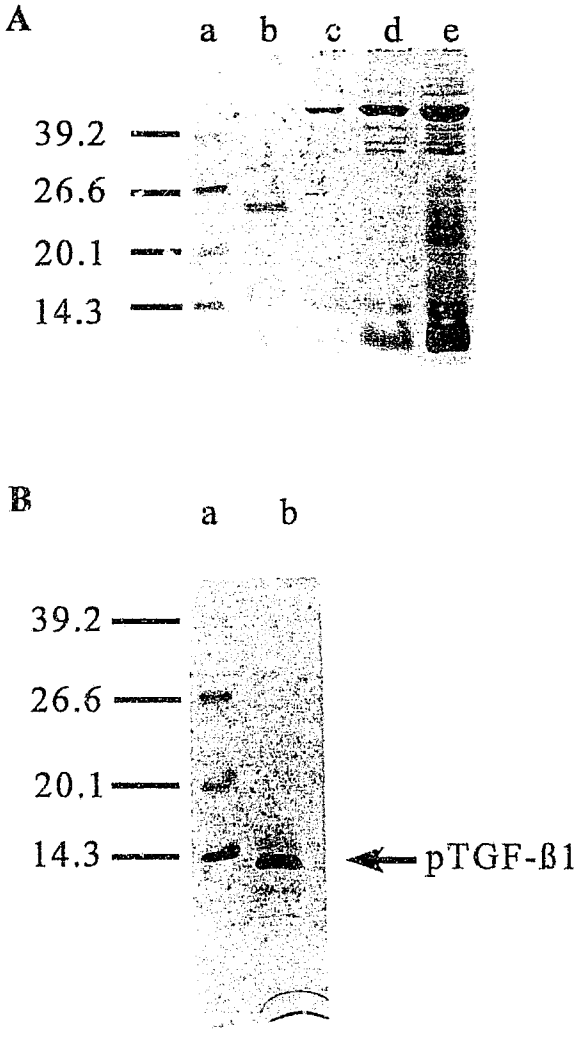
A
a b c d e
39.2
26.6
20.1
14.3
B
a b
39.2
26.6
20.1
14.3
pTGF-ß1
C
a b
pTGF-ß1

Previously, the polyacrylamide gel filtration medium Biogel P-60 (Bio-Rad) has been utilised. The 60 kDa mw exclusion range of the matrix in column dimensions of 10 cm x 100 cm resulted in yields of 500 μg of pTGF-$ß_1$ from 250 units of fresh porcine platelets. The purified pTGF-$ß_1$ was biologically active, as determined by its ability to interact synergistically with rhOP-1 in rats and primates to initiate rapid bone formation. Additionally important, the purified pTGF-$ß_1$ induced, singly, *de novo* bone formation in the rectus abdominis of the primate, at levels comparable to recombinant hTGF-$ß_1$. These results are presented in Chapter 3.

2.2 PURIFICATION OF BOVINE BONE MORPHOGENETIC PROTEINS

2.2.1 INTRODUCTION

The purification strategy adopted in this work for the purification of naturally derived BMPs (Sampath *et al.*, 1987, Luyten *et al.*, 1989; Ripamonti *et al.*, 1992) exploits the affinity of BMPs to heparin, a property deduced from the fact that pretreatment of demineralised bone matrix by soluble heparin inhibits bone formation (Reddi and Huggins, 1975). The sequence motif in BMPs that is responsible for the binding affinity to heparin has been identified (Rupert *et al.*, 1996). Immobilisation of heparin onto a polysaccharide chromatographic support such as the commercially available Sepharose (Pharmacia, Sweden) to produce heparin-Sepharose, results in a material that allows for the chromatographic adsorption of BMPs by affinity. Other components of the extracellular matrix of bone also bind to heparin (Sampath *et al.*, 1987), and further purification of osteogenin is achieved by hydroxyapaptite chromatography followed by gel filtration chromatography and finally by C18 reverse phase HPLC. The final HPLC step resulted in the 12 500-fold purification of osteogenin, but with a ten-fold loss in specific activity (Sampath *et al.*, 1987). Because of this, the HPLC was omitted in this case, and the active fractions obtained after the gel filtration step were pooled, bioassayed in rats and used in experiments to test whether pTGF-β_1 is capable of synergistic interaction with bovine BMP fractions.

2.2.2 MATERIALS AND METHODS

Preparation of bone powder

The purification of BMPs described in this work was achieved using methodologies described (Sampath and Reddi, 1981; Sampath *et al.*, 1987; Luyten *et al.*, 1989, Ripamonti *et al.*, 1992). Freshly frozen bovine femurs and tibiae of approximately 150 kg, were obtained from a local abattoir and stored at -20 °C until further use. The diaphyses were cut out using a circular butcher's saw, and epiphyses were discarded. The diaphyseal bone was then recooled to with liquid nitrogen and shattered by hammer. This exposed the marrow centre, and facilitated the removal of the marrow tissue from the bone shaft. Excess marrow was removed by brief scrubbing with a nylon brush under tap water, and fragment size was reduced further with additional cutting. Bone chips were dehydrated with absolute ethanol at 4 °C, and defatted in ether at 4 °C. Bone chips were air-dried in a fume hood. Dehydrated defatted bone chips were cooled to -70 °C using liquid nitrogen and crushed in a ring mill apparatus. Crushed bone powder was sized to 75 to 420 microns using appropriate sieves.

Demineralisation

Bone powder (5.0 Kg) was placed in an extraction tank, constructed of polypropylene and fitted with a porous polyethylene sieve (70 micron pore-size) to its bottom. The bone powder was demineralised with the addition of five volumes of 0.5 M hydrochloric acid at room temperature, under continuous stirring and pH monitoring. Successive five-volume additions of 0.5 M hydrochloric acid were made, until the pH

of the slurry stabilised at a value below 0.1, an indication that demineralisation was complete. Spent hydrochloric acid was drained between successive additions. Demineralised bone matrix was washed three times with five volumes of distilled water and the pH of the slurry adjusted with five volumes of 50 mM Tris pH 7.4. The Tris buffer was drained off, and the demineralised bone matrix was dissociatively extracted with chaotropic solvents.

Extraction of demineralised bone matrix

The extraction buffer consisted of 8 M urea, in 50 mM Tris pH 7.4 buffer, containing 1 M NaCl and the following enzyme inhibitors:

100 mM ε-aminocaproic acid

6.8 mM N-ethyl maleimide

5 mM benzamidine hydrochloride

0.5 mM phenylmethylsulphonyl fluoride.

Three volumes of the extraction buffer were added to the demineralised bone matrix. Extraction was allowed to proceed with continuous stirring at room temperature for 17 hours. The extract was filtered off, and the insoluble bone matrix was re-extracted with a second addition of three volumes of extraction buffer as before. The first and second extracts were processed separately. Extracts were exchanged into 6 M urea, 50 mM Tris pH 7.4 containing 150 mM NaCl, by the process of ultrafiltration on a 5 000 Da cutoff polyvinyldene fluoride membrane-based ultrafiltration cartridge of 6 foot square surface area (Millipore, USA). Extract was circulated at a flow volume of 6

L/minute, and at a pressure of 15 to 30 bar. 6 M urea in 50 mM Tris buffer pH7.4 was added to the concentrate in successive steps, to achieve a salt concentration of 150 mM in the extract, conditions which favour the binding of BMPs to the heparin-Sepharose affinity chromatographic step which follows.

Heparin affinity chromatography

A heparin-Sepharose CL-6B column of 5 cm diameter by 20 cm height was employed (Pharmacia Fine Chemicals, Uppsala Sweden). The extract was passed through the column at 6 cm/hr. The column was washed with 6 M urea, 50 mM Tris-chloride buffer pH 7.4 containing 150 mM NaCl, until no proteins were detected in the eluate, as determined by continuous photometric monitoring at 280 nm. Heparin bound proteins were step eluted with 6 M urea, 50 mM Tris pH 7.4 containing 500 mM NaCl. The eluting peak of absorbance was collected and exchanged into 6M urea pH 7.4, 10 mM phosphate, using a 300 ml capacity diafiltration apparatus loaded with a 10 kDa cutoff membrane (YM-10, Amicon Corp., MA, USA).

Hydroxyapatite chromatography

The heparin binding fraction was loaded onto a hydroxyapatite column (16 mm x 20 cm, Ultrogel, IBF, USA) equilibrated in 10 mM phosphate, 6 M urea, 50 mM Tris pH 7.4. The column was washed with 10 mM phosphate buffer, and osteogenic fractions eluted with 100 mM phosphate, 6 M urea, 50 mM Tris pH 7.4. The eluting peak was collected and exchanged into a minimum volume of 4 M guanidinium chloride, 50 mM Tris pH 7.4.

Sephacryl S-200 gel filtration chromatography

The fraction from the previous step, exchanged into 4 ml 4 M guanidinium chloride, was loaded onto two tandem columns (2.5 x 100 cm) of Sephacryl S-200, and run at 6 cm per hour. 20 ml fractions were collected, and 250 µl assayed in duplicate for osteogenic activity in the rat as described in section 3.2.5. Osteogenic fractions were pooled, concentrated and exchanged into 10 mM HCl using a 50 ml capacity diafiltration apparatus loaded with a 5 000 dalton cutoff membrane (Amicon Corp. MA, USA). Concentration and exchange was repeated three times to achieve removal of all guanidinium in the pooled fraction. The total amount of protein in the pooled, exchanged medium was determined by Lowry assay (Lowry *et al.*, 1951).

Alkaline phosphatase activity determination

Tissue alkaline phosphatase activity was determined by the colourimetric detection of the yellow coloured nitrophenyl phosphate resulting from enzymatic action on the substrate, para-nitrophenol phosphate (PNPP), at pH 9.3.

Substrate solution :5 mM PNPP in distilled water

Buffer :0.1 M sodium barbitol, pH 9.3

To tubes were added 1 ml of substrate solution, 1 ml of buffer solution, and temperature equilibration was made in a water-bath at 37 °C. Blanks were prepared by the addition of 0.1 N NaOH to tubes containing substrate and buffer. The assay sample was then added, and the reaction allowed to proceed for 30 minutes before stopping it with the addition of 2 ml 0.1 N NaOH. The absorbance of samples was determined spectrophotometrically at 400 nm. Alkaline phosphatase activity was expressed as units/mg solubilised explant protein. One unit of alkaline phosphatase activity is defined as that which generates 1 µmol nitrophenyl phosphate/30 min at 37 °C. This was calculated based on the extinction coefficient value of nitrophenyl phosphate, which is 218.58.

Specific activity of native osteogenic fraction

The specific activity of purified BMPs was determined from data obtained from *in vivo* bioassays in the rat subcutaneous assay as described in section *3.2.5*. One unit of osteogenic activity is defined as that amount which elicits 1 unit of alkaline phosphatase activity per mg solubilised bone explant protein in 12 day old ossicles.

2.2.3 RESULTS AND DISCUSSION

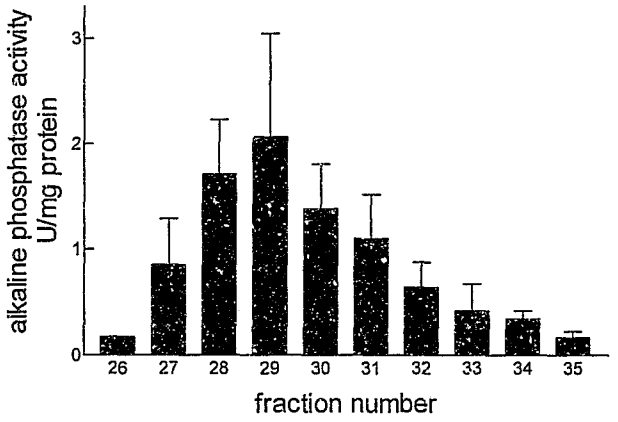

Figure 7. *Alkaline phosphatase activity of 12 day implants of rat insoluble collagenous bone matrix reconstituted with Sephacryl S-200 fractions. Osteogenic activity is confined to fractions 27-31. Fractions 27 to 31 were pooled, concentrated and exchanged into 10 ml of 10 mM HCl. The activity was expressed relative to volume of solvent (10 mM HCl). This value was 5.69 U/ml. The total activity purified was 569 units. SDS PAGE analysis showed a broad band in the region of 26 to 40 kDa (not shown).*

The majority of BMPs in its native environment is tightly bound to the collagen of the extracellular matrix of bone (Sampath *et al.*, 1987). A minority is associated with the

mineral component of bone. The purification strategy aims to expose the collagenous matrix to the extraction procedure that employs chaotropic agents such as urea or guanidinium to effect the solubilisation of BMPs. The conditions are then altered to promote the binding of BMPs to an immobilised heparin column, a first step in the purification of BMPs. The eluted BMPs are then applied to a hydroxyapatite column, to achieve further purification. Finally, gel filtration is employed to fractionate proteins on the basis of their respective molecular weights. At this stage, BMPs are still impure, but further purification is avoided, as it results in a dramatic loss of biological activity. Gel filtered fractions are collected, reconstituted with rat insoluble collagenous bone matrix and implanted in the subcutaneous space of the rat to identify osteogenic fractions. Osteogenic fractions, as determined by histology and tissue alkaline phosphatase activity, are pooled and exchanged into a medium of choice before use in experimentation. These experiments are described in Chapter 3.

3.0 CHAPTER III

BONE INDUCTIVE ACTIVITIES AND COMBINATION OSTEOGENESIS OF BMPs/OPs AND TGF-ßs

3.1 INTRODUCTION

3.1.1 *Theoretical considerations for agent interactions*

The strategy to employ combinations of agents to effect a potentiation of their activities has its roots in pharmacology, with studies aiming to show synergistic interactions for the effects, both therapeutic and toxic, of combinations of chemicals. Such studies are ubiquitous in the broad field of biomedicine. Greco *et al.* (1995) has made a comprehensive review of methodologies pertaining to the study of combinations of agents, and includes popular mathematical models for determining the nature of interaction. Over 20 000 articles in the biomedical literature from 1981 to 1987 included 'synergism' as a key word (Greco and Lawrence, 1988). The challenge of assessing the nature and intensity of agent interaction is universal and especially critical in the chemotherapy of both infectious diseases and cancer. In most applications in anticancer therapy a combination of drugs are required to cure drug-sensitive cancers (DeVita, 1989) and has given rise to the term *combination chemotherapy*. It was soon discovered that agents interact in different ways, and terminology was created to describe these interactions and includes terms such as synergy, antagonism, coalism and potentiation. *Synergism*, a word derived from the Greek '*syn*' and '*ergo*' meaning to 'work in unison', is defined in pharmacologic

contexts as an interaction between two agents which results in an effect greater than the sum of effects attributable to each agent when applied singly. It is not easy to formulate the rules by which one deems to observe a synergistic effect; for example, what magnitude of change is required before one unequivocally deems to observe a case of synergism? These and other questions will be addressed in this chapter. Other types of interactions include coalism, antagonism and potentiation. *Coalism* in an interaction which results when using a combination of agents which are inactive when applied singly, but together cause an effect. *Potentiation* is an effect resulting from the combination of an active agent and an inactive agent, which together interact to result in an increased effect. *Antagonism* is simply the opposite of synergism. These and other definitions have recently been reviewed (Greco *et al.*, 1995). However, these terminologies have not yet been standardised by world authorities, and for the purpose of this work, the umbrella term 'synergism' will define all interactions where combinations of agents result in super-additive effects when compared to the sum of effects of agents when used singly.

The interaction of two agents, where one is inactive and the other is active when applied singly, is generally easy to classify. This is the case in rats, where exogenously applied TGF-$ß_1$ in heterotopic sites is inactive, and rhOP-1 is active. Any increase in the activity of rhOP-1 when co-administered with TGF-$ß_1$ can confidently be classified as a case of synergistic interaction. However, in the vast majority of cases encountered in the literature, combinations have been studied where individual agents are all active when applied singly, making analysis of agent

interaction considerably more complicated. An example emerging from this work was the discovery that exogenously applied TGF-$ß_1$ is, like rhOP-1, osteoinductive at heterotopic sites in the baboon, making analysis of interaction more complicated. Fortunately, for the purpose of interpreting and analysing interactions where both agents in a binary combination are active, numerous mathematical models have been developed, and in the majority of cases employ a set of equations that describe agent effects in terms of their doses, and are broadly classified as response surface analyses. This methodology requires dose response data for each agent when applied singly, and response data for a set of combinatorial experiments, in which doses, $\boldsymbol{D}$, of both agents are varied. Definitions for mathematical symbols used in this section are presented in Table 2.

Table 2. Mathematical symbol definitions for interaction analysis.

Symbol	Definition
E	Measured effect, as a percent of maximal effect, E_{max}.
D, D_1, D_2	Dose of agent, agent 1, agent 2.
E_{max}	Maximum effect, or the highest E for a set of data.
ED_{50}	Dose of agent eliciting 50 % of E_{max}, derived from dose effect curves for single and binary applications of agents 1 and 2.
Dm, Dm_1, Dm_2	For stimulatory agents, Dm_1 is ED_{50} derived from dose response data of agent 1 in the absence of agent 2.

The classical analytical method for determining agent interaction is graphical **isobolographic** analysis. This approach has its origins in the work of Fraser (1871; 1872), Loewe and Muischnek (1926), Loewe (1928; 1953; 1957) and Elion *et al.* (1954). It is a general approach, and has many interpretations and variants. The data required to perform isobolographic analysis are doses of agent 1 and agent 2 (D_1 and D_2) and associated measured effects, E, both for single and applied combinations of agents. The measured data are plotted as dose effect curves on two separate graphs, graph 1 and graph 2: one showing dose effect curves for agent 1, alone, and in combination with agent 2, and another graph showing dose effect curves for agent 2, alone, and in combination with agent 1. Each graph therefore has a family of dose-effect curves which include the dose response curve for agent 1 in the absence of agent 2 (and the converse), and curves for each dosage level of the other agent. Data are expressed as percent of maximum effect E_{max}(100%) on the y-axis (see Table 2 for mathematical symbol definitions), and corresponding agent 1 and agent 2 doses (D_1 and D_2 respectively) on the x-axis of graph 1 and graph 2. Traditionally, isobolographic analysis has been performed by hand, with the aid of pencil, ruler, graph paper and possibly a French curve, a graphical aid for the drawing of curves. The advent of computers has greatly simplified these tasks, and now curves can be fitted using suitable mathematical models and specific software. A typical dose effect curve is sigmoidal in nature, and the Hill equation (reviewed in Greco *et al.*, 1995) is the model of choice for fitting data. In other cases, data may be limited, or do not converge when fitting the Hill equation, and then one has to resort to the manual determination of parameters, or else to other, more appropriate models. In

this work, the Hill equation worked well for the rat study, where dose effect data showed a typical sigmoidal relationship. In the primate study, dose effect data did not show the typical sigmoidal relationship, and the more suitable second order polynomial model was adopted using a software package for the purpose (Prism™, Graphpad Software, CA, USA). In any case, having established the dose effect curves, the next step is to determine, for each curve on graph 1, D_1 on the x-axis which corresponds to ED_{50}. Dm_1, is defined as the D_1 value corresponding to ED_{50} (at *0.5Emax),* and is determined from the ED_{50} value for the dose effect curve of agent 1 in the absence of agent 2. Alongside these D_1 values are recorded D_2, the doses of agent 2 used to generate the respective curve. The D_1 values are divided by Dm_1 and the result is denoted as D_1/Dm_1. D_2 values are divided by the Dm_2 value, the ED_{50} value of the dose response curve of agent 2 (in the absence of agent 1), and the result is denoted as D_2/Dm_2. These resulting values represent x,y co-ordinates on a cartesian plot: $(D_1/Dm_1, D_2/Dm_2)$ as depicted in figure 8. The analogous procedure is performed for agent 2 (Graph 2) to obtain the other set of D_1/Dm_1, D_2/Dm_2 co-ordinates. A thorough working of data manipulations are presented in later sections describing work in rats and primates.

The nature of agent interaction is determined geometrically on an isobologram (Figure 8) by considering the position of plotted points relative to the Loewe's line of additivity (reviewed in Greco *et al.*, 1995). Loewe's line of additivity marks the position where a binary combination of agents results in an effect which is equal to the sum of effects of each agent when used singly. Points lying below this line are

said to denote synergism, whilst points above this line denote antagonism (Figure 8). The synergistic and antagonistic interactions occur when the effect resulting from the use of the combination exceeds that attributable to the sum of effects of the agents when used singly. Points falling on the line denote additivity and zero interaction, implying that the agent combination results in an effect which equals the sum of effects of agents when applied singly. In addition, isobolographic analysis permits one to quantify the *intensity* of the interaction by calculating the ratio of the distance from the origin to the point of intersection with Loewe's line, and the distance from the origin to the plotted point. These concepts are graphically presented in Figure 8.

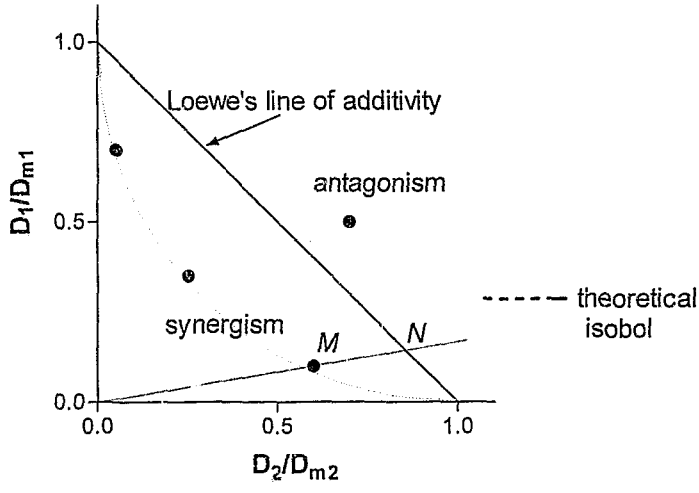

Figure 8. *An example of isobolographic analysis. Loewe's line of additivity denotes zero interaction, and indicates the graphical position where agent combinations result in an additive effect. Data points* (D_1/Dm_1, D_2/Dm_2) *represent interaction analysis for agent 1 and agent 2 combinations at of doses* D_1 *and* D_2. *Points above the line of Loewe additivity denote antagonism and points below the line of additivity*

denote synergism. The ratio of 0N to 0M is geometrically determined, and represents R, the interaction intensity (Machado, 1994). If R equals 1, then additivity is indicated. If R is > 1, then synergism is indicated. If R < 1, then antagonism is indicated. Dotted line represents the theoretical isobole, which predicts interaction for other agent combinations.

3.1.2 THE SEARCH FOR OSTEOINDUCTIVE FACTORS

Historically, the search for osteoinductive factors has relied on the use of *in vivo* bioassays at extraskeletal sites for the identification of osteogenic factors. The histological evidence of bone at the completion of the bioassay would confer the honourable status of 'osteoinductive' to the factor tested. Proteins conforming to criteria which define osteoinductive agents include the BMPs/OPs (see review, Chapter 1), GDF-5 also known as CDMP-1) (Chang *et al.* 1994; Hotten *et al.*, 1996), CDMP-2 (Erlacher *et al.*, 1998) and the phylogenetically related gene products of Drosophila melanogaster, namely DPP and 60A (Sampath *et al.*, 1993).

To date, TGF-ß either purified from natural sources such as platelets and bone matrix, or expressed recombinantly has failed to induce heterotopic bone in a number of experimental rodent models, eliciting instead, a fibrovascular response (Hammonds *et al.*, 1991; Mustoe *et al.*, 1987; Roberts *et al.*, 1986; Sampath *et al.*, 1987; Bentz *et al.*, 1991). Biological activity of TGF-ßs has instead been shown at orthotopic sites, with mixed results. Repeated injections of rhTGF-$ß_1$ into the subcutaneous tissue overlying the calvariae of neonatal mice resulted in a marked increase in the periosteal thickness and cellularity and stimulation of newly mineralised bone without a chondrogenic phase (Marcelli *et al.*, 1990). Repeated injection of TGF-$ß_1$ or -$ß_2$ subperiosteally in newborn rats resulted in local chondrogenesis and localised intramembranous bone formation (Joyce *et al.*, 1990). Injection of TGF-$ß_1$ directly into the periosteum of parietal bones of neonantal rats

stimulated membranous bone formation without a chondrogenic phase (Noda *et al.*, 1989, Tanaka *et al.*, 1993). Interestingly, injection of TGF-$ß_1$ into the pericranium of adult rats promoted endochondral osteogenesis in contrast to the membranous osteogenesis in neonates (Taniguchi *et al.*, 1993). A single application of rhTGF-$ß_1$ promoted a dose-dependent increase in intramembranous bone formation in 12 mm calvarial defects in the rabbit 28 days after treatment (Beck *et al.*, 1991). In later studies using the rabbit calvarial model, it was shown that defects treated with rhTGF-$ß_1$ were characterised by an increase in parameters of bone formation up to 49 days (Beck *et al.*, 1993). However, when implanted into calvarial defects of the baboon, rhTGF-$ß_1$ resulted histologically and histomorphometrically in limited chondro-osteogenesis confined to defect margins as evaluated on day 30 (Ripamonti *et al.*, 1996a).

Unequivocal efficacy of a recombinant factor for bone repair should be proven by day 30, a time frame of clinical significance for therapeutic applications, in which case the limited activities observed for TGF-ß in the primate at extended time periods need to be considered in clinical contexts. It is likely that differences in animal models, age of animals, defect dimensions and single versus multiple applications are of importance in determining whether osteogenesis may be promoted or indeed induced by exogenous application of TGF-$ß_1$. Paradoxically, TGF-$ß_1$ implanted in intramuscular sites of the adult baboon induced endochondral bone formation as early as day 14 post-implantation. This is the first report showing

osteoinduction by both naturally sourced and recombinantly produced TGF-β_1 at heterotopic sites of primates.

3.1.3 AIMS ADDRESSED IN CHAPTER III

Aims in rats:

i) to test osteoinductivity of single applications of recombinant human TGF-$ß_1$ (rhTGF-$ß_1$) at subcutaneous sites.

ii) to generate a dose response curve for rhOP-1 in the subcutaneous bioassay.

iii) to characterise the nature of interaction arising, in the rat subcutis,

a) from combinations of rhOP-1 and rhTGF-$ß_1$

b) from combinations of rhOP-1 and pTGF-$ß_1$

c) from combinations of porcine pTGF-$ß_1$ and bovine BMP

iv) to determine whether co-administration of anti-TGF-$ß_1$ antibodies to rhOP-1 treated implants alters parameters of tissues generated in the rat subcutis.

Aims in baboons:

i) to test the morphogenetic potential of single applications of rhTGF-$ß_1$ and pTGF-$ß_1$ in the rectus abdominis.

ii) to characterise the nature of tissue morphogenesis arising from:

a) combinations of rhOP-1 and rhTGF-$ß_1$ in heterotopic sites.

b) combinations of rhOP-1 and pTGF-$ß_1$ in heterotopic sites.

c) combinations of rhOP-1 and pTGF-$ß_1$ in orthotopic calvarial sites.

iii) to gain insights into the mechanism of combination osteogenesis by analysis of relative levels of mRNA transcripts of morphogenetic markers of endochondral bone formation in tissues generated by the various combinations of implanted morphogens in baboon intramuscular sites, including type II and type IV collagens, BMP-3, OP-1 and TGF-$ß_1$ mRNA transcripts.

3.2 MATERIALS AND METHODS

3.2.1 Experimental animals: the baboon (*Papio ursinus*) and the rat (*Rattus norvegicus*)

The demonstration of bone formation by induction at heterotopic sites in rats is a model that has been established, and has found widespread use in the field. Sites utilised are intramuscular (Urist, 1965; Urist *et al.*, 1983) or subcutaneous (Reddi, 1981; Reddi and Huggins, 1972). The induction of heterotopic bone within 12 days in response to subcutaneous implantation of morphogens is still the most reliable way to identify morphogenetic factors, to perform dose response studies and to generate tissues that can be dissected by cellular and molecular analyses. Rats were used extensively in this work to enable comparatively rapid generation of data. However, the rat is endowed with remarkable capacity for bone regeneration, and may therefore not represent an ideal model with which to directly relate data for extrapolation into primates, including humans. In addition, orthotopic experiments in rats are often difficult to perform, and are not representative of physical forces encountered in larger animals. Comparative histomorphometric studies between iliac crest bone biopsies of humans (Schnitzler *et al.*, 1990) and baboons showed a remarkable degree of similarity (Schnitzler *et al.*, 1993). This makes the adult baboon ideally suited for the study of comparative bone physiology and repair with relevance to man (Schnitzler *et al.*, 1993). Consequently, the use of primates was of critical importance to this work, and were used in the study of osteogenesis elicited

by BMPs/OPs and TGF-ßs, singly or in combination, at both heterotopic and orthotopic sites.

3.2.2 Selection of the animals

3.2.2.1 Primates.

Clinically healthy adult male Chacma baboons (*Papio ursinus*) were selected from the primate colony of the University of the Witwatersrand, Johannesburg. Criteria for selection were normal haematological and biochemical profiles (Melton and Melton, 1982) and skeletal maturity, confirmed by radiographic evidence of closure of the distal epiphyseal plate of the radius and ulna (Ripamonti, 1991). Following standard quarantine procedures, the animals were housed individually in suspended wire-mesh cages in the primate unit of the Central Animal Service of the university. Animals were kept under slight negative pressure (-25kPa) with controlled ventilation, at 22°C and humidity at ± 40%, and controlled photoperiod (lights on 06h00 to 18h00). The diet of the baboons consisted of a balanced protein-fat-carbohydrate diet with vitamins (thiamine, riboflavin and nicotinic acid) and mineral supplements (Ca:P = 1.2:1), and a soft dietary intake of sweet potatoes, pumpkins and oranges mixed in a ratio of 3:1 with a protein-vitamin-mineral dietary supplement (Dreyer and Du Bruyn, 1968). The baboons had access to tap water *ad libitum*. The research protocols were approved by the Animal Ethics Screening Committee of the university (AEC 93/120/5, later AEC 95/106/5 and AEC 96/96/5).

3.2.2.2 Rats

Long-Evans rats were supplied by the Central Animal Service of the university. Animals were housed at temperatures 23°C in groups of 5 - 8, and fed a standard rat chow. Research protocols were approved by the Animal Ethics Screening Committee of the university. Retired breeders were employed for the harvesting of tibias (AEC 96/97/05), which were processed for the making of demineralised bone matrix and insoluble collagenous bone matrix as described herein. Animals of 28 to 32 days of age were used for the subcutaneous implantation of morphogens (AEC 94/69/05 and 95/47/04), reconstituted with rat insoluble collagenous matrix as described hereunder.

3.2.3 Morphogens

3.2.3.1 Recombinant human OP-1

Recombinant human osteogenic protein-1 (rhOP-1), a kind gift of Creative BioMolecules (Hopkington, MA, USA) was expressed in Chinese hamster ovary (CHO) cells as mature glycosylated 36 kD homodimer of 139 amino acids (Sampath *et al.*, 1992). The morphogen was supplied at a purity of 95 % in 0.01% trifluoroacetic acid in 50% ethanol.

3.2.3.2 Recombinant human TGF-β_1

Recombinant human TGF-$ß_1$, a kind gift of Genentech Inc. (South San Francisco, CA, USA.), was purified from conditioned medium of transfected CHO cells as described (Derynck *et al.*, 1985). Stock solutions of rhTGF-$ß_1$ were prepared in 20 mM sodium acetate buffer, pH 5.0.

3.2.3.3 Porcine TGF-$ß_1$

Porcine TGF-$ß_1$ (pTGF-$ß_1$) was purified from lyophilised porcine platelets as described in 2.2. Stock solutions of pTGF-$ß_1$ were prepared in 20 mM sodium acetate buffer, pH 5.0.

3.2.4 Insoluble collagenous bone matrix

Insoluble collagenous bone matrix, hereafter referred to as collagenous matrix, was prepared from baboon diaphyseal bone and rat tibial diaphyseal bone (Sampath and Reddi, 1981). Bone segments were harvested, cleaned, demarrowed, defatted and then dehydrated with sequential ethanol and diethyl ether treatment, and crushed to particle size of 75 µm to 420 µm. The bone matrix was demineralised with successive additions of 5 volumes of 0.5 M HCl, until a stable pH was reached, an indication of completion of demineralisation. The demineralised bone matrix was washed three times with distilled water, neutralised with 50 mM Tris-Cl buffer pH 7.4, and washed again with five volumes of distilled water. Demineralised bone matrix was extracted twice with five volumes of 4 M guanidinium chloride, 50 mM Tris-Cl pH 7.4, containing enzyme inhibitors (100 mM ε-amino caproic acid, 5 mM N-ethyl maleimide, 5mM benzamidine-HCl, 0.5 mM phenyl methyl sulphonyl

fluoride) and washed extensively with successive additions of distilled water, and lyophilised. Implantation of allogeneic collagenous matrix into the rectus abdominis and calvarial defects of the baboon, and into the subcutis of the rat showed no evidence of osteoinductivity, confirming the inactive status of the matrix.

3.2.5 The heterotopic model in the rat

3.2.5.1 Experimental design

The subcutaneous site was chosen due to its simplicity and ease of tissue harvest at the conclusion of the experiment. The strategy employed aimed to generate data in a two-dimensional fashion by varying doses independently of both BMP/OPs and TGF-β_1 as shown in Table 3. Additional experiments were performed to test whether co-administration of anti-TGF-ß-antibodies with rhOP-1 could in any way affect endochondral bone formation.

Rats were anaesthetised with an intravenous mixture of 5:1 ketamine/rompun. The thoracical area was shaved and an incision made in the skin overlying the rib-cage. Subcutaneous connective tissue was detached with blunt dissection to create two bilateral pouches, in the region overlying the pectoralis muscles. Implants were inserted into pouches, one implant per pouch. Skin was repaired with atraumatic resorbable sutures. Implants were harvested on day 12 post-implantation and analysed by histology, histomorphometry and biochemistry as described in 3.2.8. The implantation design also includes the dose response study for rhOP-1 in the

range of 0.1 to 6.0 μg per implant in the absence of TGF-$ß_1$, and the dose response study for rhTGF-$ß_1$ in the range of 50 to 500 ng per implant in the absence of rhOP-1.

Table 3. *Heterotopic combination osteogenesis with rhTGF-$ß_1$ and rhOP-1 in the rat. The combinations of morphogens, implanted as* ***n*** *replicates between 2 and 6, were used to obtain data for the construction of the response surface, for application in isobolographic analysis of the interaction (Figure 8). Values for rhOP-1 and rhTGF-$ß_1$ are expressed as μg per 25 mg insoluble collagenous bone matrix.*

rhOP-1 / **rhTGF-$ß_1$**	**0**	**0.1**	**1**	**3**	**6**
0		6	6	6	4
0.050	2	4	4	4	
0.150	2	4	4	4	
0.500	2	4	4	4	

3.2.5.2 Preparation of rat heterotopic implants

Allogeneic insoluble collagenous bone matrix (25 mg) from Long Evans rats, was weighed into sterile 5 ml capacity polypropylene tubes. Morphogens, in their respective media, in a volume ranging from 100 µl to 500 µl, were added and vortexed thoroughly to ensure homogeneous permeation of the matrix. Chondroitin-C sulphate (100 µl) of a concentration of 10 mg/ml and 50 µl rat tail type I collagen in (5 mg/ml, 0.5 M acetic acid) were added (Muthukumaran *et al.*, 1988). Two to three volumes of chilled absolute ethanol was added and the tube vortexed. Precipitation was allowed to proceed at -20 °C for 30 minutes. Tubes were centrifuged at 500 xg for 20 minutes, to pelletise contents, and supernatant ethanol discarded. When using bovine bone purified BMPs in solvents containing guanidinium, pellets were thrice washed with 85% ethanol to remove the chaotrope. Pellets were lyophilised *in vacuo* at -70 °C. Addition of soluble type I collagen and chondroitin sulphate assists in reducing the friability of lyophilised pellets, resulting in solid plano-convex pellets ideally suited for implantation.

3.2.6 The heterotopic model in the baboon.

3.2.6.1 Experimental design

Following the serendipitous results of massive ossicles induced in the rectus abdominis of the baboon by interposed implants containing singly rhOP-1 and rhTGF-$ß_1$ (Formulation of the Hypothesis, Chapter I), it was hypothesised that the co-administration of binary combinations of rhOP-1 and rhTGF-$ß_1$ loaded onto a collagenous carrier in the respective ratio of 20:1 would lead to a reproduction of the synergistic effect. The ratio was arrived at by observing that large tissue formation had occurred at sites with juxtaposed implants of 125 µg rhOP-1 and of 5 µg rhTGF-$ß_1$ per 100 mg collagenous matrix, a ratio of 20 to 1. To further characterise combination osteogenesis, it was decided to vary the doses of both morphogens independently. Two groups of primates were employed:

Group 1: 7 adult male baboons, with a mean mass of 31.9 ± 4.3 kg, were implanted in the rectus abdominis with **rhTGF-$ß_1$** and rhOP-1 both singly and in combination. Two time periods were employed: 15 days and 30 days. rhTGF-$ß_1$ was tested singly at doses of 5 µg per 100 mg of collagenous matrix. rhOP-1 was tested singly at doses of 5, 25 and 125 µg per 100 mg of collagenous matrix, and results used to construct a dose response curve for this morphogen. rhOP-1 at doses of 25 and 125 µg was tested in combination with 0.5, 1.5 and 5 µg of rhTGF-$ß_1$.

Group 2: This group comprised 10 animals with a mean mass of 28.1 ± 6.1 kg, and were utilised for implantation in the rectus abdominis with **pTGF-ß$_1$** and rhOP-1 singly and in combination. Six baboons were scheduled for euthanasia on day 30, and 4 on day 14. Doses used for this study were restricted to those yielding optimal results when using recombinant TGF-ß$_1$ and rhOP-1. Optimal combination osteogenesis occurred for doses of 25 µg rhOP-1 in combination with rhTGF-ß$_1$, and consequently, rhOP-1 at a dose of 25 µg was tested in combination with porcine TGF-ß$_1$ at doses of 0.5, 1.5 and 5 µg respectively. Four of these animals were simultaneously utilised for the 30 day orthotopic calvarial study as described in section *3.2.7.*

3.2.6.2 Preparation of heterotopic implants

For heterotopic implants, 100 mg of baboon insoluble collagenous bone matrix was weighed into 10 ml capacity polypropylene tubes, and respective growth factors added in a volume of 100 µl of medium which was 20 mM sodium acetate pH 5.0 for TGF ß$_1$ and 10 mM HCl for rhOP-1. Four mg of bovine trachea chondroitin sulphate (Sigm Chemical Co. Mo, USA) in 400 µl water and 200 µl of baboon type I collagen in 0.5 M acetic acid (5 mg/ml) were added to each tube, vortexed, and precipitation of the entire contents achieved with the addition of 2.5 volumes of chilled absolute ethanol (-20 °C) for 30 minutes. Tubes were centifuged for 20 minutes at 0 °C at 500 x g. The ethanol supernatant was carefully poured off, and the vials with pelletised contents placed *in vacuo* at -70 °C. Lyophilised implants were stored at -70 °C until use.

3.2.6.3 *Surgical procedures and implantation design*

The surgical procedure for heterotopic implantation in the rectus abdominis of the baboon has been described in detail (Ripamonti *et al.*, 1991, 1992). Briefly, animals were immobilised with intramuscular ketamine hydrochloride (10 mg/kg) and anaesthetised with intravenous thiopentone sodium (15 mg/kg). Anaesthesia was maintained by halothane vapour in 100 percent oxygen after orotracheal intubation. Anaesthetised animals were prepared for implantation of morphogens in the rectus abdominis. Intramuscular pouches in the rectus abdominis were created by sharp and blunt dissection and implanted with pellets of lyophilised matrix. Pouches were stiched with non-resorbable silk sutures in order to demarcate position of implants at harvest. To exclude possible diffusion effects, the implantation scheme was designed to offer maximum distance between implants. In each animal, ipsilateral pouches were created such that they were separated by several centimetres of vertical as well as lateral intervening muscle (forming a zig-zag implantation design), and implanted with morphogen combinations. Contralateral pouches across the midline, were implanted with different doses of rhOP-1 in conjunction with collagenous matrix for the dose response study. Pellets containing TGF-β_1 were implanted more superiorly in the ventral musculature, at least 10 cm away from the lower dose of rhOP-1. To rule out any diffusion effects which may have led to ambiguities in the TGF-β_1 studies, TGF-β_1 was implanted in an additional baboon, without any OP-1 implants. Moreover, the collagenous matrix used as carrier was reprocessed with a further dissociative extraction with guanidinium chloride, and used as carrier for TGF-β_1.

3.2.7 The orthotopic model in the baboon

Previous studies have confirmed that 25 mm diameter calvarial defects do not heal spontaneously in the baboon. At 1, 3, and 9 months, the bone volume in untreated calvarial defects was less than 4, 11, and 20% respectively (Ripamonti, 1992, Ripamonti *et al.*, 1993).

Applications of this model have included the use of naturally derived BMPs (osteogenin) adsorbed onto porous hydroxyapatite substrata for the regeneration of calvarial defects (Ripamonti *et al.* 1992), the use of osteogenin and insoluble collagenous bone matrix (Ripamonti *et al.* 1993), autolysed antigen extracted allogeneic bone (Ripamonti, 1992) calvarial reconstruction with porous hydroxyapatites (Ripamonti *et al.* 1992), and treatment of calvarial defects with rhTGF-β_1 (Ripamonti *et al.*, 1996b) and with rhOP-1 (Ripamonti *et al.*, 1996b).

3.2.7.1 *Experimental design*

The comparatively large size of the adult male calvarium allows the surgical preparation of four symmetrically located defects each of 25 mm diameter with intervening calvarial bone of more that 25 mm between ipsilateral defects, and with intervening calvarial bone of more than 50 and 40 mm between contralateral anterior and posterior defects, respectively (Figure 9).

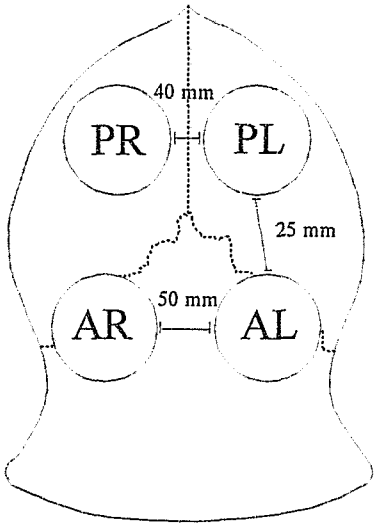

Figure 9. Calvarial model and implantation design in adult male baboons. In each animal, a balanced ipsilateral design was used to allocate the position of the implants, which contained morphogens as described Figure 10.

AR: anterior right
AL: anterior left
PR: posterior right
PL: posterior left

3.2.7.2 *Combination osteogenesis with rhOP-1 and porcine TGF-ß1 in the baboon calvarium*

Following results of combination osteogenesis in rats and baboons at heterotopic sites, it was decided to test pTGF-ß1 in combination with rhOP-1 in baboon calvarial defects. The strategy employed was to use ratios of pTGF-ß1 to rhOP-1 that had yielded optimal results in intramuscular sites of the baboon. In addition, it was decided to include a treatment modality with sub-optimal amount of rhOP-1 in calvarial defects, to determine whether pTGF-ß1 could in effect 'rescue' inferior bone induction cascade elicited by sub-optimal doses of rhOP-1. Doses of rhOP-1 were chosen such that, with the exclusion of the 20 µg dose, they were identical to historical experiments conducted previously in this laboratory. This enabled comparison of combination osteogenesis with previous experiments using single applications of rhOP-1.

3.2.7.3 *Preparation of baboon orthotopic implants*

For orthotopic use, 1 g baboon insoluble collagenous bone matrix was weighed into sterile 50 ml capacity polypropylene vials under a laminar flow cabinet. Each vial was for use for one calvarial defect. rhOP-1 and pTGF-ß1 in respective volumes of 500 µl of medium were pipetted into the vial under constant agitation by means of a vortex mixer. This allowed for the even distribution of the morphogens factors onto the collagenous matrix. Loosely capped vials were lyophilised and stored at –70 °C until implantation.

3.2.7.4 Surgical procedures and calvarial implantation design

Eight animals of the Group 2 that were assigned for calvarial studies, were divided into a 30 and 90 day study period. The rationale was to gain data on the temporal progression of osteogenesis of single and combined applications of rhOP-1 and pTGF-$ß_1$.

The calvaria of the 8 baboons allocated to the orthotopic study, were exposed and on each side of the calvaria, two full-thickness defects, 25 mm in diameter, were prepared with a craniotome under saline irrigation. The posterior defects were trephined in the posterior convexity of the parietal bone, 5 mm anterior to the lambdoid suture, and lateral to the temporal crest. The anterior defects were trephined in the fronto-parietal region of the calvaria, 5 mm lateral to the temporal crest. An ipsilateral implantation design was used to allocate the position of the implants in the 32 calvarial defects. In each animal, two ipsilateral defects were implanted with 100 µg rhOP-1 in combination with either 5 or 15 µg pTGF-$ß_1$. Contralateral defects were implanted with the lower dose of rhOP-1 (20 µg per g of collagenous matrix), singly, or in combination with 5 µg pTGF-$ß_1$. The treatment allocation was alternated anterio-posteriorly, to achieve a balanced distribution between anterior and posterior defects. Control defects containing collagenous matrix without added morphogens were omitted and instead historical results were utilised (Ripamonti *et al.*, 1993, 1996b). This allowed for the expansion of the investigation to include one additional treatment. The implantation protocol is shown in Fig. 10.

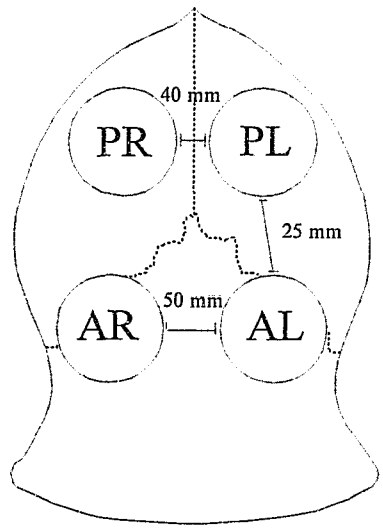

AR:	anterior right	100:15
AL:	anterior left	20:5
PR:	posterior right	100:5
PL:	posterior left	20

Figure 10. *Allocation of morphogen combinations for implantation into calvarial defects of the baboon. Doses are expressed in μg of rhOP-1:pTGF-β_1, delivered by 1 g collagenous matrix per defect site.*

3.2.8 Analytical procedures

3.2.8.1 Tissue harvest, histology and biochemistry

Rats were killed on day 12 by carbon dioxide asphyxiation. The subcutaneous area housing the implants was dissected and implants were retrieved and freed of adhering soft tissues. Anaesthetised primates were killed on days 30 and 90 after surgery with an intravenous overdose of sodium pentobarbitone (100mg/kg). Heterotopically generated tissues were excised, trimmed of adhering muscle and processed for histology and histomorphometry as described hereunder. Biochemical analyses on homogenised tissues were performed to determine tissue alkaline phosphatase and calcium as described (3.2.8.5), and used as indeces of bone formation. In addition, heterotopically generated tissues on day 30 were analysed by Northern analysis as described in section 3.2.8.7.

Bilateral carotid perfusion was performed with two litres of isotonic saline, pH 7.4, followed by two litres of 10 percent neutral buffered formaldehyde. The calvaria were then dissected, leaving a thin layer of muscle over the operative sites and the surrounding bone. The calvaria were cut into halves along the sagittal planes, using a reciprocating saw, and tissues were further fixed in 70 percent ethanol. Specimens were processed for histology.

3.2.8.2 Histomorphometry: Heterotopic specimens

A single source was selected for histomorphometry, originating at the corticalised regions of the newly generated tissue, and transversing to the interior of the section. Histomorphometry was done using the point counting technique (Parfitt, 1983) to measure fractional volumes (in percent) of each histological component: mineralised bone, osteoid, soft tissues (including fibrovascular and marrow tissue), and unresorbed implanted collagenous matrix.

3.2.8.3 Histomorphometry: Calvarial specimens

Calvarial sections were mounted after recording the position of the anterior and posterior interfaces of the defects with their corresponding calvarial margins. Consecutive sections were mounted and stained with 0.1% toluidine blue in 30% ethanol. A calibrated Zeiss Integration Platte II with 100 lattice points was used to calculate, with the point counting technique (Parfitt, 1983), the fractional volumes in percent of each histological component namely: newly formed bone, soft tissues (including fibrovascular and marrow tissue), and unresorbed implanted collagenous matrix. Bone values were computed by calculating separately its mineralised and osteoid components. Sections were analysed under a Provis AX70 research microscope (Olympus optical Co., Japan) at 40X magnification, superimposing the Zeiss graticule over five sources (Figure 11) selected for histomorphometry and defined as follows: two anterior and posterior interfacial regions (AIF and PIF), two anterior and posterior internal regions (AIN and PIN) and a central region (CEN) (Figure 11). This technique allows the histomorphometric evaluation of the

distribution of bone regeneration across the defects (Ripamonti *et al.*, 1992). Each source represents a field of 7.84 mm^2. Morphometry was performed on two sections per implant, representing two parasagittal levels, approximately 2 mm apart from each other. The cross sectional area (in mm^2) of newly generated bone tissue (mineralised bone, osteoid and bone marrow) (Parfitt *et al.*, 1987) in both heterotopic and orthotopic specimens was measured using a computerised image analysis system (Flexible Image Processing System, CSIR, South Africa). Fibrovascular tissue and residual collagenous matrix, when surrounded by newly formed bone, were included in the analysis, (Ripamonti *et al.*, 1996b).

Figure 11.

Schematic representation of a sagittal calvarial section (A=anterior, P=posterior), implanted with baboon insoluble collagenous matrix combined with morphogens as described in methods. Time of harvest was day 30 and day 90. Dashed line indicates interface of craniotomy, and boxed areas the positioning of the graticule for point-counting. The five sources selected for histomorphometry, defined as the type of regions on which quantitative morphometry was performed (Parfitt et al., 1987),were anterior and posterior interfacial regions (AIF and PIF), anterior and posterior internal regions (AIN and PIN), and a central region (CEN).

3.2.8.4 Preparation of undecalcified sections

After dehydration in ascending grades of ethanol, specimens were embedded undecalcified in a polymethylmethacrylate resin (K-Plast, Medim, Buseck, Germany). Undecalcified serial sections were cut at 7 μm using tungsten carbide knives and a motor-driven microtome (Polycut-S, Reichert-Jung, Heidelberg, Germany). Sections were stained with the free-floating method with Goldner's trichrome stain for undecalcified bone. Sections were also stained with toluidine blue for detection of cartilage matrix.

3.2.8.5 Biochemical indeces of bone formation

3.2.8.5.1 Alkaline phosphatase assay

Implant specimens were weighed and homogenised in 2 ml of ice-cold 0.15 M NaCl/ 3 mM $NaHCO_3$. Samples were centrifuged at 2 500 xg and supernatant used to determine alkaline phosphatase activity whilst sediment was used to determine calcium. Alkaline phosphatase activity was determined by the colourimetric detection of the yellow coloured nitrophenyl phosphate resulting from enzymatic action on the substrate, para-nitrophenol phosphate (PNPP), at pH 9.3.

Substrate solution: 5 mM PNPP in distilled water

Buffer: 0.1 M sodium barbitol, pH 9.3

To tubes were added 1 ml of substrate solution, 1 ml of buffer solution, and temperature equilibration was made in a water-bath at 37 °C. Blanks were prepared by the addition of 0.1 N NaOH to tubes containing substrate and buffer. The assay sample was then added, and the reaction allowed to proceed for 30 minutes before stopping with the addition of 2 ml 0.1 N NaOH. The absorbance of samples was determined spectrophotometrically at 400 nm. Alkaline phosphatase activity was expressed as units/mg solubilised explant protein. One unit of alkaline phosphatase activity is defined as that which generates 1 µmol nitrophenyl phosphate/30 min at 37 °C. This was calculated based on the extinction coefficient value of nitrophenyl phosphate, which is 218.58.

3.2.8.5.2 *Lowry assay for protein (Lowry, 1951)*

The method of Lowry (1951) was used to determine protein concentrations for the purpose of calculating alkaline phosphatase activity.

3.2.8.5.3 *Assay for calcium*

Specimens were homogenised, and centrifuged at 2 500xg to sediment insoluble materials. Pellets were washed once with 10 ml of 20 mM Tris-HCl buffer pH 7.4, and recentrifuged as before. Ten ml of 0.5 N HCl solution was added to pellets, and vortexed thoroughly to resuspend the pellet completely. Tube contents were agitated by means of magnetic bars for overnight. Tubes were spun and supernatant, containing solubilised calcium assayed for calcium in the presence of 0.06 percent lanthanum oxide, on atomic absorption flame spectrophotometer at 422.7 nm, and band width of 1.0 nm. A standard curve was constructed with $CaCl_2$ in the range of 0.5 to 6 mM Ca^{2+}.

3.2.8.6 *Statistical analysis*

The data were analysed with the Statistical Analysis System (1989). An F test was performed using the General Linear Models procedure for an analysis of variance with multiple interactions. For each treatment modality, 4 to 8 specimens were available for morphometry and biochemical analyses representing 4 to 8 alkaline phosphatase activity determinations, and 8 to 16 morphometric observations (derived from 2 serial sections from each specimen) per group. Comparison of mean values

was obtained using Sheffe's multiple comparison procedure on the dependent variables included in the analysis.

3.2.8.7 Northern analysis

3.2.8.7.1 Preparation of total RNA

Harvested tissues on day 30 from the rectus abdominis of the baboon were used for Northern analysis. For the preparation of total cellular RNA from mineralised tissues, the method of Nemeth *et al.* (1989) was employed, with modifications. All glassware was baked at 180 °C overnight, and plasticware autoclaved at 121 °C, for 20 minutes, in the presence of 0.1% diethylpyrocarbonate (DEPC) in water. Solutions were made with deionised, distilled water treated with DEPC (Sigma Chemical Co., MO USA) and autoclaved. Harvested tissues were frozen rapidly in liquid nitrogen, and stored at -70 °C. Samples, between in the range of 80 to 100 mg from replicate specimens, were crushed in heat sterilised mortar and pestle, precooled to -70 °C with liquid nitrogen. Crushed samples were homogenised on ice in 6 ml of 6 M guanidinium hydrochloride (Gdn-HCl) and 100 µl of antifoam A (Sigma Chemical Co., MO., USA) with an IKA Ultra-Turrax T-25 tissue homogeniser at 20 000 rpm (Janke & Kunkel, Staufen, Germany). Following homogenisation, samples were centrifuged at 9 000 rpm on a Beckman Ti-75 rotor at 18 °C for 2 hours. The pellet was discarded, and the supernantant filtered through 0.5 µm filter (Millex SR, Millipore Co. MA USA). Potassium acetate (135 µl of 2.0 M

pH 5.0, adjusted with glacial acetic acid) was added to the filtrate, which was vortexed and then layered over a 4 ml 5.6 M cesium chloride cushion in a polyallomer (14 x 89 mm) ultracentrifuge tube (Beckman Instruments, CA., USA). Tubes were spun at 32 000 rpm in a Beckman SW-41 ultracentrifuge rotor for 18 h at 18 °C. The supernatant was aspirated, and the RNA pellet dissolved in 200 µl of DEPC-treated water. Instead of the precipitation step with 4M sodium acetate described by Nemeth *et al.* (1989), it was decided to further purify the RNA using an RNA purification kit (RNeasy total RNA kit, Qiagen, Hilden, Germany). RNA was thus purified using the instructions supplied by the kit, which employs the selective binding properties of silica gel-based membranes in a miniature spin column design. The RNA was finally redissolved in a volume of 60 µl of DEPC-treated water. The concentration of the RNA was determined spectrophotometrically at 260 nm, by employing an extinction coefficient of 1 representing a concentration of 40µg/ml. The quality of the RNA was judged by the A260/A280 ratio of absorbance of the sample, by scrutiny of the quality of the ribosomal RNA bands visualised on agarose gels and by the quality of ß-actin signal on Northern blots.

3.2.8.7.2 Formaldehyde-Agarose gel electrophoresis for fractionation of RNA

Reagents

2 % Stock agarose (electrophoresis grade) gel was made with DEPC-treated water and autoclaved. Agarose gel was utilised as required by melting the preformed gel in a microwave oven.

Gel loading buffer

50 % glycerol

1 mM EDTA

0.25 g bromophenol blue

Electrophoresis buffer, 5x concentrate

0.1 M MOPS

40 mM sodium acetate, pH 7.0

5 mM EDTA

The required amount of molten agarose was mixed with a volume of concentrated electrophoresis buffer to give a 1x concentration in the final preparation, and with formaldehyde (Merck, Darmstadt, Germany) to give a 2.2 M final concentration. The mixture was poured into an electrophoresis apparatus (Hybaid, UK). Agarose gels were generally prepared as 1% to 1.2 % agarose.

3.2.8.7.3 Sample preparation and electrophoresis

Prior to electrophoresis, samples of RNA containing 5 to 20 μg of RNA, were denatured at 65 °C for 15 minutes in a solution containing 50 % formamide (Merck, Darmstadt, Germany), 17.5 % formaldehyde and 1 x electrophoresis buffer. Samples were then mixed with 10 % of their volume with gel loading buffer, and electrophoresis was commenced at 3-5 volts per centimetre, until the bromophenol blue dye had reached two-thirds of the gel length. The gel was then stained with ethidium bromide (Sigma Chemical Co.) 10 ng/ml in 0.1 M ammonium acetate for 1 hour, and then destained for overnight with changes of DEPC treated water. The gel was photodocumented.

3.2.8.7.4 Transfer of RNA to membrane

Transfer and hybridisation solution: Saline Sodium Citrate (SSC)

A 20 x concentrate of this solution was prepared by adding 175.3 g of NaCl and 88.2 g of tri-sodium citrate to a final volume of 1 litre of water, and adjusting the pH to 7.0. Solution was sterilised by autoclaving.

Transfer of RNA to nylon membrane (Hybond N+, Amersham) was carried out by capillary blotting in an apparatus specific for the purpose (Life Science Technologies, UK) for 48 hours in the presence of 20 x SSC as described (Sambrook

et al., 1989). The membrane was baked *in vacuo* at 80 °C for 2 hours to effect crosslinking of RNA to membrane.

3.2.8.7.5 Probes and hybridisation

The following probes were used:

Type II collagen was a 2.2 kb fragment of the human gene, coding from amino acid 343 of the triple helix to 70 amino acids inside the C-propeptide (Baldwin *et al.*, 1989). cDNA for human type IV collagen alpha 2 was most of the collagenous domain and part of the non-collagenous domain (Hostikka *et al.*, 1988). cDNAs for collagens and gamma-actin were gifts of W. de Wet (University of the Witwatersrand, Johannesburg). cDNA for hOP-1, comprising a 679 bp fragment harboured within pÖ320 and covering amino acids 63-263 of the proregion and the first 25 amino acids of the mature polypeptide (Helder *et al.*, 1995), and cDNA for human TGF-$ß_1$ (pRK5-ß1E) containing the unmodified wild type TGF-$ß_1$ precursor (Derynck *et al.*, 1985) were kind gifts of S. Vukicevic (University of Zagreb, Croatia). cDNA for BMP-3 containing a 1508 bp insert including the full coding region of hBMP-3 (Wozney *et al.*, 1988) was a kind gift of A.H. Reddi, (Johns Hopkins University, Maryland, USA).

3.2.8.7.6 Amplification of constructs in E. coli

Eschericia coli strain XL1 blue was a kind gift of W de Wet, Department of Medical Biochemistry of the university. These were cultured in Luria-Bertani medium at 37 °C containing 1 % bacto-tryptone, 0.5 % bacto-yeast extract and 1 % NaCl (Life Technologies, UK), adjusted to pH 7.0 and autoclaved at 121°C for 20 minutes. Bacteria were grown on plates containing Luria-Bertani (LB) medium solidified by the presence of 1.5 % agar (Life Technologies, UK). These bacteria were made competent for transformation using the calcium chloride procedure of Cohen *et al.* (1972). A single colony was picked from a fresh plate and transferred to 100 ml LB broth and shaken vigorously for 3 hours at 37°C. Cells were transferred aseptically to sterile ice-cold 50 ml polypropylene tubes, and cultures cooled to 0°C by storing the tubes on ice for 10 minutes. Cells were recovered by centrifugation at 4000 rpm for 10 minutes at 4°C in an MSE centrifuge with type 43114-143 rotor. The pellet was resuspended in 10 ml of ice-cold 0.1 M $CaCl_2$ and left on ice for 10 minutes. Cells were recovered with centrifugation as before, and pellets resuspended in 4 ml of ice-cold 0.1 M $CaCl_2$. Cells were quick-frozen to -70°C in liquid nitrogen, and stored at -70°C until further use.

3.2.8.7.7 Transformation of E. coli

The method of Sambrook *et al.* (1989) was modified for execution on a small scale (W. de Wet, personal communication). Competent E. coli were thawed on ice and plasmid DNA, 50 ng in approximately 10-20 µl of sterile water was added and

mixed by gentle agitation. The tubes were stored on ice for 30 minutes. Tubes were transferred to a 42°C water bath for 90 seconds, then rapidly transferred to an ice bath for 1 to 2 minutes. An addition of 800 µl LB medium was made to the tube, and incubation at 37°C commenced for 45 minutes, to allow expression of selectable markers harboured on plasmid vectors. An aliquot of 200 µl was then streaked onto an agar LB plate, containing the specific antibiotic for selection of transformed bacteria, and plates incubated overnight at 37°C in an inverted position.

3.2.8.7.8 Preparation of plasmid DNA.

A kit for the purpose was obtained from Qiagen (Hilden, Germany). The method employes silica gel-membrane technology for the selective binding of DNA, and a combination of the alkaline lysis method of Birnboim and Doly (1979). Transformed colonies were picked for overnight culture in 2 ml of LB at 37°C. Cells were collected by centrifugation in a microcentrifuge (Hettich, Germany). Cells were lysed and total DNA extracted and adsorbed onto the spin column membrane supplied by the kit. DNA was washed free of contaminants and eluted in 10 mM Tris-HCl, 1 mM EDTA, pH 7.4 (TE buffer).

3.2.8.7.9 Preparation of probe labeled with alpha^{32}PdCTP.

The insert was cleaved from the vector DNA using suitable restriction endonucleases. Inserts were further purified to remove unwanted vector DNA, or used directly following the digestion reaction, with no effect upon the results.

Restriction digests of plasmid vectors (1 μg) and molecular weight markers (lamda phage DNA restricted with HindIII, Life Technologies) were run on an agarose gel (1.2 % agarose, containing Tris-borate buffer pH 8.0) at 5 volts per centimetre. DNA was visualised by UV irradiation on a transilluminator (UVP, CA., USA). The insert was identified according to molecular weight, and gel containing the fragment cut out with a scalpel blade. The DNA insert was purified from the gel using a kit (Qiagen, Qiaquick gel extraction kit, Hilden, Germany). The concentration of the DNA was determined spectrophotometrically at 260 nm, where an absorbance of 1 unit represents a DNA concentration of 50 μg per ml. DNA (25 ng) was labelled with alpha (^{32}P)dCTP (Amersham, UK) using a random prime labeling kit (Megaprime DNA labeling kit, Amerhsham, UK). Unincorporated label was removed using a DNA purification kit (Qiaquick, Qiagen, Hilden, Germany) and the purified probe used for hybridisation.

3.2.8.7.10 Hybridisation of probes and detection

Hybridisation was carried out in 50 ml conical polypropylene tubes in a hybridisation oven (Hybaid Corp. UK). Probe was mixed with 100 µl of sonicated, fragmented, denatured salmon sperm DNA (10 mg/ml) and boiled for 2 minutes. Membranes were prehybridised with a hybridisation reagent (3 ml) supplied commercially for this purpose (QuickHyb, Stratagene, La Jolla, CA., USA) for 20 minutes at 68 °C. Probe was added and hybridisation commenced for one to two hours at 68 °C, except for type IV collagen detection, which was done at 72 °C, owing to non-specific binding of the probe to GC rich sequences of ribosomal RNA at lower temperatures (W. de Wet, personal communication). Membranes were washed twice for 15 minutes at room temperature with 150 ml of 2 x SSC, 0.1 % SDS, followed by a single wash at 68 °C with 0.1 x SSC, 0.1 % SDS. The type IV collagen blot was washed at 72 °C to achieve a higher stringency. Membranes were briefly blotted dry and covered with Saran wrap. Autoradiography was performed with Kodak Biomax MS film at - 70 °C for given time periods, ranging between 16 hours to 5 days. Films were processed and photographed.

3.2.8.7.11 Signal quantitation

The signal intensity for each lane was quantitated by scanning densitometry (Biomed Instruments Inc., CA., USA), and normalised against values obtained for the γ-actin signal. Values were arbitrarily adjusted to relative densitometric units onto a scale of 100.

3.3 RESULTS AND DISCUSSION

3.3.1 THE HETEROTOPIC STUDY IN THE RAT

3.3.1.1 Histological and biochemical analyses

Figure 12 (next page). *Representative toluidine blue stained sections of tissues generated in the subcutaneous space of the rat by morphogen combinations on day 12. 1 μg rhOP-1 (A) was combined with 50 (B), 150 (C) and 500 ng (D) rhTGF-β1 per 25 mg collagenous matrix. Note dose dependent increase in cartilage formation in implants containing rhTGF-β1. Original magnification 25x.*

A
B
C
D

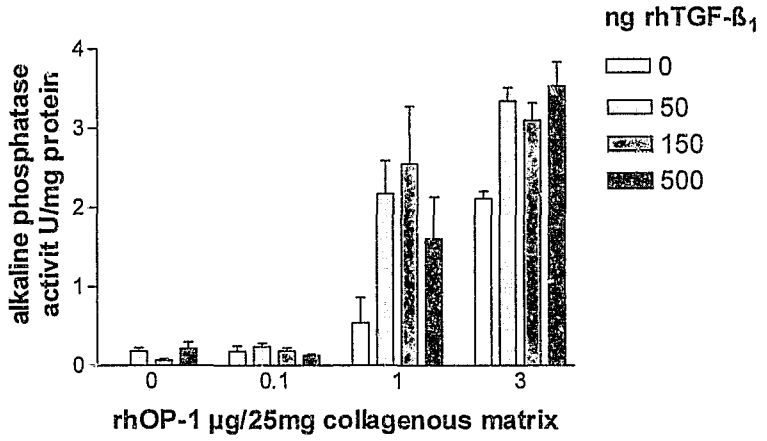

Figure 13. *Implantation of rhOP-1 and rhTGF-ß1, both singly and in combination in the rat subcutis as described in Methods. Generated tissues were harvested at 12 days post-implantation and alkaline phosphatase activity determined as described in Methods. Single applications of rhOP-1 induced dose dependent changes in alkaline phosphatase activity (p=0.000022), whereas rhTGF-ß1 did not. The two morphogens, when in combination, induced significant increases in alkaline phosphatase (p=0.0096).*

In rats, single applications of rhTGF-$ß_1$ were inactive at the doses tested (Figure 13). Single applications of rhOP-1 gave rise to a dose dependent response in alkaline phosphatase activity. Addition of comparatively low amounts of rhTGF-$ß_1$ to implants containing 1 and 3 µg rhOP-1 gave rise to a two to four-fold rise in alkaline phosphatase activity. Due to the fact that single applications of rhTGF-$ß_1$ are inactive (as confirmed histologically with lack of cartilage or bone formation), all cases where binary combinations of the two morphogens caused increases in alkaline phosphatase activity (Figure 13) are classified as cases of synergistic interaction

(Greco *et al.*, 1995). Strong synergistic interaction was shown for combinations of 1 µg rhOP-1 with 50 ng of rhTGF-$ß_1$ that gave rise to activity equal to that elicited by single application of 3µg rhOP-1. Data were used in isobolographic analysis, to confirm synergistic interaction, and to measure the intensity of the interaction (section *3.3.1.2*).

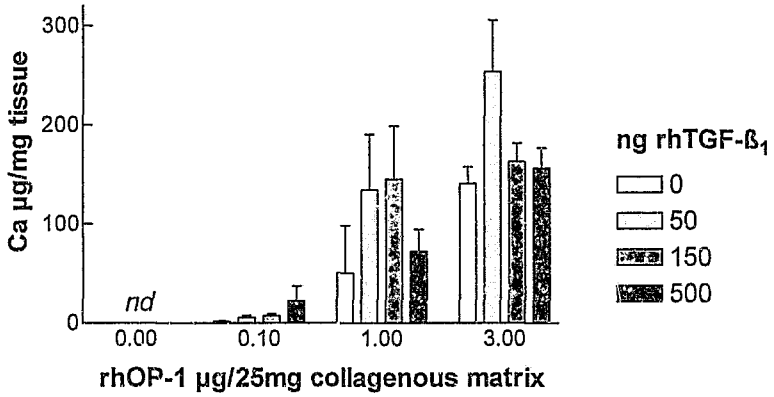

Figure 14. *Calcium content of tissues generated by rhOP-1 and rhTGF-ß1, both singly and in combination in the rat subcutis on day 12. Single applications of OP-1 caused dose dependent increases in calcium content (p=0.0035), whereas rhTGF-ß1 did not. The interaction of the two morphogens, resulted in increases in calcium content, however, this increase was not statistically significant at the sample size chosen (p=0.292).*

Tissues generated by single applications of rhTGF-$ß_1$ were inactive at the doses tested, and was reflected in the undetectable levels of calcium (*nd*, Figure 14). Single

applications of rhOP-1 gave rise to a dose dependent increase in calcium content. Addition of comparatively low amounts of TGF-$ß_1$ to implants containing 1 and 3 µg rhOP-1 gave rise to a two-fold rise in calcium content of the newly induced ossicles. Combinations of 1 µg rhOP-1 with 50 and 150 ng of rhTGF-$ß_1$ gave rise to calcium content equivalent to that elicited by 3 µg rhOP-1 alone. Interestingly, synergism occurred in a biphasic manner related to dose of rhTGF-$ß_1$. At higher doses of rhTGF-$ß_1$, there was a decrease in the observed synergistic effect in terms of calcium content. It may be that generated tissue growth exceeds mineralisation rate, causing a drop in the ratio of calcium to tissue mass. Alternatively, the biphasic mode of action might be analogous to that described by Rosen *et al.* (1990), where it was suggested that TGF-ßs may stimulate bone formation at low levels, cartilage formation at higher levels and fibrosis at even higher levels. Indeed, histologic examination of generated tissues showed a strong correlation between doses of rhTGF-$ß_1$ and induction of cartilage tissue in combinations with 1 µg rhOP-1 (Figure 12).

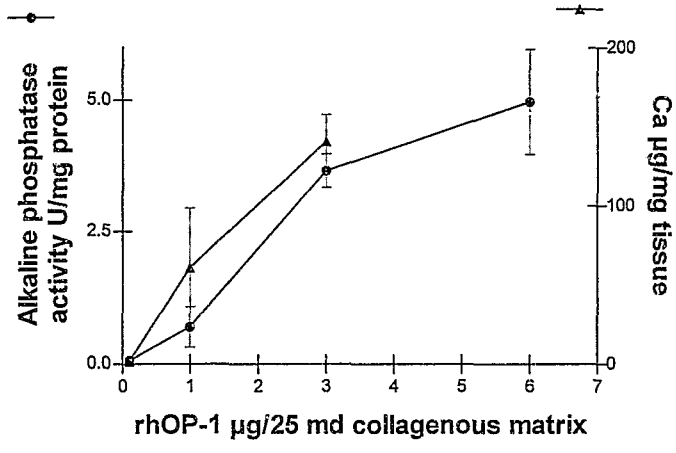

Figure 15. *Dose response curve showing changes in alkaline phosphatase activity and calcium content in response to rhOP-1 implanted in the rat subcutaneous space. Calcium content at the 6 µg dose was not available. Alkaline phosphatase activity and calcium content changes were significant (p=0.00002 and p= 0.0013 respectively).*

Implantation of rhOP-1 at doses of 0.1, 1, 3 and 6 µg/25 mg collagenous matrix in the in subcutaneous space of the rat, resulted in a dose dependent increase in the parameters of calcium content and alkaline phosphatase activity. The curve was classically sigmoidal nature, showing strong response in the range of 1 to 3 µg and plateauing off at 6 µg of rhOP-1.

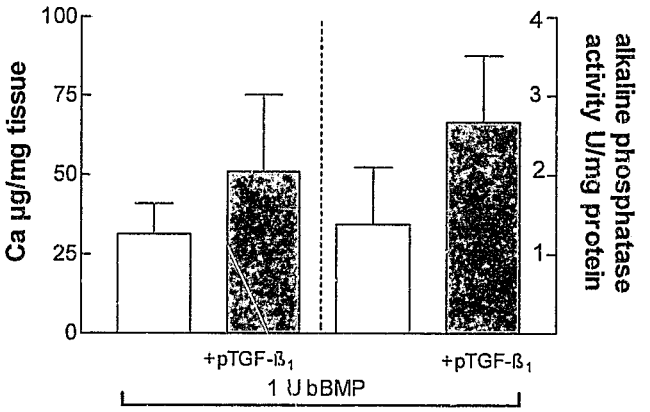

Figure 16. *Calcium content and alkaline phosphatase activity of tissues generated in the rat subcutis with binary combinations of porcine TGF-β_1 and bovine BMP. Alkaline phosphatase activity was significantly higher for the morphogen combination ($p=0.042$).*

BMP purified from bovine bone was implanted into the subcutaneous space of the rat at a dose of 1 unit alkaline phosphatase activity/25 mg collagenous matrix. The criteria used to define bovine BMP activity have been described in Chapter 2. Contralateral sites were implanted with the same dose of bBMP in conjunction with 150 ng of pTGF-β_1. Generated tissues were harvested at 12 days post implantation and analysed for alkaline phosphatase activity (right panel) and calcium content (left panel, Figure 16). A 50% increase in calcium content and a 100% increase in alkaline phosphatase was measured in bone generated with combinations of bBMP and pTGF-β_1. Since TGF-β_1 is inactive in the rat subcutis, the combined actions of

the two morphogens conform to the criteria for synergism, eliciting an activity which is greater than the sum total of their individual activities.

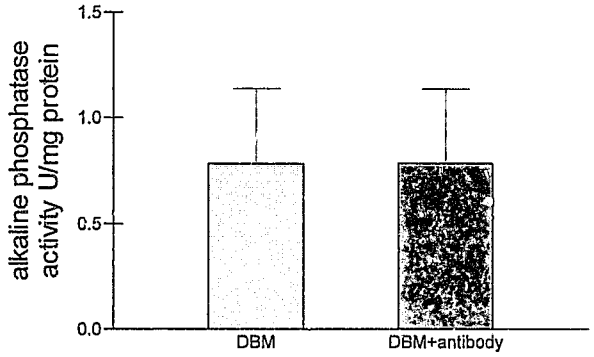

Figure 17. *Effect of single application of anti-TGF-$\beta_{1/1.2}$-antibody on heterotopic osteogenesis by demineralised bone matrix in the rat.*

Rat demineralised bone matrix (DBM) was implanted in the rat subcutis, and contralateral sites were implanted with DBM containing 10 µg of chicken anti-pTGF-β_1 and -ß1.2 (R&D Systems, OX, UK, product no. AB-101-NA), known to have cross-reactivity with murine TGF-β_1. This experiment aimed to show, at the doses tested, whether inactivation of TGF-ß by anti-body binding might have an effect on the osteoinductive cascade elicited by DBM. Explants at 12 days were analysed for alkaline phosphatase activity (Figure 17). No significant differences were found between the two groups ($p>0.05$, two-tailed t-test).

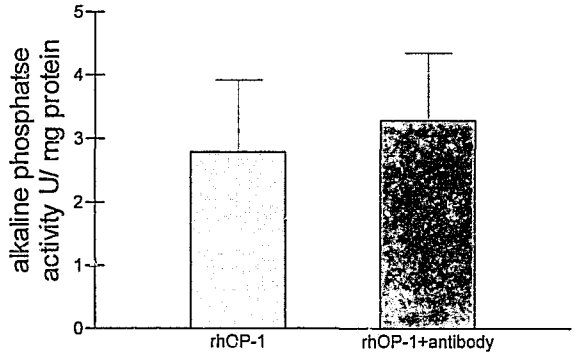

Figure 18. *Effect of single application of anti-TGF-$\beta_{1/1.2}$-antibody on heterotopic osteogenesis by rhOP-1 in the rat.*

Insoluble collagenous bone matrix containing 3 µg of rhOP-1 was implanted in the rat subcutis as described, and contralateral sites were implanted with the same dose containing in addition 10 µg chicken anti-pTGF-β_1 and -$\beta_{1.2}$ (R&D Systems, OX., UK, product no. AB-101-NA), known to have cross-reactivity to murine TGF-β_1. This experiment aimed to show whether anti-TGF-ß antibody might have an effect on the osteoinductive cascade elicited by rhOP-1. Explants were analysed at 12 days for alkaline phosphatase. No significant differences were found between the two groups ($p>0.05$, two-tailed t-test). At the doses tested, it appears that a single application of specific anti-TGF-ß antibodies does not alter significantly the bone induction cascade elicited by BMPs/OPs. Whether the dosage range was correct for purposes of the investigation will require further experiments with wider dosage ranges, multiple applications and different antigen specificities.

3.3.1.2 ISOBOLOGRAPHIC ANALYSIS OF INTERACTION OF rhOP-1 AND rhTGF-$ß_1$ IN THE RAT SUBCUTANEOUS BIOASSAY.

Isobolographic analysis is effectively a way to represent a three-dimensional array of data on two sets of two-dimensionl graphs. In effect, isobolographic analysis is a response surface method (Greco *et al.*, 1995). A response surface, as the name implies, is comprised of three dimensions; an az (vertical) dimension representing the effect *E*, alkaline phosphatase in the present case, and an xy plane representing doses of agent 1 (x) and agent 2 (y) respectively. The response surface of alkaline phosphatase activity for combinations of rhOP-1 and rhTGF-$ß_1$ is shown in Figure 19B. Figure 19A, is the predicted response surface calculated from dose effect data of single applications of rhOP-1 and rhTGF-$ß_1$. Since rhTGF-$ß_1$ is inactive when applied singly, then the predicted outcome for combinations of the two morphogens is essentially the effect (E) for rhOP-1 alone. Figure 19B demonstrates clearly how addition of rhTGF-$ß_1$ to rhOP-1 increases alkaline phosphatase activity (E).

Figure 19 (next page). *Response surface plots. Alkaline phosphatase activity data for tissues generated by single and combined applications of rhOP-1 and rhTGF-β_1 in the rat, were plotted on an xyz set of axes.*

A: predicted response surface from data of single applications of rhOP-1 and rhTGF-β_1, assuming additive interaction. Since rhTGF-β_1 was inactive in the rat, the plot in A is essentially contribution from rhOP-1 only.

B: response surface plot of data obtained from rats, for single and combined applications of rhOP-1 and rhTGF-β_1. rhTGF-β_1 was inactive when used singly, in the dosage range 0 to 500 ng per 25 mg collagenous matrix. Single applications of rhOP-1 dose dependently increased alkaline phosphatase activity in the range from 0 to 3 μg rhOP-1/25 mg collagenous bone matrix. Combined applications of rhOP-1 and rhTGF-β_1 interacted synergistically to increase alkaline phosphatase activity in tissues generated in the subcutaneous space of the rat by day 12.

a

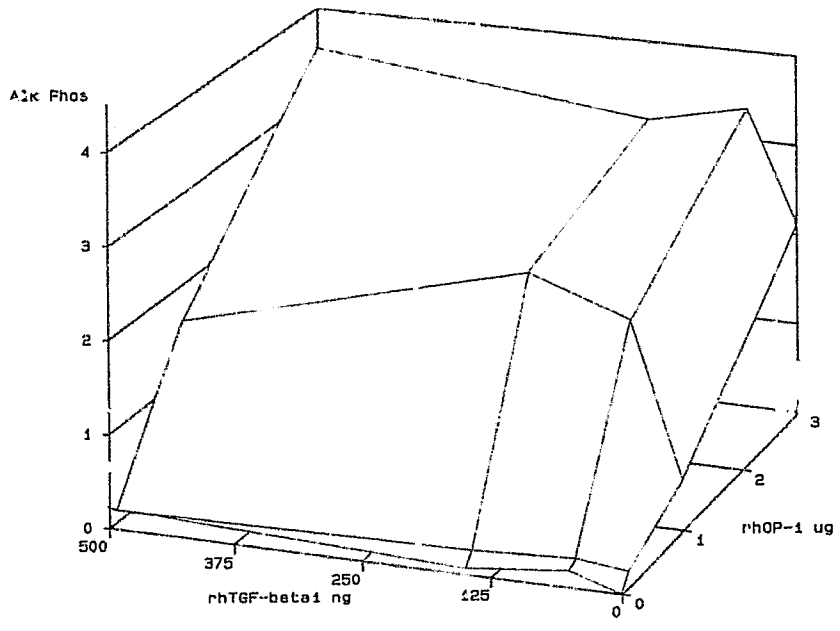
Alk Phos
4
3
2
1
0
500
375
250
125
0
rhTGF-beta1 ng
0
1
2
3
rhOP-1 ug

b

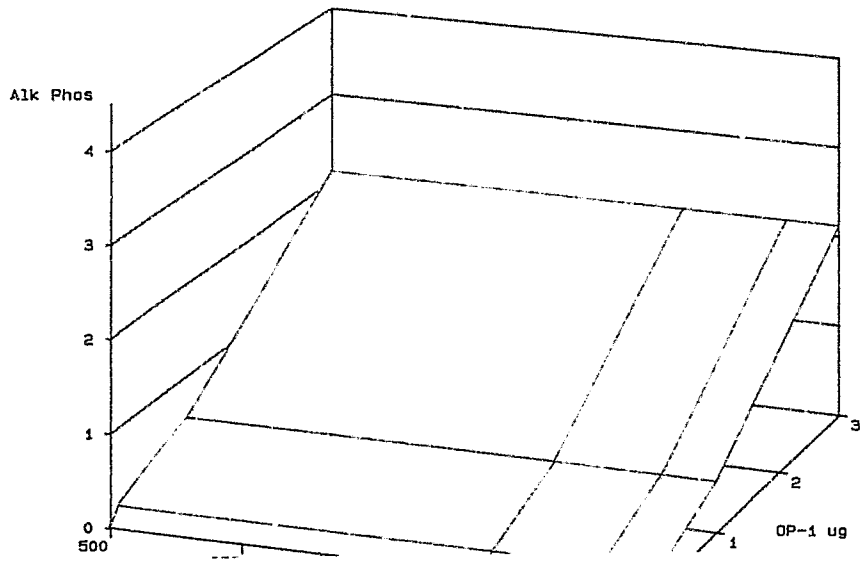
Alk Phos
4
3
2
1
0
500
0
1
2
3
OP-1 ug

Figure 20 (opposite). *Calculation of $D_{OP\text{-}1}/Dm_{OP\text{-}1}$, $D_{TGF\text{-}\beta 1}/Dm_{TGF\text{-}\beta 1}$, for use in isobolographic analysis of morphogen interaction in heterotopic sites of the rat on day 12. Dose effect data (alkaline phosphatase activity) for rhOP-1, in combination with different doses of rhTGF-β_1 were plotted in:*

A: rhOP-1 for given levels of rhTGF-ß

B: rhTGF-β_1 for given levels of rhOP-1.

The Hill model in A, and a second order polynomial equation in B was applied using a computer program for the purpose (Prism™, GraphPad Software, CA, USA), and $D_{OP\text{-}1}$ and $D_{TGF\text{-}\beta 1}$ (ED_{50}) on the x-axis, corresponding to 50% Emax on the y-axis, determined. $Dm_{OP\text{-}1}$ and $Dm_{TGF\text{-}\beta 1}$ was obtained from A and B at dose levels of 0 µg for rhTGF-β_1 and 0 µg for rhOP1 respectively. The data obtained and manipulations leading to the calculation of $D_{OP\text{-}1}/Dm_{OP\text{-}1}$, $D_{TGF\text{-}\beta 1}/Dm_{TGF\text{-}\beta 1}$ (Table 4), are the cartesian co-ordinates employed for isobolographic analysis (Figure 20).

For dose effect curves of rhOP-1 (Figure 20A), synergistic intensity, as judged by ED_{50} values, was strongest with combinations of the lower doses of rhTGF-β_1 of 150 and 50 ng, and weaker at 500 ng rgTGF-β_1. Inspection of dose effect curves of rhTGF-β_1 (Figure 20B), showed TGF-β_1 to be ineffective at all doses, including cases when in combination with 100 ng rhOP-1. At higher dosage levels of rhOP-1, TGF-β_1 caused a biphasic change in alkaline phosphatase activity (Figure 20B).

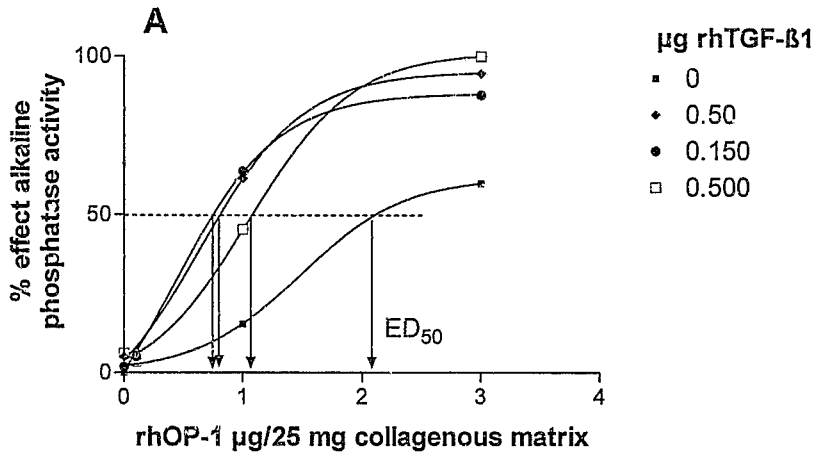
A
% effect alkaline phosphatase activity
100
50
0
0
1
2
3
4
ED50
rhOP-1 µg/25 mg collagenous matrix
µg rhTGF-ß1
0
0.50
0.150
0.500

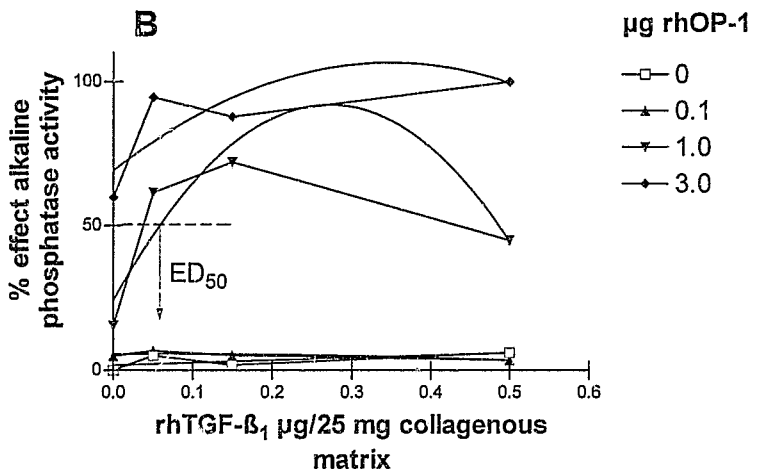
B
% effect alkaline phosphatase activity
100
50
0
0.0
0.1
0.2
0.3
0.4
0.5
0.6
ED50
rhTGF-ß1 µg/25 mg collagenous matrix
µg rhOP-1
0
0.1
1.0
3.0

Table 4. *Calculation of $D_{OP\text{-}1}/Dm_{OP\text{-}1}$, $D_{TGF\text{-}\beta1}/Dm_{TGF\text{-}\beta1}$, for use in isobolographic analysis of morphogen interaction in heterotopic sites of the rat on day 12.*

$D_{TGF\text{-}\beta1}$ µg	$D_{ED50,OP1}$	$D_{ED50,OP1}/Dm_{OP\text{-}1}$	$D_{TGF\text{-}\beta}/Dm_{TGF\text{-}\beta}$	$D_{OP\text{-}1}$ µg	$D_{ED50,TGF\text{-}\beta1}$	$D_{ED50,TGF\text{-}\beta1}/Dm_{TGF\text{-}\beta1}$	$D_{OP\text{-}1}/Dm_{OP\text{-}1}$
0	2.111 =$Dm_{OP\text{-}1}$			0	5.669 =$Dm_{TGF\text{-}\beta1}$		
0.05	0.809	0.383	0.0089	0.1			
0.15	0.751	0.356	0.026	1	0.068	0.012	0.474
0.50	1.079	0.511	0.088	3			

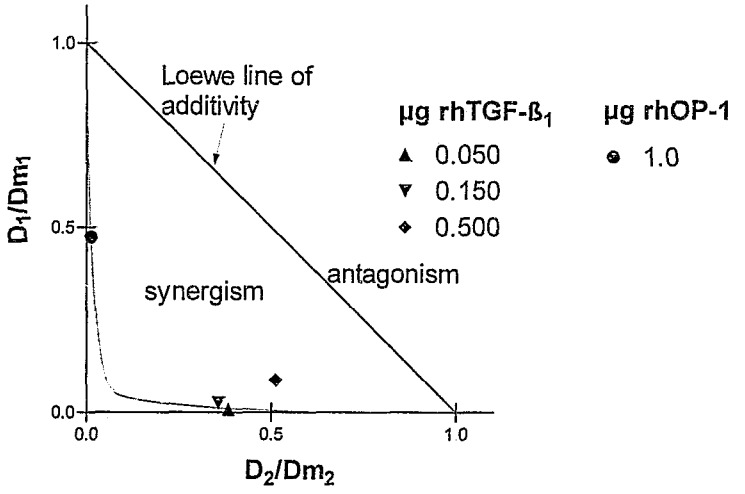

Figure 21. *Isobolographic analysis of morphogen interaction in heterotopic sites of the rat on day 12. Isobologram shows data derived from alkaline phosphatase activity values obtained from tissues generated by single and combined applications of rhOP-1 and rhTGF-β_1 in the subcutaneous space of the rat. The position of points below Loewe's line of additivity indicates that rhOP-1 and rhTGF-β_1 interact synergistically to induce changes in alkaline phosphatase activity. For dose effect curves of rhOP-1, synergistic intensity was strongest for 150 and 50 ng rhTGF-β_1, being weaker for 500 ng TGF-β_1. Only one point could be obtained for TGF-β_1 dose effect curves (Figure 20 B), since TGF-β_1 itself was inactive, and the dose effect curve of rhTGF-β_1 in combination with 3 µg rhOP-1 was already above 50% of Emax.*

The isobolographic analysis (Fig. 21) reflects accurately classical synergism where TGF-$ß_1$, itself inactive, is capable of increasing parameters of bone formation induced by rhOP-1 when in binary combinations. The isobole points therefore, fall very closely to the x and y axis. In conclusion, the type of interaction arising out of binary combinations of rhTGF-ß1 and rhOP-1 in the rat heterotopic assay, is synergism as defined by Greco *et al.*, (1995).

3.3.2 THE HETEROTOPIC INTRAMUSCULAR STUDY IN THE BABOON

Gross observations

Palpation of the rectus abdominis of both Group 1 and Group 2 primates at the time of harvest revealed the larger size of tissue generated with combinations of TGF-$ß_1$ and rhOP-1, and which appeared to depend on the doses of TGF-$ß_1$ used. Ossicles were excised with a small layer of surrounding muscle, and cut through the plane of greatest diameter. Exposed surfaces showed mineralisation of the external cortex and were reddish-brown in the gross indicating the presence of bone marrow and associated highly vascular tissue. Samples were processed for histology and histomorphometric analysis. Samples were further analysed for alkaline phosphatase activity, calcium content and used for isolation of total RNA for Northern analysis.

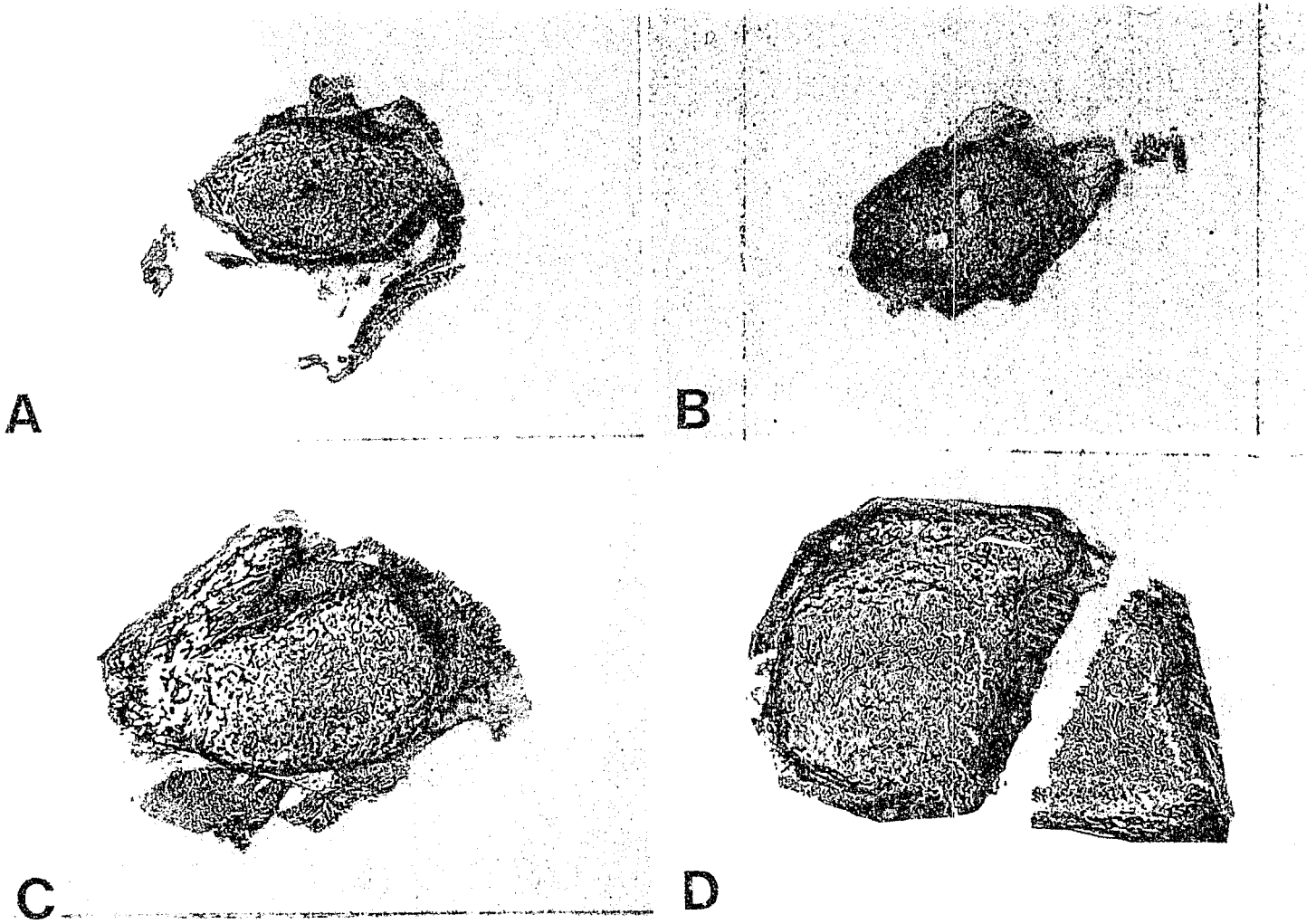
A
B
C
D

3.3.2.1 Group 1 Primates: heterotopic study with recombinant OP-1 and recombinant TGF-$ß_1$

3.3.2.1.1 30 day study

Histology

Figure 22 (opposite). *Synergistic activity of rhOP-1 and rhTGF-$ß_1$ in the rectus abdominis of the baboon on day 30. rhOP-1 and rhTGF-$ß_1$ were implanted singly and in combination, delivered with 100 mg collagenous matrix as carrier.*

A and B: bone induction by a single administration of 5 µg rhTGF-$ß_1$ (A) and 25 µg rhOP-1 (B).

C and D: Ossicles generated by 25 µg rhOP-1 combined with 0.5 (C) and 1.5 µg rhTGF-$ß_1$ (D). Original magnification (A, B, C and D) 3.5X.

Single applications of rhOP-1 and rhTGF-$ß_1$ induced new bone formation by day 30, as shown histologically (Figures 22A and 22B). The co-administration of comparatively low doses of rhTGF-$ß_1$ with rhOP-1 resulted in large corticalised ossicles with marrow. Generated bone tissue showed typical histological features of mineralised bone covered by osteoid seams, and populated by contiguous osteoblasts.

Figure 23 (opposite). *Synergistic tissue morphogenesis by combinatorial action of doses of recombinant morphogens in the rectus abdominis of the baboon, 30 days post-implantation.*

A and B: Ossicles generated by 25 μg rhOP-1 combined with 1.5 (A) and 5 μg rhTGF-β_1 (B).

C and D: Large ossicles generated by 125 μg rhOP-1 combined with 5 μg rhTGF-β_1. Note the maturational gradient of tissue organisation from the periphery to the centre of the ossicles, with 'voids' surrounded by delicate trabeculae of newly formed bone and, occasionally, by scattered remnants of collagenous matrix (A, B, C and D: Goldner's trichrome stain, original magnification x3).

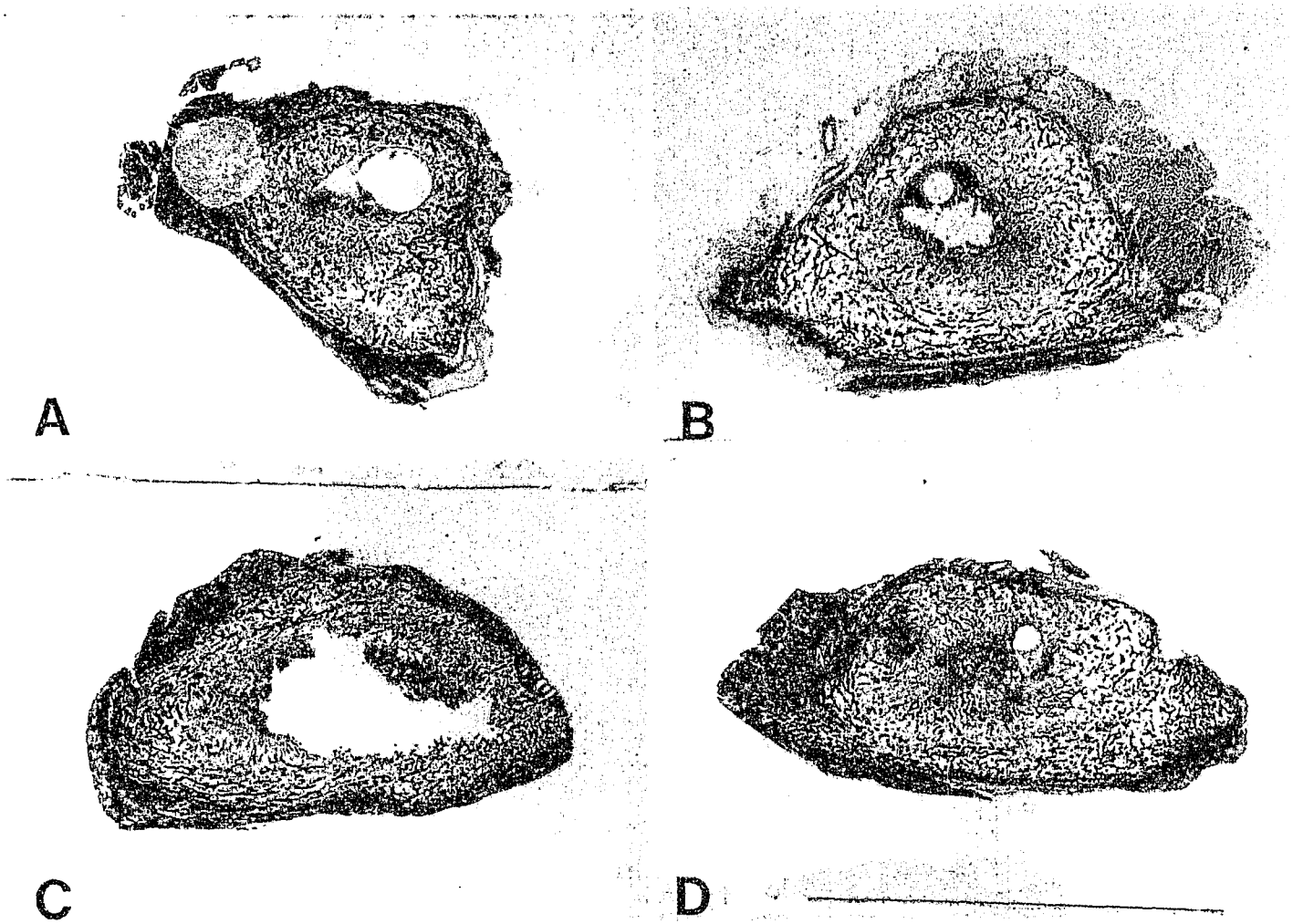
A
B
C
D

Histomorphometry

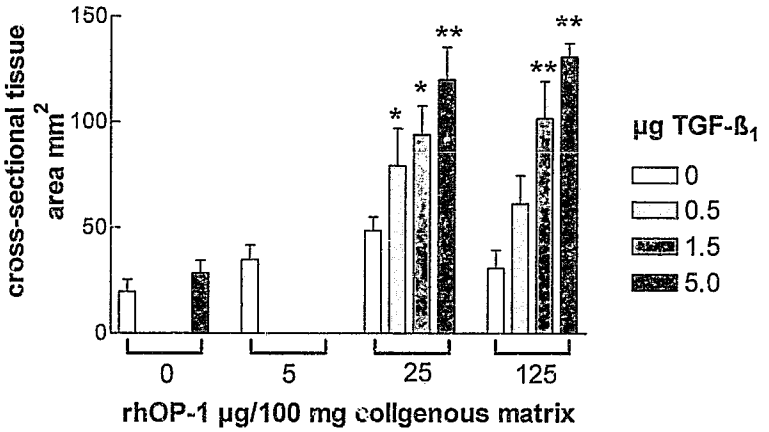

Figure 24. *Computerised analysis of histologic cross-sectional tissue area for tissues generated by single and combined applications of rhTGF-β_1 and rhOP-1 in the rectus abdominis of the baboon on day 30. Values are mean ±SEM of 4 to 8 observations per group. *P<0.05 vs rhOP-1 of single application; **P<0.05 vs the combination of 25 and 0.5, 1.5 µg rhTGF-β_1, and vs 125 µg rhOP-1 combined with 0.5 µg rhTGF-β_1 respectively. At the 25 µg rhOP-1 dose alone, cross-sectional tissue area was significantly greater than any other dose, except for 5µg rhOP-1 .*

The addition of rhTGF-β_1 to rhOP-1 dose-dependently increased cross-sectional tissue areas to a maximal two- and three-fold for doses of 25 µg and 125 µg rhOP-1

respectively (Fig. 24). Interestingly, single application of rhOP-1 showed a dose-dependent biphasic relationship with cross-sectional area of generated tissue, so that there was little difference between parameters of the 25 μg rhOP-1 group and the 125 μg rhOP-1 group.

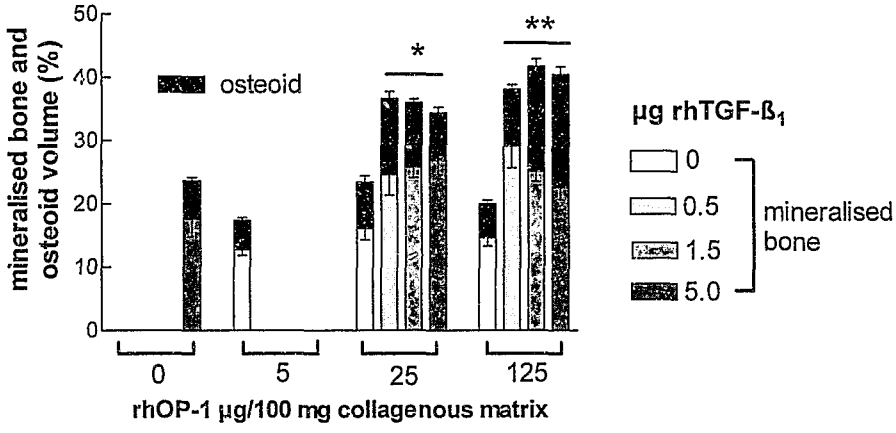

Figure 25. *Volume fractions (in %) of mineralised bone and osteoid on day 30, of ossicles generated at heterotopic sites in the baboon by single and combined applications of rhTGF-ß1 and rhOP-1. *P<0.05 vs 25 µg rhOP-1 dose response; **P<0.05 vs single application of 125 µg rhOP-1.*

As for cross-sectional tissue area, single application of rhOP-1 did not yield the typical sigmoidal dose relationship when evaluated on day 30, but rather a biphasic one, in which there is an initial dose-dependent increase in mineralised bone and osteoid, followed by a reduction in said parameters at the highest dose, though not of statistical significance (Figure 25). Addition of rhTGF-ß1 at doses of 0.5, 1.5 and 5 µg to rhOP-1 at doses of 25 and 125 µg per 100 mg collagenous matrix, increased mineralised bone up to two-fold at doses as low as 0.5 µg rhTGF-ß1. Addition of rhTGF-ß1 to rhOP-1 had a marked effect on osteoid volume, causing a 4-fold increase for combinations of 125 µg rhOP-1 and 5 µg rhTGF-ß1. Single application of rhTGF-ß1 of 5 µg per 100 mg collagenous matrix induced mineralised bone and

osteoid volumes similar to that elicited by single applications of rhOP-1. This is a first account of bone induction in heterotopic sites by any TGF-ß isoform.

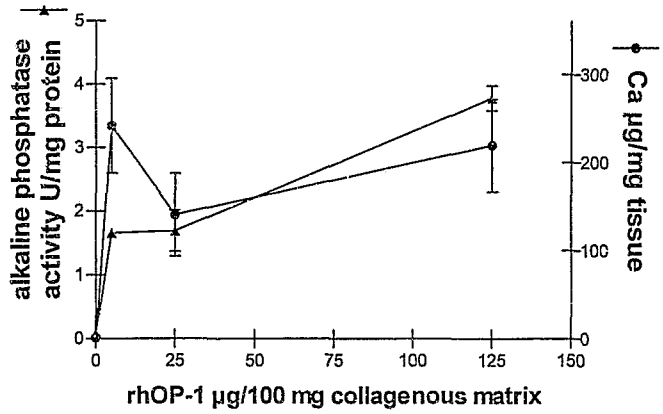

Figure 26. *Dose response curve on day 30, showing changes in alkaline phosphatase activity and calcium content of ossicles generated in response to single application of rhOP-1 implanted in the rectus abdominis of the baboon. Changes in alkaline phosphatase activity were significantly higher for the 125 µg rhOP-1 dose ($p<0.5$). The intermediate dose of 25µg rhOP-1 induced significantly less calcium content in generated tissues when compared to the 5 and 125 µg dose of rhOP-1.*

At the time period evaluated of 30 days, the classic sigmoidal relationship, was not evidenced (Figure 26). Instead, there was a decrease in the said parameters for the intermediate dose of rhOP-1, which coincided with histomorphometrical *increases* in mineralised bone and osteoid volumes. The same experiment conducted over a 15 day evaluation period (section 3.3.2.1.3) however yielded dose-dependent changes in biochemical parameters. The data suggest that the observed trends may be a function

of time. There was a correlation between day 30 calcium content and alkaline phosphatase activity changes, demonstrating a direct relationship between the two indices of bone formation. The synthesis of alkaline phosphatase is a dynamic process during bone induction, reaching a peak before decreasing to steady state levels. Interpretation of the results is difficult without additional time point data.

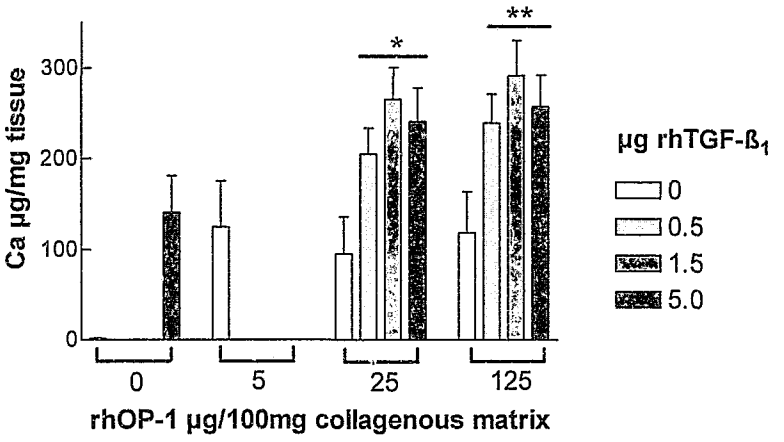

Figure 27. *Calcium content on day 30 of tissues generated by single and combined applications of rhOP-1 and rhTGF-β_1 in the rectus abdominis of the baboon. Values are mean ± SEM for 4 to 8 observations per group. *P<0.05 vs 25 µg rhOP-1; **P<0.05 vs 125 µg rhOP-1.*

The calcium content on day 30 of tissues generated by single and combined applications of rhOP-1 and rhTGF-β_1 are shown in Figure 27. A dose of 5 µg of rhTGF-β_1 induced mineralisation comparable to that of single applications of rhOP-1. The morphogens interacted optimally at the intermediate dose of 25µg rhOP-1, where the addition of comparatively low doses of rhTGF-β_1 initiated a dose dependent increase in calcium content. The combination of 1.5 µg of rhTGF-β_1 and 25 µg of rhOP-1 resulted in a 2.8-fold increase in calcium content with respect to single application of rhOP-1 and a 2.0 fold increase with respect to single application of 5 µg rhTGF-β_1. Furthermore, the said combination resulted in tissue bearing twice the mineral content when compared to single application of a 5-fold higher rhOP-1

dose of 125 μg or a 3.3-fold higher dose of rhTGF-β_1 (5 μg). The data suggest that the two morphogens may interact synergistically during heterotopic bone formation in the primate. This notion was confirmed by isobolographic analysis.

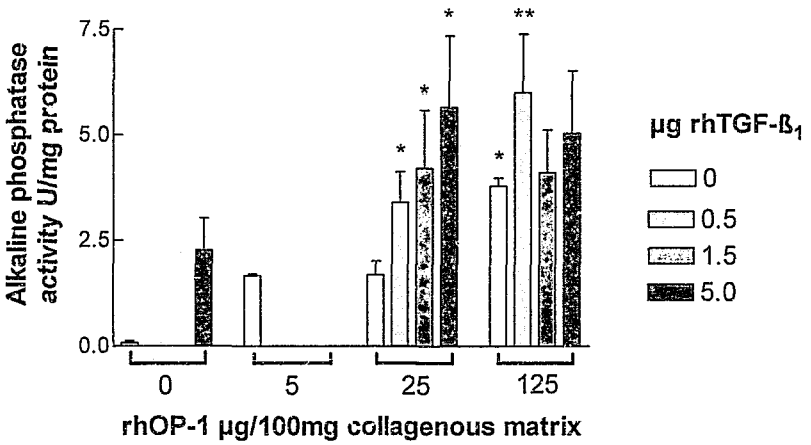

Figure 28. *Alkaline phosphatase activity on day 30 of tissues generated by the implantation of single and combined applications of rhOP-1 and rhTGF-ß1 in the rectus abdominis of the baboon. Values are mean ±SEM for 4 to 8 observations per group. *P<0.05 vs 25 µg rhOP-1; **P< 0.05 vs 5 and 25 µg rhOP-1.*

5 µg of rhTGF-ß1 induced alkaline phosphatase activity comparable to levels induced by single applications of rhOP-1 (Fig. 28). The addition of comparatively low doses of rhTGF-ß1 caused a dose dependent increase in alkaline phosphatase activity. The combination of 5 µg of rhTGF-ß1 and 25 µg of rhOP-1 resulted in a 3.5-fold increase in alkaline phosphatase activity with respect to rhOP-1 and a 2.5 fold increase with respect to rhTGF-ß1, a level surpassing by 30 % that elicited by single application of 125 µg of rhOP-1. These data demonstrate that the observed combination osteogenesis conforms with the criteria of synergism. At higher doses of 125 µg rhOP-1, co-administration of TGF-ß1 caused increase in alkaline

phosphatase activity which were less marked, and with no clearly discernible trend. Since the most concrete method of scoring bone formation is morphometrical analysis, and alkaline phosphatase activity is a dynamic expression in the developing ossicle which experiences a peak of activity during the developmental cascade (Cunningham *et al.*, 1992), results were further interpreted with the combined consideration of histomorphometric data. To determine the nature of the morphogen interaction, isobolographic analysis was performed.

3.3.2.1.2 Group 1 Primates: Isobolographic analysis

Figure 29. *Determination of $D_{OP\text{-}1}/Dm_{OP\text{-}1}$, $D_{TGF\text{-}\beta1}/Dm_{TGF\text{-}\beta1}$, for use in isobolographic analysis of morphogen interaction in heterotopic sites of the baboon on day 30.*

Dose effect data (alkaline phosphatase activity) for rhOP-1, in combination with different doses of rhTGF-β_1 were plotted in;

A: rhOP-1 for given levels of rhTGF-β_1

B: rhTGF-β_1 for given levels of rhOP-1.

A second order polynomial model was applied using a computer program for the purpose (Prism™, GraphPad Software, CA, USA), and D obtained for 50% Emax. $Dm_{OP\text{-}1}$ and $Dm_{TGF\text{-}\beta1}$ was obtained from A and B at dose levels of 0 µg for rhTGF-β_1 and 0 µg for rhOP1 respectively. The data obtained were used to calculate $D_{OP\text{-}1}/Dm_{OP\text{-}1}$, $D_{TGF\text{-}\beta1}/Dm_{TGF\text{-}\beta1}$, which are the cartesian co-ordinates that were used to construct the isobologram (Figure 30).

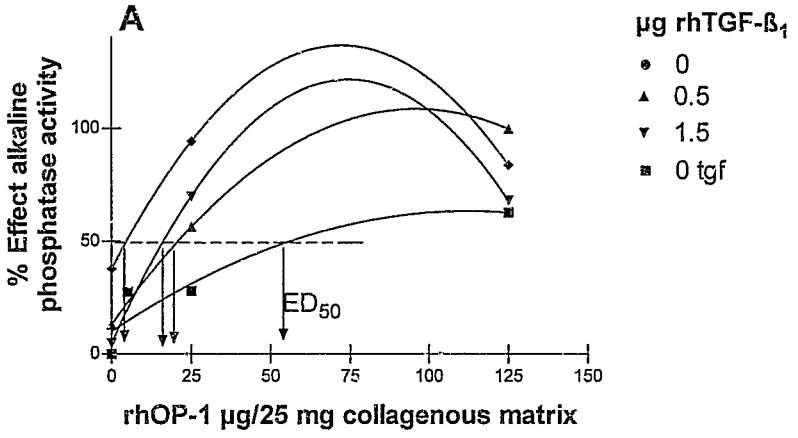
A
% Effect alkaline phosphatase activity
100
50
0
0
25
50
75
100
125
150
ED50
rhOP-1 µg/25 mg collagenous matrix
µg rhTGF-ß1
0
0.5
1.5
0 tgf

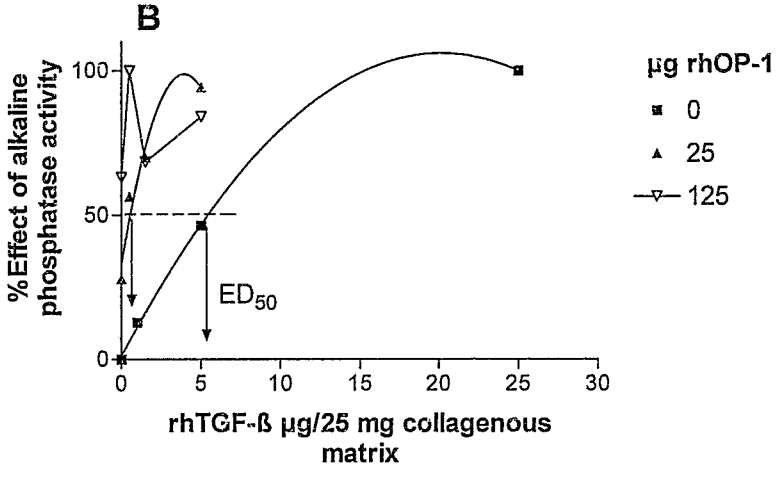
B
%Effect of alkaline phosphatase activity
100
50
0
0
5
10
15
20
25
30
ED50
rhTGF-ß µg/25 mg collagenous matrix
µg rhOP-1
0
25
125

Table 5. Parameters obtained from graphs A and B of Figure 29 for calculation of $D_{OP\text{-}1}/Dm_{OP\text{-}1}$, $D_{TGF\text{-}\beta 1}/Dm_{TGF\text{-}\beta 1}$, for use in isobolographic analysis.

$D_{TGF\text{-}\beta 1}$	$D_{ED50,OP1}$	$D_{ED50,OP1}/Dm_{OP\text{-}1}$	$D_{TGF\text{-}\beta}/Dm_{TGF\text{-}\beta}$	$D_{OP\text{-}1}$	$D_{ED50,TGF\text{-}\beta 1}$	$D_{ED50,TGF\text{-}\beta 1}/Dm_{TGF\text{-}\beta 1}$	$D_{OP\text{-}1}/Dm_{OP\text{-}1}$
0	55.97 $=Dm_{OP\text{-}1}$			0	5.42 $=Dm_{TGF\text{-}\beta 1}$		
0.5	20.79	0.371	0.09	5			
1	16.19	0.289	0.18	25	0.554	0.102	0.447
5	4.65	0.083	0.922	125			

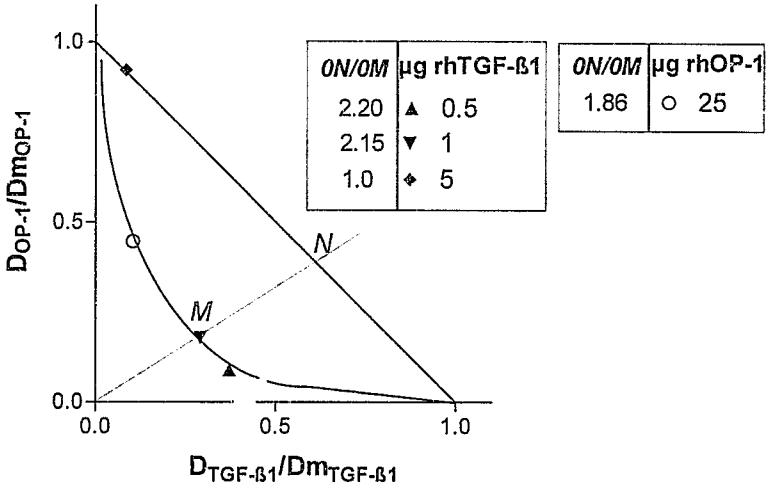

Figure 30. *Isobologram constructed from parameters (Table 5) derived from Figures 29 A and 29 B for the analysis of interaction of binary combinations of rhOP-1 and rhTGF-ß1 in the rectus abdominis of the baboon on day 30.*

The curve (Fig. 30) represents the isobol which can be used to predict interaction for other morphogen combinations. Solid points represent data obtained from Fig. 29 A (dose effect curves of rhOP-1 for given levels of rhTGF-$ß_1$; inset, left panel), and open points represent data obtained from Fig. 29 B (dose effect curves of rhTGF-$ß_1$ for given levels of rhOP-1; inset, right panel). The ratio of ON/OM represents synergistic intensity. Values of ON/OM decreased as rhTGF-$ß_1$ dose was increased (inset). This may reflect the biphasic properties of rhTGF-$ß_1$ in numerous systems reviewed in Chapter 1. In the present case, higher doses of rhTGF-$ß_1$ conferred a biphasic nature to the dose effect curve for rhOP-1, where *E* was seen to be was reduced at higher doses of rhTGF-$ß_1$ (Figure 29A).

3.3.2.1.3 Group 1 Primates: 15 Day Study

Based on results from the 30 day combination osteogenesis study, a 15 day study was conducted in order to gain insights into the developmental cascade of the synergistic interaction. The study was limited to a fixed dose of 25 μg rhOP-1 in combination of different doses of rhTGF-$ß_1$, having been found to be optimal for the 30 day study.

Figure 31. *Histological details of tissues generated by single and combined applications of rhOP-1 and rhTGF-$ß_1$ on days 15 and 30.*

A: bone induced by 5 μg rhTGF-$ß_1$ in the rectus abdominis of the baboon on day 30 (detail of Figure 22A). Note peripheral corticalisation by thick trabeculae of mineralised bone with more delicate trabeculae and thicker osteoid seams towards the internal and central areas of the ossicle. Areas indicate islands of cartilage (original magnification x30).

B and C: Rapid and extensive induction of bone in a specimen generated by 25 μg rhOP-1 combined with 0.5 μg rhTGF-$ß_1$ on day 15. Mineralised trabeculae of newly formed bone are covered by thick osteoid seams populated by contiguous osteoblasts. Note colonies of haemopoietic cells adjacent to cavernous sinuses, with trabeculae of bone extending between muscle fibres (B and C: original magnification x30 and x75 respectively).

D: Chondro-osteogenesis induced by 25 μg rhOP-1 combined with 1.5 μg rhTGF-$ß_1$ on day 15 (toluidine blue stain, original magnification x75)

E and F: Histological details of Figure 23A and 23C, respectively. Trabeculae of newly formed bone covered by thick osteoid seams (E) generated by 25 μg rhOP-1 combined with 1.5 μg rhTGF-$ß_1$ on day 30. Endochondral bone formation at the periphery of the ossicle generated by 125 μg rhOP-1 combined with 5 μg rhTGF-$ß_1$ on day 30 (F, original magnification x30).

A
D
E
F

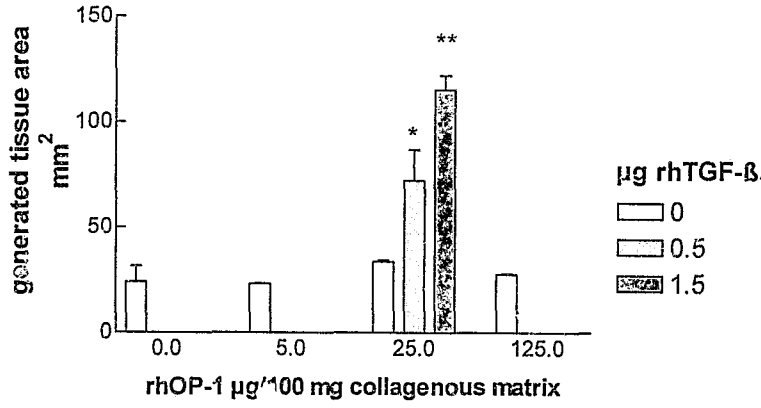

Figure 32. *Computerised analysis of histologic cross-sectional tissue area for tissues generated by single and combined applications of rhTGF-β_1 and rhOP-1 in the rectus abdominis of the baboon on day 15. Values are mean ± SEM of 4 to 8 observations per group. *P<0.05 vs rhOP-1 dose response; **P<0.05 vs the combination of 25 µg rhOP-1 and 0.5 µg rhTGF-β_1.*

Single applications of rhOP-1 showed minimal dose-dependent changes in cross-sectional tissue areas of generated tissues on day 15 (Fig. 32). However, addition of 0.5 and 1.5 µg of rhTGF-β_1 to 25 µg rhOP-1 resulted in a dose-dependent increase in generated tissue area of up to 3.5-fold (Fig. 32). When compared to cross-sectional tissue area data on day 30 (Figure 24), it is evident that ossicle size of tissues generated by morphogen combinations has changed little when compared to day 15 (Figure 32). In marked contrast, tissue generated by single application of rhOP-1 had increased significantly in size between day 15 and 30. Hence, combinations of the

two morphogens resulted in early determination of the final size of the generated tissue, whereas single application of rhOP-1 required longer time periods for size determination. Following these results, additional experiments were performed with pTGF-β_1 tested singly at doses of 0.5, 1.5 and 5 μg, in order to determine this morphogen's dose response curve (section 3.3.2.2), without which, the mode of interaction cannot be determined.

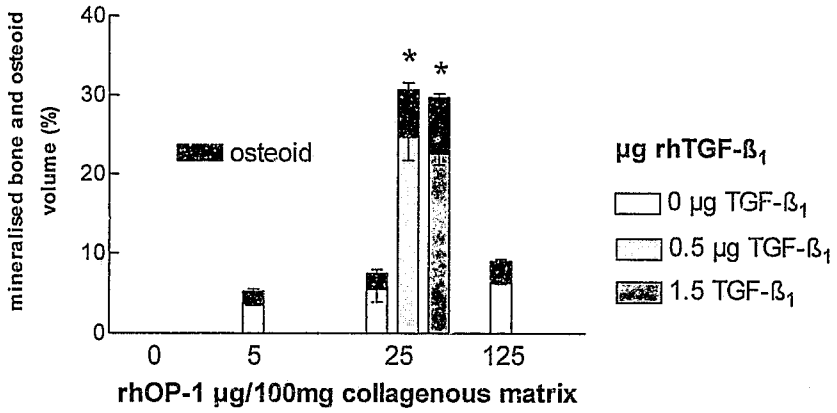

Figure 33. *Bone and osteoid volumes (in %) of ossicles on day 15 generated by heterotopic implantation of single and combined applications of rhTGF-β_1 and rhOP-1. *P<0.01 vs single application of rhOP-1.*

The co-administration of rhTGF-β_1 with 25 µg rhOP-1 caused significant increase in bone and osteoid volumes when compared to single applications of rhOP-1 (Fig. 33). The addition of the comparatively low dose of rhTGF-β_1 of 0.5 µg caused a 4.3-fold increase in mineralised bone parameter over single application of rhOP-1, and osteoid showed a 3.4-fold increase (Figure 33). Tissues generated with morphogen combinations underwent little change in mineralised bone volume between day 15 (Fig. 33) and day 30 (Fig. 25), indicating that morphogen combinations caused early determination of said parameters of the generated tissue. In contrast, tissues generated by single application of rhOP-1 of 25 µg underwent a 2.8 fold increase in mineralised bone volume between day 15 (Fig. 33) and day 30 (Fig. 25). The data

- indicate that morphogen combinations caused an acceleration of the osteogenic cascade, resulting in earlier bone formation and determination of the fate of the generated tissue.

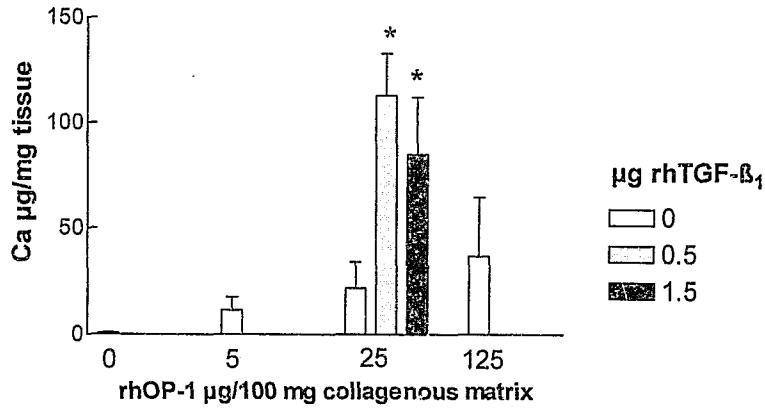

Figure 34. *Calcium content on day 15 of tissues generated by the implantation of single and combined applications of rhOP-1 and rhTGF-β_1 in the rectus abdominis of the baboon as described. Values are mean ±SFM for 4 to 8 observations per group. *P<0.05 vs single application of rhOP-1. Increases in calcium content were significantly greater than control for the 25 and 125 µg rhOP-1 (p<0.1).*

At the early time period of 15 days, single application of rhOP-1 showed a dose dependent increase in calcium content of tissues (Figure 34). This is in contrast to 30 days post-implantation, where a biphasic effect is observed in most parameters of bone formation that were measured. The addition of the comparatively low dose of 0.5 µg rhTGF-β_1 to 25 µg rhOP-1 resulted in a 5.2-fold increase in calcium content of generated tissues.

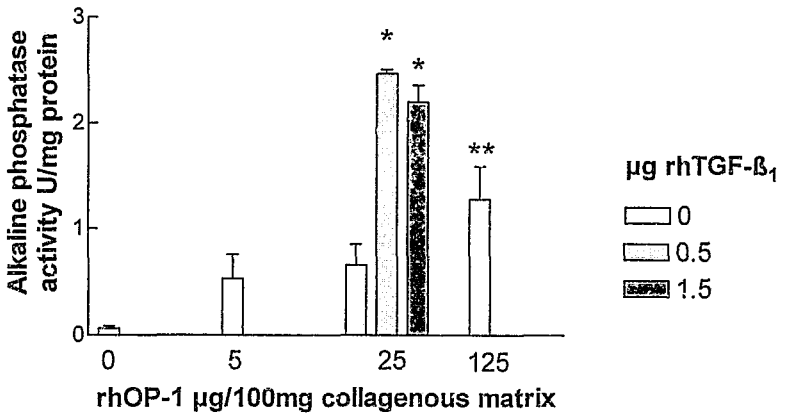

Figure 35. *Alkaline phosphatase activity on day 15 of tissues generated by single and combined applications of rhOP-1 and rhTGF-β_1. Values are mean ± SEM for 4 to 8 observations per group. *P<0.05 vs rhOP-1 dose response. **P<0.05 vs 5 and 25 µg rhOP-1.*

The addition of 0.5 µg of rhTGF-β_1 to 25 µg rhOP-1 resulted in a three-fold increase in alkaline phosphatase, reaching a level which was two-fold greater than that attained by a single application of the highest dose of rhOP-1 (Fig. 35). At this early time point, there is a clear dose dependent increase in alkaline phosphatase activity in relation to rhOP-1 alone.

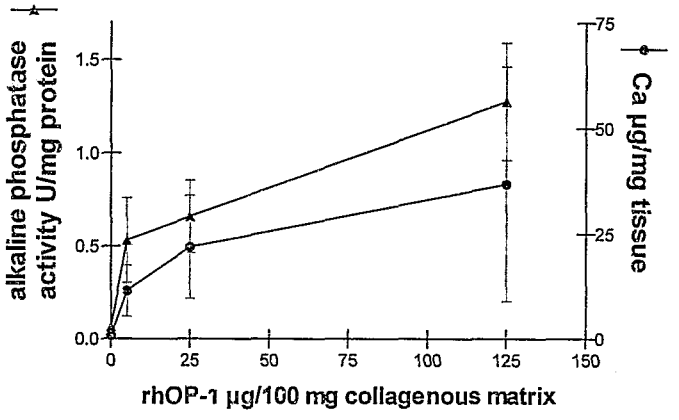

Figure 36. *Dose response curve on day 15, showing changes in alkaline phosphatase activity and calcium content of ossicles generated in response to single application of rhOP-1 implanted in the rectus abdominis of the baboon. Doses were of 0, 5, 25 and 125 µg of rhOP-1 per 100 mg collagenous matrix. Doses of 25 and 125 µg rhOP-1 induced significantly higher alkaline phosphatase activity when compared to control ($p<0.05$).*

There was a dose dependent increase in alkaline phosphatase activity and calcium content of tissues generated by single application of rhOP-1 (Fig. 36). The greatest responsiveness occurred for doses in the range up to 25 µg rhOP-1, whereafter increases in bone forming activity occurred at a reduced rate, approaching a plateau at 125 µg. There was a correlation between calcium content and alkaline phosphatase activity increases, demonstrating a direct relationship between the two markers of bone formation. At this early time(t) period (t=15d), alkaline phosphatase activity represents approximately a third of the activity attained on day 30 (2t) (Fig. 29)

whereas calcium content represented one quarter of the value attained on day 30 (2t) (Fig. 28). The data suggest that changes in parameters of bone formation during the bone induction cascade do not proceed in a linear fashion with respect to time, leading instead to comparatively larger increases in the said parameters in the period 15 days to 30 days post-implantation.

3.3.2.2 GROUP 2 PRIMATES: PORCINE TGF-β_1 AND rhOP-1

30 and 14 day study

3.3.2.2.1 Histology, histomorphometry and biochemistry

Figure 37. *Bone induction by single and combined application on day 30 of rhOP-1 and pTGF-β_1 implanted in the rectus abdominis of the baboon.*

A and B: Bone induction by a single application of 25 μg rhOP-1 (A) and 5 μg pTGF-β_1 (B) delivered by 100 mg of guanidinium inactivated collagenous matrix.

C and D: Large ossicles generated by 25 μg rhOP-1 combined with 1.5 (C) and 5 μg pTGF-β_1 (D). Areas of chondrogenesis (arrows in C) at the periphery of the newly generated tissue and corticalisation of the ossicles. Goldner's trichrome stain, original magnification x4.

To determine tissue induction and morphogenesis by rhOP-1 and pTGF-β_1, morphogens were added singly to 100 mg of collagenous matrix as carrier and implanted in the rectus abdominis of the baboon. As expected, 5 and 25 μg of rhOP-1 induced bone formation by day 30 in the rectus abdominis (Figure 37A). In marked contrast to previously published negative results in rodents, histological analysis of specimens of collagenous matrix combined with 5 μg of pTGF-β_1 showed

A

B

C

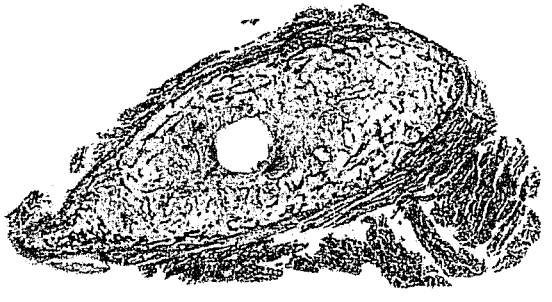

D

endochondral bone formation by day 30 (Figure 37B). The addition of comparatively low doses of pTGF-$ß_1$ (0.5, 1.5 and 5 μg) to 25 μg rhOP-1 resulted in the generation of large corticalised ossicles displacing the muscle fibres of the rectus abdominis.

Figure 38. *Histological details of chondro-osteogenic tissue generated in the rectus abdominis of the baboon on day 30 by 25 μg rhOP-1 combined with 1.5 (A) and 5 μg pTGF-β1 (B).*

A: Higher magnification of Figure 37 showing classic features of chondrogenesis and osteogenesis with a gradient of morphological structures highly suggestive of a rudimentary growth plate. Subjacent to columns of progressively maturing chondroblasts there is vascular invasion with chondrolysis and generation of trabeculae of bone with bone marrow. Trabeculae of newly formed bone are lined by contiguous osteoblasts. Original magnification in A, x30; B: toluidine blue stain, original magnification x75.

A
B

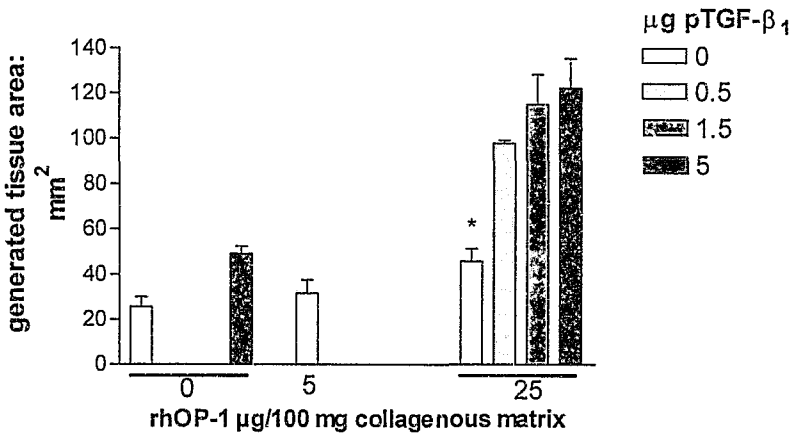

Figure 39. *Histologic cross-sectional tissue areas on day 30 for tissues generated by single and combined applications of porcine TGF-β_1 and rhOP-1 in the rectus abdominis of the baboon. *P < 0.05 versus values for morphogen combinations.*

Cross-sectional generated tissue areas on day 30 for single on binary applications of rhOP-1 and pTGF-β_1 in the rectus abdominis of the baboon are shown in Figure 39. The addition of pTGF-β_1 to rhOP-1 dose dependently increased generated tissue area. The addition of comparatively low dose of pTGF-β_1 of 0.5 μg resulted in a two-fold increase in the said parameter.

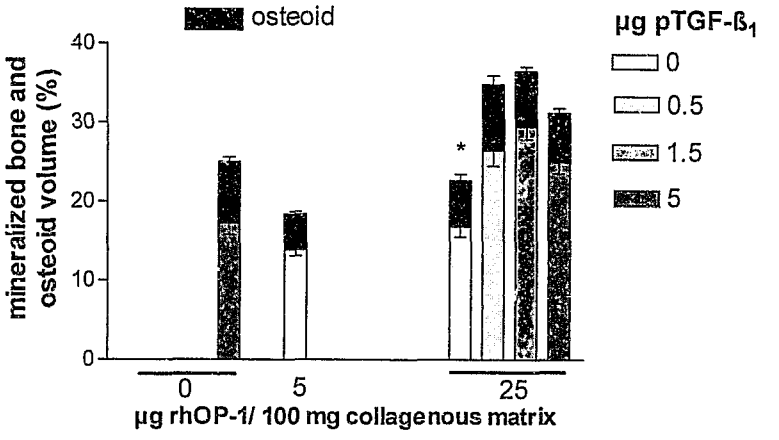

Figure 40. *Mineralised bone and osteoid volumes of ossicles on day 30, generated by heterotopic implantation of single and combined applications of pTGF-ß1 and rhOP-1. *P < 0.05 versus values for morphogen combinations.*

pTGF-ß1 and rhOP-1 were implanted singly and in combination in the rectus abdominis of the baboon, and generated tissues harvested on day 30 and processed for histology. Histomorphometric parameters are shown in Figure 40. Addition of comparatively low doses of pTGF-ß1 to rhOP-1 caused a significant increase in mineralised bone and osteoid volumes. The combination of 1.5 µg pTGF-ß1 with 25 µg rhOP-1 resulted in a 0.5-fold increase in mineralised bone over single application of rhOP-1.

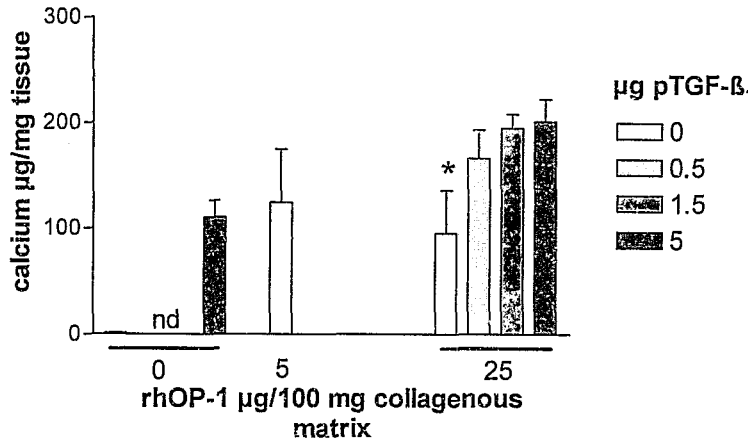

Figure 41. *Calcium content on day 30 of tissues generated by single and combined applications of rhOP-1 and pTGF-β_1 in the rectus abdominis of the baboon. *P < 0.05 versus morphogen combinations. Addition of 0.5, 1.5 and 5 µg pTGF-β_1 to 25 µg rhOP-1 caused significant increases in calcium content when compared to single application of rhOP-1 ($p<0.05$).*

pTGF-β_1 at a dose of 5µg per 100 mg collagenous matrix generated ossicles with a calcium content comparable to that induced by single applications of rhOP-1 (Fig. 41). The co-administration of pTGF-β_1 with rhOP-1 resulted in increases in the calcium content of the generated ossicles, in a manner which was dose dependent on pTGF-β_1. The addition of the comparatively low dose of 0.5 µg pTGF-β_1 to 25 µg rhOP-1, resulted in a 75 % increase in calcium content when compared to single application of rhOP-1.

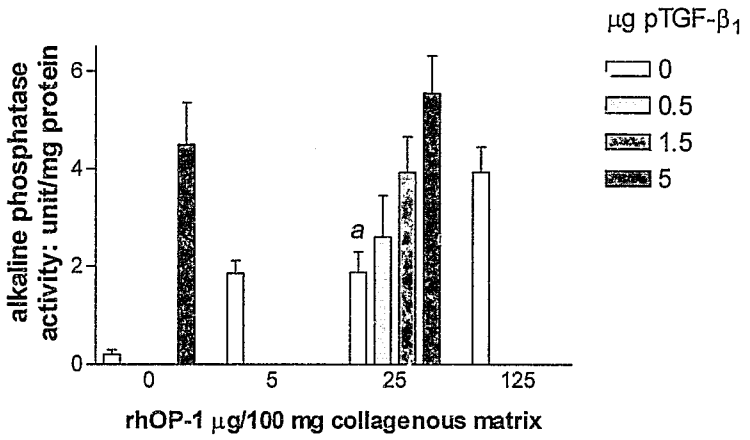

Figure 42. *Alkaline phosphatase activity on day 30 of tissues generated by the implantation of single and combined applications of rhOP-1 and pTGF-β1 in the rectus abdominis of the baboon. Each value represents the mean of four replicates (n=4), generated using two primates.* $^{a}P < 0.05$ *when compared to values for morphogen combinations.*

The high level of alkaline phosphatase activity in osseous tissue generated by single application of 5 µg pTGF-β_1 is striking (Fig. 42). When combined with 25 µg rhOP-1, pTGF-β_1 caused a dose-dependent rise in alkaline phosphatase activity of generated tissues. Since pTGF-β_1 alone induced high levels of alkaline phosphatase activity, it was not clear at this time point, whether this parameter was increased synergistically during bone formation induced by morphogen combinations. A similar experiment was therefore performed at the earlier time point of 14 days to gain further insights into the interaction of these two morphogens.

Figure 43 (opposite). *Synergistic interaction of pTGF-ß1 and rhOP-1 on day 14. Values are mean ± SEM of 4 to 8 specimens per group. A, computerised analysis of newly formed bone tissue cross-sectional area (mm^2) (mineralised bone, osteoid and marrow)(Parfitt et al., 1987) induced by doses of morphogens, singly or in binary applications. B, mineralised bone and osteoid volume (in %) generated by doses of pTGF-ß1 and rhOP-1, singly, or in combination. C, effect of pTGF-ß1 on alkaline phosphatase activity in the newly generated tissues harvested on day 14.* ***a*** *indicates significant differences with morphogen combinations, with the exclusion of the 0.5 µg pTGF-ß1 and 25 µg rhOP-1 combination in C.*

On day 14, binary applications of pTGF-1 and rhOP-1 resulted in synergistic induction of tissue morphogenesis as determined by histomorphometry and biochemistry (Figures 43). Combinations of 1.5 and 5 µg pTGF-$ß_1$ with 25 µg rhOP-1 induced extensive amounts of osteoid and mineralised bone with foci of chondrogenic tissue mainly localised at the periphery of the newly generated ossicles (not shown). Bone tissue (mm^2) and mineralised bone and osteoid volumes (%) in specimens generated by morphogen combinations were increased synergistically by several fold when compared to single applications of 25 or even 125 µg rhOP-1 (Figures 43A and 43B). The data at the early time-point of 14 days indicate unequivocally, that the two morphogens interact synergistically when inducing new bone formation as binary combinations.

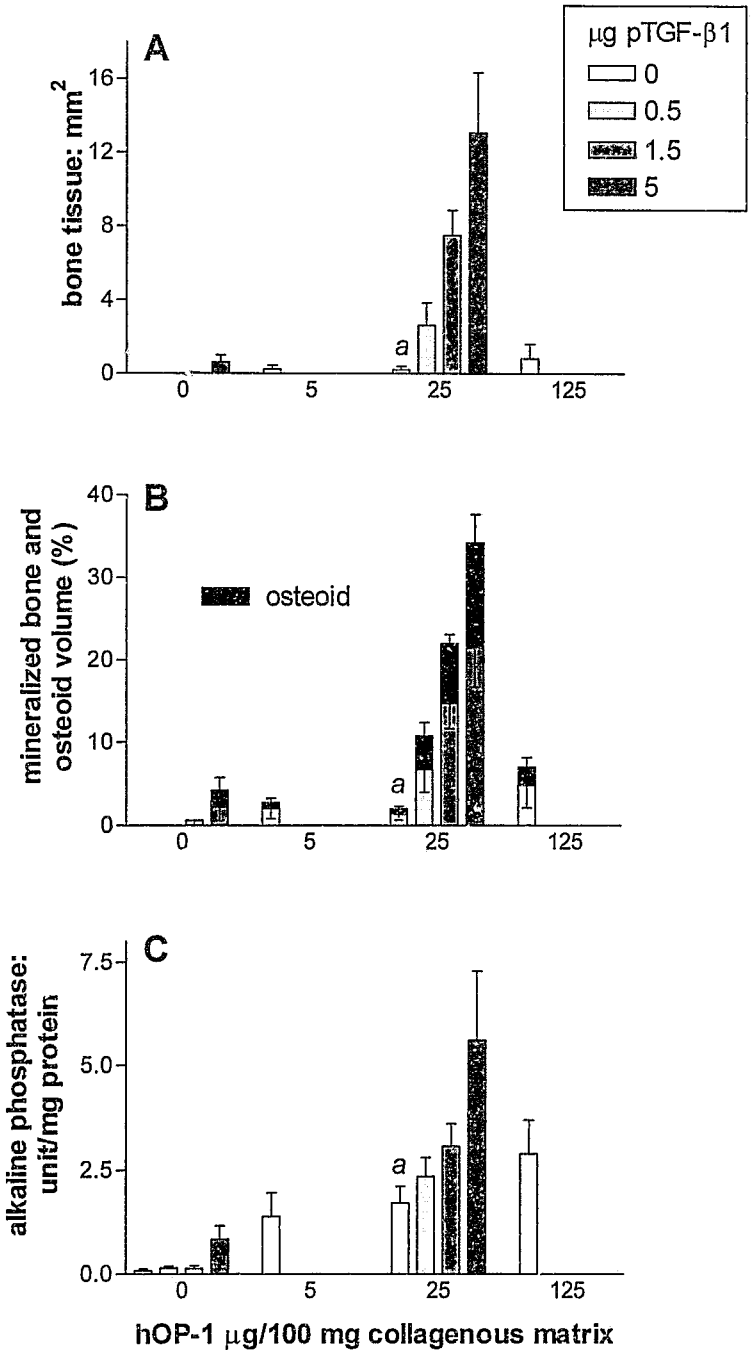
A
bone tissue: mm²
16
12
8
4
0
a
0
5
25
125
μg pTGF-β1
0
0.5
1.5
5
B
mineralized bone and osteoid volume (%)
40
30
20
10
0
osteoid
a
0
5
25
125
C
alkaline phosphatase: unit/mg protein
7.5
5.0
2.5
0.0
a
0
5
25
125
hOP-1 μg/100 mg collagenous matrix

3.3.2.2.2 NORTHERN ANALYSIS OF SELECTED mRNA SPECIES EXPRESSED IN TISSUES GENERATED IN THE BABOON RECTUS ABDOMINIS BY SINGLE AND COMBINED APPLICATIONS OF rhOP-1 AND pTGF-$ß_1$.

Figure 44. *Northern analysis of OP-1, BMP-3, TGF-$ß_1$, type II and type IV collagens mRNA expression of tissues generated by rhOP-1 and pTGF-$ß_1$. rhOP-1 and pTGF-$ß_1$ were implanted singly and in combination with collagenous matrix in the rectus abdominis of the baboon, and replicate generated tissues (n=4) were harvested on day 30, pooled, and total RNA extracted as described in Methods. Samples of total RNA were subjected to Northern analysis for type II and type IV collagens (5 µg per lane) and for OP-1, BMP-3 and TGF-$ß_1$ (20 µg per lane). The gamma-actin mRNA, and the 18S and 28S ribosomal RNA signals were used as standard for size determination. mRNA levels are expressed in relative densitometric units.*

Single applications of 5 µg pTGF-$ß_1$ induced endochondral bone formation in the baboon by day 30. Northern blot analysis of this tissue showed that OP-1, BMP-3 and TGF-ß message was highly expressed. This is the first account showing osteoinduction by TGF-$ß_1$ at heterotopic sites of any animal model. It is noteworthy that bone morphogenesis induced by TGF-$ß_1$ requires, at least in part, the mRNA

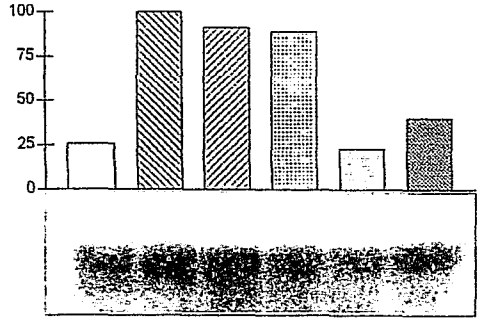

OP-1

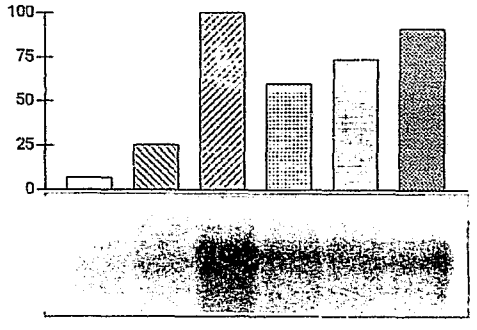

type II
collag

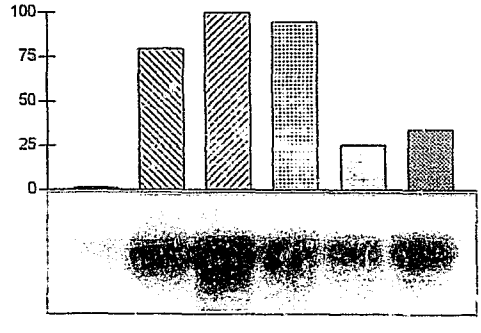

BMP-3

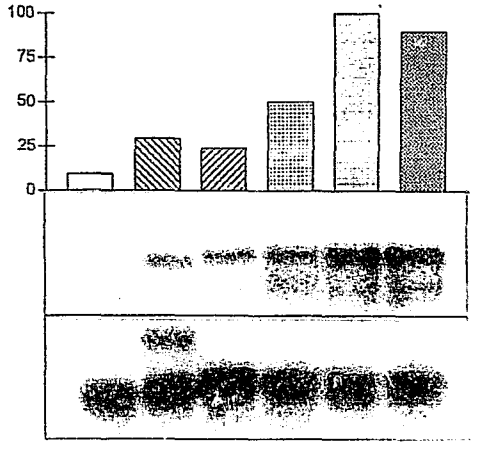

type IV
collag

γ-actin

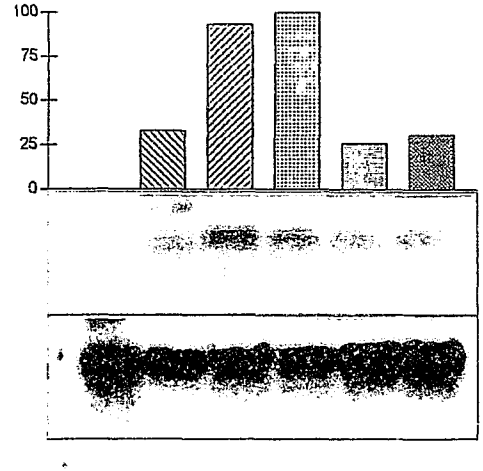

TGF-ß1

γ-actin

hOP-1 µg	pTGF-ß1 µg
0	0
25	0
0	5
25	0.5
25	1.5
25	5

expression of members of the BMP/OP family. rhOP-1 also induced endochondral bone expressing OP-1, BMP-3 and TGF-ß mRNA, though the latter mRNA transcript was more than two-fold less than in tissue generated by pTGF-$ß_1$. BMP-3, OP-1 and TGF-$ß_1$ mRNA synthesis was three-fold lower in ossicles generated by combinations of 1.5 and 5 µg pTGF-$ß_1$ combined with 25 µg rhOP-1 (Fig. 44). Comparison of histomorphometrical and biochemical data of tissue generated on day 15 and 30 showed that morphogen combinations accelerate the osteoinductive cascade. The decrease in mRNA expression of morphogen species in tissues generated by higher doses of pTGF-$ß_1$ combined with 25 µg rhOP-1 may signify a temporal acceleration of the induction cascade, and thus with decreased OP-1, BMP-3 and TGF-$ß_1$ mRNA synthesis on day 30. Additional insights will require Northern analyses at multiple time points. Of interest is the synthesis, albeit limited, of OP-1 mRNA in control tissue. Control tissue was generated by the implantation of collagenous matrix without any added morphogens, in the rectus abdominis of the baboon. Histologically, the tissue showed fibrovascular tissue invasion with no evidence of bone formation. OP-1 may therefore be involved in soft tissue repair mechanisms, though further insights will require additional experiments.

The expression of high levels of mRNA for type II collagen, a marker for chondrogenesis, in tissues generated by single application of pTGF-$ß_1$ is not surprising. This morphogen has been implicated in chondrogenesis following numerous *in vivo* and *in vitro* experiments (literature review, Chapter 1). Single application of 5 µg pTGF-$ß_1$ induced 4-fold more type II collagen mRNA expression

than single application of 25 μg rhOP-1. In combinations, pTGF-ß$_1$ dose dependently increased levels of type II collagen expression approaching levels induced by pTGF-ß$_1$ alone (Figure 44). Single applications of pTGF-ß$_1$ and rhOP-1 synergistically upregulated type IV collagen mRNA synthesis, a marker for angiogenesis. Angiogenesis and vascular invasion are prerequisites for osteogenesis, and consequently, this effect may by part of the mechanism whereby rhOP-1 and pTGF-ß$_1$ interact synergistically during combination osteogenesis. These results are of clinical significance for the design of molecular therapeutics which are capable of initiating the rapid and optimal induction of new bone in clinical contexts.

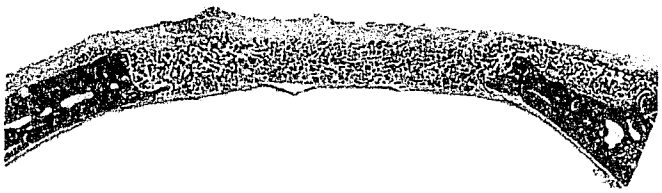

A

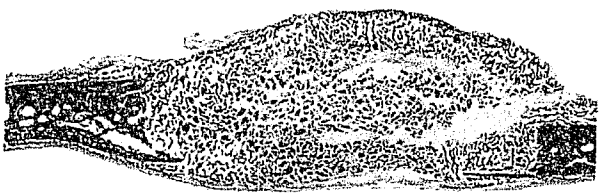

B

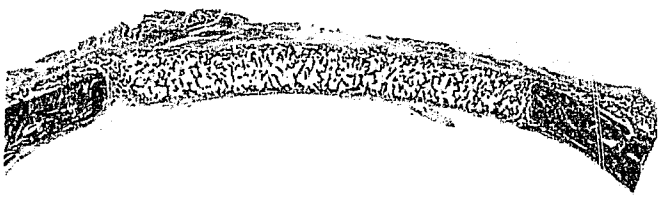

C

D

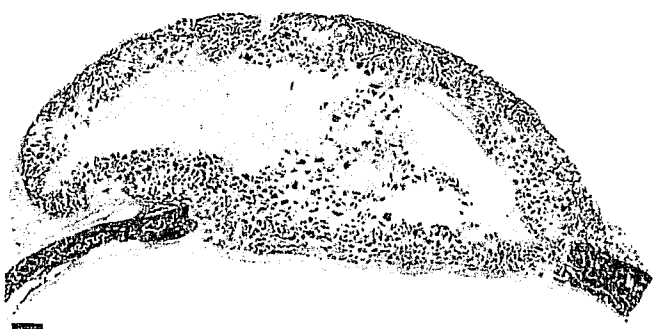

E

F

3.3.3 The orthotopic study in the baboon: Group 2 Primates

Figure 45. *Tissue induction and morphogenesis of bone in calvarial defects by implantation of rhOP-1 alone, and in combination with doses of pTGF-β_1 on day 30.*

A and B: Low power photomicrographs of defects treated with 20 μg rhOP-1 (A) and with 20 μg rhOP-1 combined with 5 μg pTGF-β_1 (B).

C, D, E and F: Calvarial defects treated with 100 μg rhOP-1 alone (C) and in combination with 5 (D and E) and 15 μg pTGF-β_1 (F). Formation of trabeculae of mineralised bone across the entire defect but within the profile of the original calvaria following treatment with single administration of 100 μg rhOP-1 (C). Extensive pericranial osteogenesis in specimens treated with morphogen combinations, culminating in gross displacement of the pericranial tissues (E and F). Goldner's trichrome stain, original magnification x2.8.

Using the baboon calvarial model, it has recently been shown that a single application of 100 μg of rhOP-1, delivered by an identical collagenous matrix preparation as described in the present study, induced complete regeneration of the calvarial defects by day 90 (Ripamonti *et al.*, 1996b). In marked contrast, 5, 30 and 100 μg of recombinant hTGF-β_1, delivered by the same collagenous matrix, failed to regenerate calvarial defects in the adult baboon, resulting in limited chondro-osteogenesis at the margins of the defects, and in enhanced fibrosis and vascular invasion when compared to controls of collagenous matrix alone (Ripamonti *et al.*, 1996a). In the present study, an experiment was conducted with binary combinations of rhOP-1 and pTGF-β_1 to investigate the combinatorial action of both

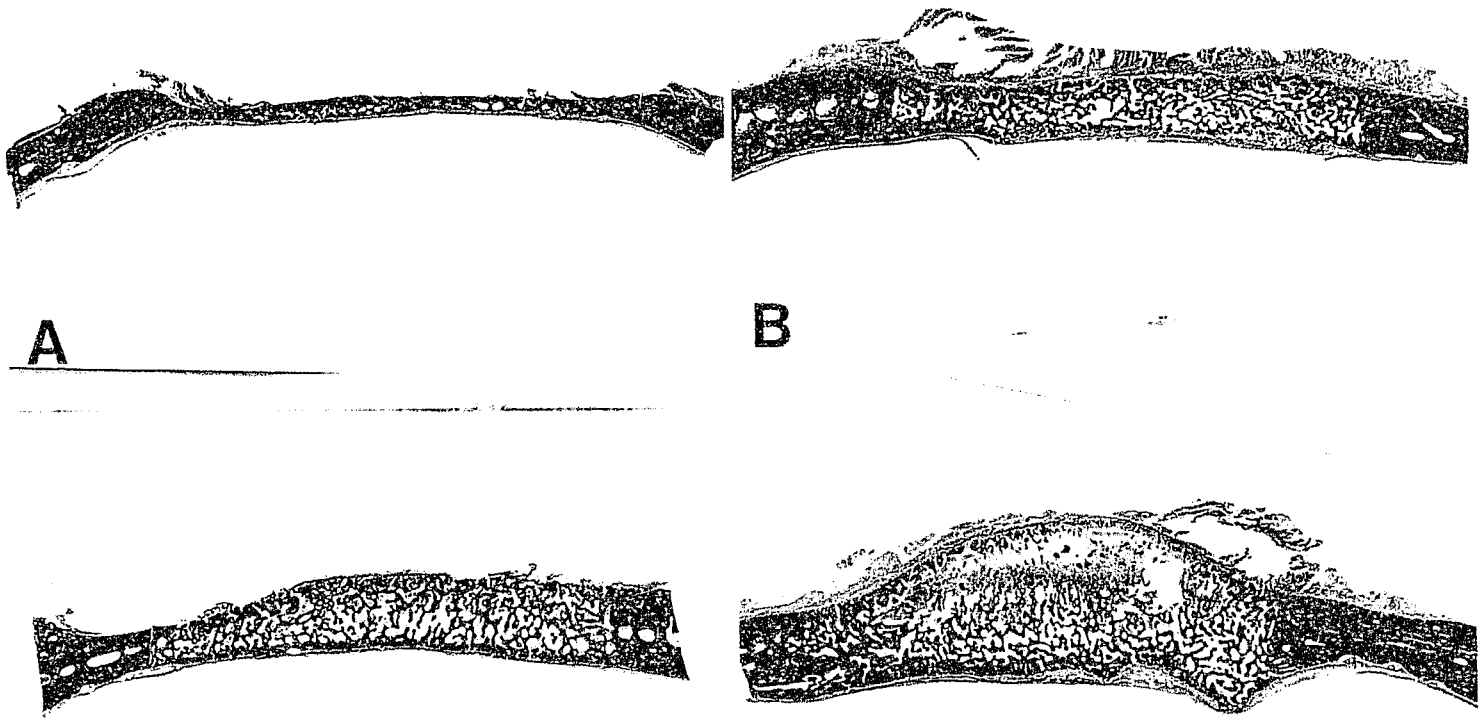
A
B
C
D

morphogens in 32 calvarial defects prepared in 8 adult baboons. At harvest, calvarial specimens treated with combinations of rhOP-1 and pTGF-$ß_1$ on day 30 showed displacement of the pericranium and associated temporalis muscle. Cut surfaces were brownish-red in the gross, indicating prominent angiogenesis and vascular invasion. On day 30, treatment with 20 μg of rhOP-1 initiated sparse bone formation pericranially and in proximity to the defect margins (Figure 45A). The addition of 5 μg pTGF-$ß_1$ to 20 μg rhOP-1 resulted in pericranial and endocranial osteogenesis across the treated defects (Figure 45B). When compared to a single application of 100 μg rhOP-1 (Figure 45C), the addition of 5 and 15 μg of pTGF-$ß_1$ to 100 μg of rhOP-1 resulted in prominent pericranial osteogenesis with pronounced lifting of the newly formed mineralized bone pericranially, grossly displacing the temporalis muscle (Figures 45D, 45E and 45F). The mineralized bone that had formed beneath the temporalis muscle and along the dura was separated by a loose connective tissue, characterised by the presence of an internal, dividing zone with prominent vascular invasion and scattered remnants of collagenous matrix (Figures 45D, 45E and 45F). Numerous delicate trabeculae of newly formed bone, covered by continuous osteoid seams populated by contiguous osteoblasts, characterised the pericranial zone of osteogenesis. The histological features seen on specimens generated by morphogen combinations were remarkably similar to the histological results obtained using higher doses of rhOP-1 (0.5 and 2.5 mg rhOP-1 per g of collagenous matrix) as evaluated on day 30 in the adult baboon (Ripamonti *et al.*, 1996b). Both treatments (morphogen combinations and high doses of rhOP-1) resulted in a marked proliferative and inductive phase at the periphery of the implanted matrix,

particularly at the level of the pericranium and temporalis muscle, followed by an exuberant osteogenic effect that resulted in the loss of cohesiveness between the pericranial and endocranial osteogenic sites (Figures 45D and 45E).

Figure 46. *Morphology of calvarial regeneration by rhOP-1, alone, and in combination with doses of pTGF-ß1 on day 90.*

A and B: Low power photomicrographs of defects treated with 20 µg rhOP-1 (A) and with 20 µg rhOP-1 combined with 5 µg pTGF-ß1 (B).

C and D: Calvarial defects treated with 100 µg rhOP-1 alone (C) and in combination with 15 µg pTGF-ß1 (D). Goldner's trichrome stain, original magnification x2.8.

On day 90 (Figure 46), defects treated with 20 µg rhOP-1 were markedly thinner when compared to regenerates obtained by the combination of 5 µg pTGF-ß1 and 20 µg rhOP-1 (Figure 46A and 46B). Defects treated with 100 µg rhOP-1 in combination with 15 µg pTGF-ß1 showed marked and exuberant osteogenesis, persistence of pericranial lifting with temporalis muscle displacement and of zones of fibrovascular tissue influx with scattered collagenous matrix particles (Figure 46D). The addition of comparatively low dose of 5 µg pTGF-ß1 to 20 µg rhOP-1 (Figure 46B) markedly increased bone formation induced by single application of 20 µg rhOP-1 (Figure 46A), approaching levels of bone tissue formation elicited by single application of 100 µg rhOP-1 (C). The addition of 15 µg pTGF-ß1 to 100 µg rhOP-1 induced tissue with distorted pericranial profile in one specimen (Figure 46D) with scattered remnants of collagenous matrix within a zone of fibrovascular tissue beneath the pericranial corticalised bone layer.

Table 6. *Effect of pTGF-ß$_1$ on bone induction by rhOP-1 in 32 calvarial defects in 8 adult male baboons.*

Day	Morphogen Combinations:µg rhOP-1	pTGF-ß$_1$	Bone %	Osteoid %	Matrix %
30	20	0	18.1±1.4	4.6±0.3	33.9±1.6
	20	5	24.5±1.4[b]	6.7±4.4[b]	13.0±11.7[f]
	100[a]	0	29.1±0.6[c]	4.5±0.2	7.7±0.6[f]
	100	5	31.7±1.4[c]	9.0±0.5[e]	7.0±0.6[f]
	100	15	24.7±1.2	7.0±0.3[e]	9.2±1.4[f]
	0	100	8.5±1.5	1.0±0.2	30.7±2.6
90	20	0	35.5±1.9	3.1±0.2	6.3±1.3
	20	5	49.2±1.6[b]	4.2±0.3[h]	2.7±0.5
	100[a]	0	53.3±1.5[d]	2.6±0.1	0.3±0.1
	100	5	46.6±1.6	4.5±0.2[e]	1.6±0.6
	100	15	56.9±1.7[d]	6.9±0.3[e]	0.7±0.2

Single and binary applications of morphogens were applied once at the time of surgery and delivered by 1 g of baboon collagenous matrix. Operated sites were harvested on day 30 and 90, and serial undecalcified section, cut at 7 µm, were analysed by morphometry. Volume fractions of tissue components (in %) were calculated using a Zeiss integration Platte II with 100 lattice points superimposed over two sagittal sections used for analysis as described in methods. Bone indicates mineral plus osteoid. Bone indicates mineralised bone plus osteoid, matrix indicates the residual collagenous carrier used for local delivery of morphogens. Values are means ± SEM of 4 calvarial specimens per group. Levels of significance were determined using the Statistical Analysis System General Linear Models Procedure with multiple interactions on a balanced set of data. [a]The 5 and 15 µg doses of TGF-ß$_1$ refer to purified porcine TGF-ß$_1$ used in the present experiments, whilst the 100 µg dose refers to previously published data on day 30 in 4 adult male baboons implanted with 100 µg of recombinant human TGF-ß$_1$ (Ripamonti *et al.*, 1996a). The 100 µg dose of rhOP-1 alone represents data from 8 calvarial defects on day 30 and 90 (Ripamonti *et al.*, 1996b), implanted in conjunction with an identical preparation of collagenous matrix used in the present experiments.

[b]*P<0.05 vs 20 µg rhOP-1 alone on day 30 and 90*

[c]*P<0.05 vs 100 µg rhOP-1 and 15 µg pTGF-ß$_1$ on day 30*

[d]*P<0.05 vs 100 µg rhOP-1 and 5 µg pTGF-ß$_1$.*

[e]*P<0.05 vs 100 µg rhOP-1 alone on day 30 and 90.*

[f] *P<0.05 vs 20 µg rhOP-1 and 100 µg hTGF-ß$_1$ on day 30.*

Volume fractions (with level of significance) of bone, osteoid and residual matrix of regenerated tissue, in defects treated with rhOP-1 and TGF-$ß_1$, singly or in combination, are presented in Table 6. Histomorphometric data of the present series of calvarial defects were compared with previously published results using 100 µg of rhOP-1 (Ripamonti *et al.*, 1996b) and 100 µg of recombinant rhTGF-$ß_1$ (Ripamonti *et al.*, 1996a), delivered by an identical preparation of collagenous matrix. On day 30, all doses of rhOP-1, either singly or in combination with 5 or 15 µg of pTGF-$ß_1$, induced greater amounts of bone and osteoid volumes when compared with specimens treated with 100 µg rhTGF-$ß_1$ ($P<0.01$, Table 6). Specimens treated with 20 µg rhOP-1 in combination with 5 µg pTGF-$ß_1$ induced greater amounts of bone and osteoid when compared with specimens treated with a single application of 20 µg rhOP-1 ($P<0.05$, Table 6). Specimens treated with 100 µg rhOP-1 induced equal and greater amounts of bone when compared with 100 µg rhOP-1 combined with 5 and 15 µg pTGF-$ß_1$, respectively (Table 6). However, morphogen combinations resulted in greater amounts of osteoid volumes when compared with specimens treated with 100 µg rhOP-1 alone ($P<0.05$, Table 6).

On day 90, on average, greater amounts of bone and osteoid volumes were found in specimens treated with 100 µg rhOP-1 combined with 15 µg pTGF-$ß_1$. This difference, however, was significant only for osteoid volume ($P<0.05$, Table 6), indicating substantial osteoid deposition (7.0 and 6.9 % on day 30 and 90, respectively) sustained by continuous osteoblastic synthesis in specimens treated with the 15 µg dose of pTGF-$ß_1$. Treatment with 100 µg rhOP-1 combined with 5 µg pTGF-$ß_1$ showed significantly less bone but greater osteoid volume when compared with specimens treated with 100 µg rhOP-1 alone ($P<0.05$, Table 6). The histomorphometric results indicate a 2 fold increase in bone volume between day 30 and 90 in specimens treated with 20 µg rhOP-1 alone and in combination with 5 µg pTGF-$ß_1$, and in specimens treated with 100 µg rhOP-1 in combination with 15 µg pTGF-$ß_1$ (Table 6). Specimens treated with 100 µg rhOP-1 in combination with 5 µg pTGF-$ß_1$ showed the least fold increase in bone volume on day 90, in spite of the highest osteoid volume present on day 30 (Table 6).

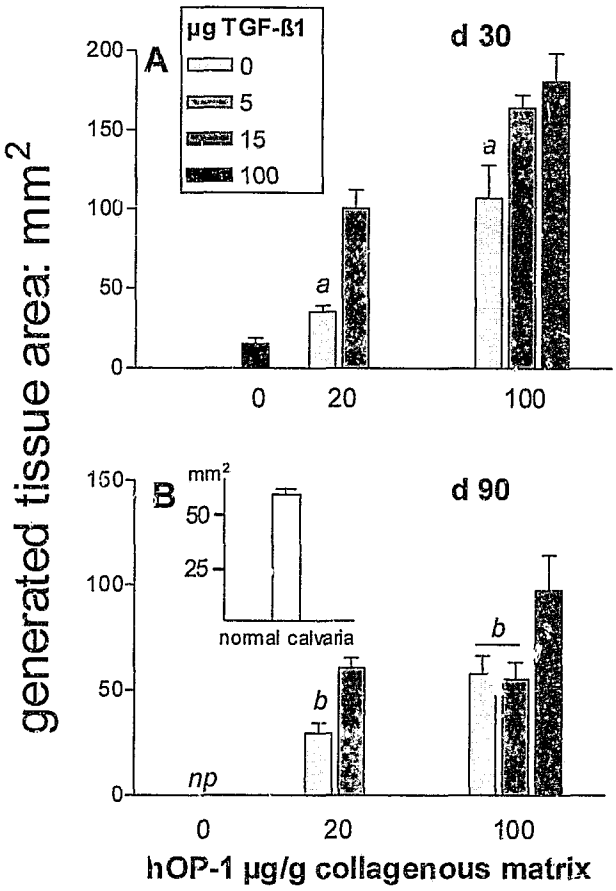

Figure 47. *Computerised analysis of generated tissue area (mineralised bone, osteoid, marrow, and other fibrovascular tissue and residual collagenous matrix on day 30 when surrounded by mineralised bone) in calvarial defects of the baboon on day 30 (A) and day 90 (B). a and b denote significant differences between single application of rhOP-1 when compared to combined application of rhOP-1 and TGF-ß1.*

Computer generated data of cross-sectional areas (in mm^2) of morphogen-treated calvarial defects are shown in Figure 47. Exuberant bone and fibrovascular tissue formation induced on day 30 by morphogen combinations showed a significant increase in tissue area when compared with specimens treated with both doses of rhOP-1 alone ($P<0.05$, Figure 47A). This exuberant tissue formation was remodelled rapidly to near normal calvariae (mean cross-sectional area: 60.8 ± 3.1 mm^2) (Ripamonti *et al., 1996b*) by day 90 (Figure 47B). In contrast to the other treatment modalities, specimens treated with 100 μg rhOP-1 combined with 1[illegible] pTGF-$ß_1$ showed persistence of exuberant tissue formation when compared with the profile of the normal baboon calvaria, in spite of 50% reduction of bone and fibrovascular tissue between the two time periods (Figure 47). It is noteworthy that on day 90 the combination of 20 μg rhOP-1 and 5 μg pTGF-$ß_1$ resulted in a two fold increase in bone tissue when compared to specimens treated with 20 μg of rhOP-1 alone, and approached levels of generated tissue area comparable with the higher dose of rhOP-1 (Figure 47B).

The most apparent effect of pTGF-$ß_1$ in binary combinations with rhOP-1 was that it caused marked increases in cross-sectional tissue areas of tissues generated in calvarial defects on day 30 and 90 post-implantation. Osteoid synthesis (Table 6) showed strong response to added pTGF-$ß_1$, which at comparatively low levels of 5 and 15 μg per defect site, was capable of increasing osteoid volumes in excess of 50 % on days 30 and 90. The data indicate that the addition of pTGF-$ß_1$ to rhOP-1 upregulated osteoblast matrix synthesis and deposition. Indeed, when seen histologically, tissues generated by morphogen combinations, both heterotopically

and orthotopically, showed marked thickening of osteoid seams. In terms of mineralised bone volumes, differences were particularly evident for low doses of rhOP-1, where the addition of 5 μg pTGF-$ß_1$ caused significant increases on day 30 and 90. Combinations of 20 μg rhOP-1 with 5 μpTGF-$ß_1$ also caused a significant resorption of the implanted collagenous matrix when compared to single application of rhOP-1 on both time periods (Table 6).

A first demonstration that TGF-ß could enhance the osteogenic activity of bone derives osteogenic fractions was reported by Bentz *et al.* (1989). They isolated a crude osteoinductive fraction from bone, and showed that when purified further, osteoinductive activity was lost. Osteogenic activity could however be recovered when TGF-$ß_2$, itself inactive in the heterotopic bioassay, was tested in combination with the putative osteoinductive factor in the same assay. Although the active factor was misidentified as the osteogenically inactive osteoglycin, it was however, a demonstration of synergism between two crude principles, inactive alone, but when in combination, were capable of eliciting of a substantial biologic response. This type of synergism would be pharmacologically classified as coalism (Greco *et al.*, 1995). Later, Bentz *et al.* (1991) showed that the osteoinductive fraction they were working with was a cocktail of proteins containing traces of BMP-2 and BMP-3, which was osteogenic in the rat subcutis assay, and whose activity was potentiated by TGF-$ß_2$. The ratio of cartilage to bone was increased by combinations containing increasing doses of TGF-$ß_2$. Bone and cartilage were essentially absent at at the lower threshold limit of 25 ng osteoinductive fraction/implant, whereas co-

implantation of 140 ng TGF-$ß_2$ more than doubled alkaline phosphatase activity and bone volume.

The same synergistic interaction of TGF-ßs with native fractions containing BMP-2 and BMP-3 was reported by Ogawa *et al.* (1992). Implants containing combinations of naturally sourced TGF-$ß_2$ and BMP fractions resulted in an abundance of cartilage when compared to BMP alone in rats. This was dose dependent for TGF-$ß_2$, with increases in cartilage noted at higher amounts of the morphogen. Optimal combinations of BMP fractions and TGF-$ß_2$ resulted in an 8-fold increase in alkaline phosphatase activity at 14 days when compared to controls containing BMP alone. Interestingly, they also noted that synergism occurred with combinations of another member of the TGF-ß superfamily: activin. Activin in combination with native BMP fractions resulted in an 8-fold increase in alkaline phosphatase activity on day 14. Notably, the response was somewhat attenuated at higher levels of activin. Histological examination revealed the presence of well developed bone with minimal levels of cartilage. When implants containing all three factors, namely activin, TGF-$ß_2$ and BMP were implanted, the resulting tissue appeared disorganised, with patches of fibrous connective tissue, fibrocartilage and bone. Activin A stimulates DNA synthesis in foetal rat parietal osteoblast cultures, and the synthesis of collagen and non-collagenous proteins (Centrella *et al.*, 1991) thus suggesting that TGF-ß and activin may have different, as well as common roles during bone formation, in view of the unique receptors to which these factors bind to.

An experiment which may indirectly demonstrate synergism between TGF-$ß_1$ and BMPs was in a rabbit craniofacial onlay model (Kibblewhite *et al.*, 1993). In this experiment, recombinant TGF-$ß_1$ was added to demineralised bone matrix at different doses. It was shown that with respect to control demineralised bone matrix, the TGF-$ß_1$ fortified implant induced significantly higher amounts of bone and greater resorption of implanted matrix in a dose dependent manner. They concluded that TGF-$ß_1$ is a potent inducer of osteoinduction when used in conjunction with demineralised bone matrix. It is likely however, that the observed biologic activity of TGF-$ß_1$ was dependent upon interactions with BMPs/OPs present in the demineralised bone matrix preparation. This experiment may be in fact an *in vivo* demonstration of synergy between BMPs/OPs bound to the demineralised bone matrix and the exogenously applied recombinant TGF-$ß_1$ at orthotopic sites.

That BMPs/OPs may act synergistically with TGF-ßs in bone formation has also been postulated by Cunningham *et al.,* (1992). They suggested that BMPs may have early effects in bone induction by stimulating the chemotaxis of monocytes to the area. Once attracted, the monocytes are stimulated to produce a number of chemotactic and mitogenic cytokines and growth factors including TGF-ßs as shown by Northern blot analysis (Cunningham *et al.*,1992). Expressed TGF-ß may thus recruit mesenchymal cells and promote the synthesis of collagen and other extracellular matrix constituents. It is accepted that vascular invasion is a prerequisite for bone formation (Foidart and Reddi, 1980).

3.4 OVERVIEW OF RESULTS AND CONCLUDING STATEMENTS

A striking and discriminatory feature of BMPs/OPs is their capacity to singly initiate bone formation in heterotopic sites, recapitulating events which occur in the normal course of embryonic bone development (Reddi, 1992; Wozney, 1992; Reddi, 1994), a phenomenon so far shared by other members of the TGF-ß superfamily but not by TGF-$ß_1$ or - $ß_2$ (Hammonds *et al.*, 1991; Roberts *et al.*, 1986; Sampath *et al.*, 1987). As predicted from results obtained in rodents (Sampath *et al.,* 1992), rhOP-1, at doses of 5 and 25 µg per 100 mg of collagenous matrix as carrier, initiated bone formation by induction in heterotopic sites of the adult baboon. Platelet-derived pTGF-$ß_1$ or recombinantly produced hTGF-$ß_1$ combined with guanidinium-inactivated collagenous matrix, also induced heterotopic endochondral bone formation with an inductive efficiency comparable to doses of 5 and 25 µg rhOP-1 as determined by key parameters of bone formation. This remarkable result obtained in adult baboons contrasts markedly with previous studies in rodents, where heterotopic implantation of TGF-$ß_1$ or - 2, combined with either the insoluble collagenous matrix or purified collagen in conjunction with ceramic carriers, induces a fibrogenic response, without signs of cartilage or bone formation (Hammonds *et al.*, 1991; Roberts *et al.*, 1986; Sampath *et al.*, 1987; Bentz *et al.*, 1989; Bentz *et al.*, 1991).

The present finding of bone induction by TGF-$ß_1$ must be viewed within the context of biological experiment. One cannot completely dismiss the possibility that specific BMPs/OPs, binding to the matrix from systemic circulation or endogenously upregulated during heterotopic wound healing, might have synergized with the

exogenously-applied pTGF-ß$_1$ or rhTGF-ß$_1$. The recent immunolocalization of OP-1 in basement membranes of epithelia and endothelium in absence of detectable mRNA expression (Vukicevic *et al.*, 1994a), strongly indicates deposition within basement membranes at distance from sites of BMPs/OPs synthesis (Ozkaynak *et al.*, 1992; Helder *et al.*, 1995; Vukicevic *et al.*, 1994b). In the studies presented here, TGF-ß$_1$ was purified from porcine platelets, cellular elements known to contain other potent growth factors (Assoian *et al.*, 1984), so that the potency of the purified morphogen could be the result of other activities. To rule out this possibility, recombinant hTGF-ß$_1$, purified from medium of transfected CHO cells (Derynk *et al.*, 1985) was used and found to induce endochondral bone formation in the rectus abdominis of the baboon with an efficacy comparable to porcine TGF-ß$_1$. These results make it extremely unlikely that the bone inductive activity observed when using naturally derived TGF-ß$_1$ is due to impurities in the pTGF-ß$_1$ preparation.

The presence of multiple molecular forms with osteogenic activity raises important questions about the biological relevance of this apparent redundancy, and suggests multiple interactions during endochondral bone formation (Reddi, 1992; Wozney, 1992; Centrella *et al.*, 1994). It is natural to envision that a plurality of morphogens are required, if not to singly initiate, to promote synchronously and sequentially the cascade of bone formation. Data indicating that factors isolated from bone may act in concert to induce heterotopic osteoinduction were reported using demineralized bone matrix (Carrington *et al.*, 1988), and bone-derived fractions containing BMP-2 and -3 combined with bone-derived TGF-ß2 (Bentz *et al.*, 1989; Bentz *et al.*, 1991). In rat

experiments, the ratio of cartilage to bone was increased by combination of BMP fractions co-administered with increasing doses of bone-derived TGF-ß2 (Bentz *et al.*, 1989; Bentz *et al.*, 1991). In the experiments presented here, the addition of comparatively low doses of pTGF-$ß_1$ (0.5, 1.5 and 5 µg) to 25 µg rhOP-1 resulted in the generation of large corticalized ossicles complete with bone marrow in the rectus abdominis of the baboon. The finding that the addition of 0.5 and 1.5 µg pTGF-$ß_1$ increased more than 2 fold the inductive efficiency of 25 µg rhOP-1 indicates that the two morphogens interact synergistically during the induction of endochondral bone formation. Additionally, it was shown that TGF-$ß_1$ was inactive in the rat subcutaneous site, and that co-administration with rhOP-1 led to synergistic induction of bone formation. This is a classic example of synergistic interaction between two agents, where one is active, and the other inactive (Greco *et al.*, 1995). In calvarial defects of the baboon where TGF-$ß_1$ is inactive when applied singly, binary applications of rhOP-1 and pTGF-$ß_1$ induced tissue morphogenesis greater than the sum of the effects of both morphogens implanted singly. The unexpected osteoinductive activity of single applications of TGF-$ß_1$ in heterotopic sites of the baboon makes analysis of interaction with rhOP-1 difficult without additional analytical tools such as isobolographic techniques. These were used to show that in intramuscular sites of the primate, TGF-$ß_1$ and rhOP-1 interact synergistically to induce endochondral bone.

Ossicles generated by morphogen combinations showed chondrogenic zones with a degree of structural organization highly suggestive of rudimentary embryonic growth

plates, indicating that common molecular and cellular mechanisms are deployed for embryonic development and the induction of bone formation in postnatal life. The many-fold increase in type IV collagen mRNA synthesis over a single application of rhOP-1 and pTGF-$ß_1$, suggests that the two morphogens interact synergistically to induce angiogenesis and vascular invasion. Since angiogenesis is a prerequisite for osteogenesis, enhanced vascularization (including sinusoidal capillaries in the marrow compartment), may be part of the mechanism whereby rhOP-1 and TGF-$ß_1$ synergize in heterotopic bone induction.

Tissue generated by a single application of either morphogen showed high expression levels of their own mRNAs, suggesting an autoinductive effect, which, for TGF-$ß_1$, is in agreement with previous results obtained *in vitro* (Robey *et al.*, 1987) and *in vivo* (Joyce *et al.*, 1990). It is worth noting that tissue generated by pTGF-$ß_1$ showed OP-1 and BMP-3 mRNA synthesis, indicating that bone formation induced by pTGF-$ß_1$ in the rectus abdominis requires, at least in part, synthesis of members of the BMP/OP family. The high levels of type II collagen mRNA transcripts found in tissue generated by a single application of pTGF-$ß_1$ highlights the well-known chondrogenic potential of TGF-$ß_1$ (Sporn and Roberts, 1992; Centrella, 1994; Joyce, 1990). Addition of pTGF-$ß_1$ to rhOP-1 caused a dose-dependent rise in type II collagen mRNA synthesis, approaching levels induced by pTGF-$ß_1$ alone. The moderate expression of OP-1 and BMP-3 in tissue generated by morphogen combinations at doses of 1.5 and 5 μg pTGF-$ß_1$ may signify a temporal

acceleration of the induction cascade, and thus with decreased OP-1, BMP-3 and TGF-β_1 mRNA synthesis on day 30.

Evidence that TGF-ßs stimulate local osteogenesis *in vivo* consists of experiments where repeated applications of the morphogen were delivered subperiosteally in mice and rats (Joyce *et al.*, 1990; Noda and Camilliere, 1989), and, after a single administration, in calvarial defects of rabbits (Beck *et al.*, 1991; Beck *et al.*, 1993) and in humeral defects in dogs (Sumner *et al.*, 1995). In the primate, however, recombinant hTGF-β_1 failed to regenerate defects of the calvarial membranous bone (Ripamonti *et al.*, 1996a). These paradoxical effects of TGF-β_1 in the primate (osteoinductive in heterotopic but not in orthotopic sites) should be viewed in the context of the contradictory biphasic effects of TGF-β_1 on proliferation and differentiated functions of osteoprogenitor and osteoblastic cells *in vitro* (Sporn and Roberts, 1992; Centrella *et al.*, 1994), and more recently *in vivo* (Cassiede *et al.*, 1996). It is difficult to reconcile the apparent site specificity of TGF-β_1, osteoinductive at heterotopic sites but not at orthotopic sites of the primate. This apparent paradoxical behaviour of TGF-β_1 has been considered by others (Cassiede *et al.*, 1996), with the hypothesis that the effect of exogenously applied TGF-β_1 on the chondro-osteogenic potential of progenitor cells may be predicted from their anatomical location. Their hypothesis was conceived from the consideration of numerous results performed by different research groups seeking to analyse the effect of exogenous TGF-ß on the osteo-chondrogenic potential of progenitor cells. Osteo-chondrogenic progenitor cells can be separated into two distinct groups, based on their anatomical location in relation to the shaft of cortical bone (Cassiede *et al.*,

1996). The periosteum (progenitor cells in apposition to, but outside the shaft of cortical bone) constitutes one group, whereas endosteum and bone marrow the second group. Addition of TGF-ß to the first group triggers the differentiation of progenitor cells towards bone and cartilage differentiation. In the second group, the addition of TGF-ß to osteoprogenitor cells diverts cells from both chondrogenic and osteogenic lineages. There seems to be some analogy to the paradoxical effects of TGF-$ß_1$ presented in this work. When implanted into full thickness calvarial defects, TGF-$ß_1$ may act according to the hypothesis of Cassiede *et al.* (1996) to divert endosteal and marrow-derived osteochondro-progenitor cells from their chondrogenic and osteogenic lineage. If we may allow the periosteal criterion to be extended to surrounding muscle as well, then TGF-$ß_1$ may be expected to promote the differentiation of progenitor cells, presumably a mesenchymal stem cell, into the osteo-chondrogenic lineage, resulting in bone formation by induction. Whether responding cells and different signalling pathways, capable of imparting chondro-osteogenic differentiation after exogenous application of TGF-$ß_1$ are more readily available in the primate rectus abdominis than in a calvarial osseous wound, will require further studies.

rhOP-1, on the other hand, is capable of inducing bone differentiation in both heterotopic and orthotopic sites, changing the fate of cellular elements irrespective of their tissue location. In the context of the calvarial wound, rhOP-1 induces bone cell differentiation and TGF-$ß_1$ on the other hand, acts synergistically with rhOP-1 to promote the inductive events, but does not in itself induce bone formation. These

effects are specific, and are evidenced by the histological analysis of the tissue regenerates induced when rhOP-1 and TGF-$ß_1$ are applied singly to the calvarial wound (Ripamonti *et al.*, 1996a; Ripamonti *et al.*, 1996b). The latter morphogen induces and promotes the influx of mesenchymal elements resulting in exuberant bone formation in the presence of rhOP-1, and in a marked dose-dependent fibrogenic response when applied alone (Ripamonti *et al.*, 1996a). Co-administration of pTGF-$ß_1$ and rhOP-1 caused the induction of exuberant regenerates well above the profile of the normal calvaria with displacement of the temporalis muscle. This synergistic activity is possibly the result of superior cell migration and recruitment at site of implantation as well as enhancement of differentiated functions of osteoblasts, as documented by increased osteoid volumes. The orthotopic study further demonstrates that the co-administration of 5 µg pTGF-$ß_1$ improved dramatically the regenerates obtained by 20 µg rhOP-1, resulting in bone volumes comparable to a single administration of 100 µg rhOP-1, and in regenerates with geometric and architectural configurations equal to those obtained by a 5 fold higher amount of rhOP-1.

The current data obtained in the adult baboon, a primate that shares a remarkably similar bone remodelling with man (Schnitzler *et al.*, 1993), are relevant to therapeutic tissue engineering of bone. The results of the heterotopic and orthotopic studies indicate a synergistic interaction between two related but different members of the TGF-ß superfamily. TGF-$ß_1$ may act as chemotactic and mitogenic factor for responding precursor cells for subsequent induction by rhOP-1, as previously

suggested for a combination of bovine bone-derived TGF-ß$_2$ and BMP fractions (Bentz *et al.*, 1989; Bentz *et al.*, 1991), and possibly with simultaneous shift and redistribution in receptor binding profiles for TGF-ß$_1$ regulated by rhOP-1 (Centrella *et al.*, 1995). Ultimately, predictable and rapid bone regeneration for the treatment of human skeletal defects will require information concerning the expression and cross-regulation of members of the TGF-ß superfamily during tissue morphogenesis and regeneration induced by single or combined morphogen applications. In this study, the expression of multiple members of the TGF-ß superfamily indicates complex autocrine and paracrine activities of the ligands and different signalling pathways on responding cells during the cascade of endochondral bone formation in the primate. This may provide the scientific basis for synergistic molecular therapeutics for cartilage and bone regeneration in clinical contexts.

4.0 REFERENCES

Assoian, R.K., Komoriya, A., & Meyers, C.A., et al. 1983. Transforming growth factor-beta in human platelets. Identification of a major storage site, purification, and characterization. *J Biol Chem*, 258: 7155-7160.

Assoian, R.K., Grotendorst, G.R., & Miller, D.M. 1984. Cellular transformation by coordinated action of three peptide growth factors from human platelets. *Nature* (Lond.), 309: 804-806.

Assoian, R.K. 1987. Purification of type-beta transforming growth factor from human platelets. *Methods Enzymol*, 146: 153-163.

Attisano, L., Cárcamo, J., & Ventura, F. et al. 1993. Identification of human activin and TGFβ type I receptors that form heteromeric kinase complexes with type II receptors. *Cell*, 75: 671-680.

Baldwin, C.T., Reginato, A.M., & Smith, C., et al. 1989. Structure of cDNA clones coding for human type II procollagen. The alpha 1 (II) chain is more similar to the alpha 1 (I) chain than two other alpha chains of fibrillar collagen. *Biochem J*, 262: 521-528.

Bascom, C.C., Wolfshohl, J.R., & Coffey, R.J. Jr, et al. 1989. Complex regulation of transforming growth factor beta 1, beta 2, and beta 3 mRNA expression in mouse fibroblasts and keratinocytes by transforming growth factors beta 1 and beta 2. *Mol Cell Biol*, 9: 5508-5515.

Bassing, C.H., Yingling, J.M., & Howe, D.J., et al. 1994. A transforming growth factor beta type I receptor that signals to activate gene expression. *Science*, 263: 87-89.

Beck, L.S., DeGuzman, L., & Lee, W.P., et al. 1991. TGF-β1 induces bone closure of skull defects. *J Bone Min Res*, 6: 1257-1265.

Beck, L.S., Amento, E.P., & Xu, Y., et al. 1993. TGF-β1 induces bone closure of skull defects: Temporal dynamics of bone formation in defects exposed to rhTGF-β1. *J Bone Min Res*, 8: 753-761.

Bentz, H., Nathan, R.M., & Rosen, D., et al. 1989. Purification and characterization of an unique osteoinductive factor from bovine bone. *J Biol Chem*, 264: 20805-20810.

Bentz, H., Thompson, A., & Armstrong, R., et al. 1991. Transforming growth factor-β2 enhances the osteoinductive activity of a bovine bone-derived fraction containing bone morphogenetic protein-2 and 3. *Matrix*, 11: 269-275.

Bohme, K., Winterhalter, K.H., & Bruckner, P. 1995. Terminal differentiation of chondrocytes in culture is a spontaneous process and is arrested by transforming growth factor-beta 2 and basic fibroblast growth factor in synergy. *Exp Cell Res*, 216: 191-198.

Bonewald, L.F., & Dallas, S.L. 1994. Role of active and latent transforming growth factor β in bone formation. *J Cell Biochem*, 55: 350-357.

Bostrom, M., Lane, J.M., & Tomin, E., et al. 1996. Use of bone morphogenetic protein-2 in the rabbit ulnar nonunion model. *Clin Orthop*, 327: 272-282.

Bradshaw, R.A., Blundell, T.L., & Lapatto, R., et al. 1993. Nerve growth factor revisited. *Trends Biochem Sci*, 18: 48-52.

Carcamo, J., Weis, F.M., & Ventura, F., et al. 1994. Type I receptors specify growth-

inhibitory and transcriptional responses to transforming growth factor beta and activin. *Mol Cell Biol*, 14: 3810-3821.

Carrington, J.L., Roberts A.B. & Flanders K.C. 1988. Mesenchymal progenitor cells exposed to TGF-ß1 or PDGF-BB as assayed in vivo and in vitro. *J Bone Min Res*, 11: 1264-1273.

Cassiede, P., Dennis, J.E., & Ma, F., et al. 1996. Osteochondrogenic potential of marrow mesenchymal progenitor cells exposed to TGF-beta 1 or PDGF-BB as assayed in vivo and in vitro. *J Bone Miner Res*, 11: 1264-1273.

Celeste, A.J., Iannazzi J.A., & Taylor, R.C., et al. 1990. Identification of transforming growth factor β family members present in bone-inductive protein purified from bovine bone. *Proc Natl Acad Sci USA*, 87: 9843-9847.

Centrella, M., McCarthy, T.L., & Canalis, E. 1987. Transforming growth factor beta is a bifunctional regulator of replication and collagen synthesis in osteoblast-enriched cell cultures from fetal rat bone. *J Biol Chem*, 262: 2869-2874.

Centrella, M., McCarthy, T.L., & Canalis, E. 1991. Activin-A binding and biochemical effects in osteoblast-enriched cultures from fetal-rat parietal bone. *Mol Cell Biol*, 11: 250-258.

Centrella, M., Horwitz M.C., & Wozney, J.M., et al. 1994. Transforming growth factor-β gene family members and bone. *Endocr Rev*, 15: 27-39.

Centrella, M., Casinghino, S., & Kim, J., et al. 1995. Independent changes in type I and type II receptors for transforming growth factor β induced by bone morphogenetic protein 2 parallel expression of the osteoblast phenotype. *Mol Cell Biol*, 15: 3273-3281.

Chang, S.C., Hoang, B., & Thomas, J.T., et al. 1994. Cartilage-derived morphogenetic proteins. New members of the transforming growth factor-beta superfamily predominantly expressed in long bones during human embryonic development. *J Biol Chem*, 269: 28227-28234.

Cheifetz, S., Hernandez, H., & Laiho, M., et al. 1990. Distinct transforming growth factor-beta (TGF-beta) receptor subsets as determinants of cellular responsiveness to three TGF-beta isoforms. *J Biol Chem*, 265: 20533-20538.

Cohen, S.N., Chang, A.C., & Hsu, L. 1972. Nonchromosomal antibiotic resistance in bacteria: genetic transformation of Escherichia coli by R-factor DNA. *Proc Natl Acad Sci USA*, 69: 2110-2114.

Cook, S.D., Baffes, G.C., & Wolfe, M.W., et al. 1994. Recombinant human bone morphogenetic protein-7 induces healing in a canine long-bone segmental defect model. *Clin Orthop*, 301: 302-311

Cook, S.D., Wolfe, M.W., & Salkeld, S.L., et al. 1995. Effect of recombinant human osteogenic protein-1 on healing of segmental defects in non-human primates. *J Bone Joint Surg*, 77: 734-746.

Cook, S.D. & Rueger, D. 1996. Osteogenic protein-1. *Clin Orthop*, 324: 29-38.

Cunningham, N.S., Paralkar, V., & Reddi, A.H. 1992. Osteogenin ad recombinant bone morphogenetic protein 2B are chemotactic for human monocytes and stimulate transforming growth factor β_1 mRNA expression. *Proc Natl Acad Sci USA*, 89: 11740-11744.

Cunningham, N.S., Jenkins, N.A., & Gilbert, D.J., et al. 1995. Growth/differentiation factor-10: A new member of the transforming growth factor-β superfamily related to bone morphogenetic protein-3. *Growth Factors*, 0: 1-11.

Daopin, S., Piez, K.A., & Ogawa, Y., et al. 1992. Crystal structure of transforming growth factor-beta 2: an unusual fold for the superfamily. *Science*, 257: 369-373.

Darnell, J.E. Jr., Kerr, I.M., & Stark, G.R. 1994. Jak-STAT pathways and transcriptional activation in response to IFNs and other extracellular signaling proteins. *Science*, 264: 1415-1421.

Derynk, R., Jarret, J.A., & Chen, E.Y., et al. 1985. Human transforming growth factor-ß complementary DNA sequence and expression in normal and transformed cells. *Nature (Lond.)*, 316: 701-705.

Derynck, R., Lindquist, P.B., & Lee, A., et al. 1988. A new type of transforming growth factor-beta, TGF-beta 3. *EMBO J*, 7: 3737-3743.

Derynk, R. 1994. The biological complexity of transforming growth factor-β. In: The Cytokine Handbook. A Thompson, editor. Academic Press, Boston. 319-342.

DeVita, V.T. Jr. 1989. Principles of chemotherapy. In: Cancer Principles and Practice of Oncology. DeVita, V.T. Jr, Hellman, S., & Rosenberg, S.A., ed. J.B. Lippincott, Philadelphia. 276-300.

Dieudonné, S.C., Semeins, C.M., & Goei, S.W., et al. 1994. Opposite effects of osteogenic protein and transforming growth factor β on chondrogenesis in cultured long bone rudiments. *J Bone Miner Res*, 9: 771-780.

Ducy, P., Desbois, C., & Boyce, B., et al. 1996. Increased bone formation in osteocalcin-deficient mice. *Nature*, 382: 448-452.

Dudley, A.T., Lyons, K.M., & Robertson, E.J. 1995. A requirement for bone morphogenetic protein-7 during development of the mammalian kidney and eye. *Genes & Dev*, 9: 2795-2807.

Dudley, A.T., & Robertson, E.J. 1997. Overlapping expression domains of bone morphogenetic protein family members potentially account for limited tissue defects in BMP7 deficient embryos. *Dev Dyn*, 208: 349-362.

Ebner, R., Chen, R.H., & Lawler, S., et al. 1993. Determination of type I receptor specificity by the type II receptors for TGF-beta or activin. *Science*, 262: 900-902.

Ebner, R., Chen, R-H., & Shum, L., et al. 1993. Cloning of a type I TGF-β receptor and its effect on TGF-ß binding of the type II receptor. *Science*, 260: 1344-1348.

Edwards, D.R., Murphy, G., & Reynolds, J.J., et al. 1987. Transforming growth factor beta modulates the expression of collagenase and metalloproteinase inhibitor. *EMBO J*, 6: 1899-1904.

Elion, G.B., Singer, S., & Hitchings, G.H. 1954. Antagonists of nucleic acid derivatives. Part VIII. Synergism in combinations of biochemically related antimetabolites. *J Biol Chem*, 208: 477-488.

Erlacher, L., McCartney, J., Piek, E., ten Dijke, P., Yanagishita, M., Oppermann, H., Luyten, FP. (1998) Cartilage-derived morphogenetic proteins and osteogenic protein-1 differentially regulate osteogenesis. *J Bone Miner Res* 13(3):383-392.

Erlebacher, A., & Derynck, R. 1996. Increased expression of TGF-ß2 in osteoblasts results in osteoporosis-like phenotype. *J Cell Biol*, 132: 195-210.

Ewen, M.E., Sluss, H.K., & Whitehouse, L.L., et al. 1993. TGF beta inhibition of Cdk4 synthesis is linked to cell cycle arrest. *Cell*, 74: 1009-1020.
Ferguson, E.L., & Anderson, K.V. 1992. Decapentaplegic acts as a morphogen to organize dorsal-ventral pattern in the Drosophila embryo. *Cell*, 71: 451-461.

Foidart, J.M., & Reddi, A.H. 1980. Immunofluorescent localization of type IV collagen and laminin during endochondral bone differentiation and regulation by pituitary growth hormone. *Dev Biol*, 75: 130-136.

Francis, P.H., Richardson, K., & Brickell, P.M., et al. 1994. Bone morphogenetic proteins and a signalling pathway that controls patterning in the developing chick limb. *Development*, 120: 209-218.

Franzén, P., ten Dijke, P., & Ichijo, H., et al. 1993. Cloning of a TGF-β type I receptor that forms a heteromeric complex with the TGF-β type II receptor. *Cell*, 75: 681-692.

Franzén, P., Heldin, C-H., & Miyazono, K. 1995. The Gs domain of the transforming growth factor-β type I receptor is important in signal transduction. *Biochem Biophys Res Commun*, 270: 682-689.

Fraser, T. R. 1871. An experimental research on the antagonism between the actions of physostigma and atropia. *Proc R Soc Edinb*, 7: 506-511.

Fraser, T.R. 1872. The antagonism between the actions of active substances. *Br Med J*, 2: 485-487.

Gerhart, T.N., Kirker-Head, C.A., & Vet, M.A., et al. 1994. Healing segmental

femoral defects in sheep using recombinant bone morphogenetic protein. *Clin Orthop*, 28: 1149-1161.

Globus, R.K., Bikle, D.D., & Morey-Holton, E. 1986. The temporal response of bone to unloading. *Endocrinology*, 118: 733-742.

Greco, W.R., & Lawrence, D.L. 1988. Assessment of the degree of drug interaction where the response variable is discrete. American Statistical Association, Proceedings of the Biopharmaceutical Section, 226-231.

Greco, W.R., Bravo, G., & Parsons, J.C. 1995. The search for synergy: a critical review from a response surface perspective. *Pharmacol Rev*, 47: 331-385.

Griffith, D.L., Keck, P.C., & Sampath, T.K., et al. 1996. Three-dimensional structure of recombinant human osteogenic protein 1: Structural paradigm for the transforming growth factor β superfamily. *Proc Natl Acad Sci USA*, 93: 878-883.

Halstead, J., Kemp, K., & Ignotz, R.A. 1995. Evidence for involvement of phosphatidylcholine-phospholipase C and protein kinase C in transforming growth factor-beta signaling. *J Biol Chem*, 270: 13600-13603.

Hammmonds, R.G., Schwall, R., & Dudley, A., et al. 1991. Bone inducing activity of mature BMP-2b produced from a hybrid BMP-2a/2b precursor. *Mol Endocrinol*, 5: 149-155.

Harland, R.M. 1994. The transforming growth factor ß family and induction of the vertebrate mesoderm: Bone morphogenetic proteins are ventral inducers. *Proc Natl Acad Sci USA*, 91: 10243-10246.

Harris, S.E., Bonewald, L.F., & Harris, M.A., et al. 1994. Effects of transforming growth factor beta on bone nodule formation and expression of bone morphogenetic protein 2, osteocalcin, osteopontin, alkaline phosphatase, and type I collagen mRNA in long term cultures of fetal rat calvarial osteoblasts. *J Bone Mineral Res*, 9: 855-863.

Hayashi, H., Abdollah, S., & Qiu, Y., et al. 1997. The MAD-related protein Smad7 associates with the TGF-beta receptor and functions as an antagonist of TGF beta signalling. *Cell*, 89: 1165-1173.

Heine, U.I., Munoz, E.F., & Flanders, K.C., et al. 1987. Role of transforming growth factor-β in the development of the mouse embryo. *J Cell Biol*, 105: 2861-2876.

Helder, M.N., Özkaynak, E., & Sampath, T.K. et al. 1995. Expression pattern of osteogenic protein-1 (bone morphogenetic protein-7) in human and mouse development. *J Histochem Cytochem*, 43: 1035-1044.

Heldin, C.H. 1992. Structural and functional studies on platelet-derived growth factor. *EMBO J*, 11: 4251-4259.

Heldin, C.H., Ostman, A., & Eriksson, A., et al. 1992. Platelet-derived growth factor: isoform-specific signalling via heterodimeric or homodimeric receptor complexes. *Kidney Int*, 41: 571-574.

Hill, D.J., Strain, A.J., & Elstow, S.F., et al. 1986. Bi-functional action of transforming growth factor-beta on DNA synthesis in early passage human fetal fibroblasts. *J Cell Physiol*, 128: 322-328.

Hostikka, S.L., & Tryggvason, K. 1988. The complete primary structure of the alpha 2 chain of human type IV collagen and comparison with the alpha 1 (IV) chain. *J Biol Chem*, 263: 19488-19493.

Hötten, G., Neidhardt, H., Jacobowsky, B., Pohl, J. (1994) Cloning and expression of recombinant human growth/differentiation factor 5. *Biochem Biophys Res Commun* 28;204(2):646-652.

Hötten, G.C., Matsumoto, T., & Kimura, M., et al. 1996. Recombinant human growth/differentiation factor 5 stimulates mesenchyme aggregation and chondrogenesis responsible for the skeletal development of limbs. *Growth Factors*, 13: 65-74.

Ibanez, C.F., Ebendal, T., & Barbany, G., et al. 1992. Disruption of the low affinity receptor-binding site in NGF allows neuronal survival and differentiation by binding to the trk gene product. *Cell*, 69: 329-341.

Ignotz, R.A., & Massague, J. 1986. Transforming growth factor-beta stimulates the expression of fibronectin and collagen and their incorporation into the extracellular matrix. *J Biol Chem*, 261: 4337-4345.

Imamura, T., Takase, M., & Nishihara, A., et al. 1997. Smad6 inhibits signalling by the TGF-beta superfamily. *Nature*, 389:622-626.

Israel, D.I., Nove, J., & Kerns, K.M., et al. 1992. Expression and characterization of bone morphogenetic protein-2 in Chinese hamster ovary cells. *Growth Factors*, 7: 139-150.

Jennings, J.C., Mohan, S., & Linkhart, T.A., et al. 1988. Comparison of the biological actions of TGF beta-1 and TGF beta-2: differential activity in endothelial cells. *J Cell Physiol*, 137: 167-172.

Johnson, E.E., Urist, M.R., & Finerman, G.A. 1988. Bone morphogenetic protein augmentation grafting of resistant femoral nonunions. A preliminary report. *Clin*

Orthop, 230: 257-265

Johnson, E.E., Urist, M.R., & Finerman, G.A. 1988. Repair of segmental defects of the tibia with cancellous bone grafts augmented with human bone morphogenetic protein. A preliminary report. *Clin Orthop*, 236: 249-257.

Johnson, E.E., Urist, M.R., & Finerman, G.A. 1990. Distal metaphyseal tibial nonunion. Deformity and bone loss treated by open reduction, internal fixation, and human bone morphogenetic protein (hBMP). *Clin Orthop*, 250: 234-240.

Jones, C.M., Lyons, K.M., & Hogan, B.L. 1991. Involvement of Bone Morphogenetic Protein-4 (BMP-4) and Vgr-1 in morphogenesis and neurogenesis in the mouse. *Development*, 111: 531-542.

Joyce, M.E., Roberts, A.B., & Sporn, M.B., et al. 1990. Transforming growth factor-β and the initiation of chondrogenesis and osteogenesis in the rat femur. *J Cell Biol*, 110: 2195-2207.

Kawabata, M., Imamura, T., & Miyazono, K., et al. 1995. Interaction of the transforming growth factor-beta type I receptor with farnesyl-protein transferase-alpha. *J Biol Chem*, 270: 29628-29631.

Keller, J.R., Mantel, C., & Sing, G.K., et al. 1988. Transforming growth factor beta 1 selectively regulates early murine hematopoietic progenitors and inhibits the growth of IL-3-dependent myeloid leukemia cell lines. *Exp Med*, 168: 737-750.

Keller, J.R., Jacobsen, S.E., & Sill, K.T., et al. 1991. Stimulation of granulopoiesis by transforming growth factor beta: synergy with granulocyte/macrophage-colony-stimulating factor. *Proc Natl Acad Sci USA*, 88: 7190-7194.

Kenley, R., den, .L, & Turek, T., et al. 1994. Osseous regeneration in the rat calvarium

using novel delivery systems for recombinant human bone morphogenetic protein-2 (rhBMP-2). *J Biomed Mater Res*, 28: 1139-1147.

Kessler, E., Takahara, K., & Biniaminov, L., et al. 1996. Bone morphogenetic protein-1: the type I procollagen C-proteinase. *Science*, 271: 360-362.

Khouri, R.K., Koudsi, B.,& Reddi, A.H. 1991. Tissue transformation into bone in vivo. A potential practical application. *JAMA*, 266: 1953-1955.

Khouri, R.K., Brown, D.M., Koudsi, B., Deune, E.G., Gilula, L.A., Cooley, B.C., Reddi, A.H. (1996) Repair of calvarial defects with flap tissue: role of bone morphogenetic proteins and competent responding tissues. Plast Reconstr Surg 98(1):103-109.

Kibblewhite, D.J., Bruce, A.G., & Strong, D.M., et al. 1993. Transforming growth factor-beta accelerates osteoinduction in a craniofacial onlay model. *Growth Factors*, 9: 185-193.

Kingsley, D. 1994. The TGF-(superfamily: new members, new receptors, and new genetic tests of functions in different organisms. *Genes & Dev*, 8: 133-146.

Kirker-Head, C.A., Gerhart, T.N., & Schelling, S.H., et al. 1995. Long-term healing of bone using recombinant human bone morphogenetic protein-2. *Clin Orthop*, 318: 222-234

Koff, A., Ohtsuki, M., & Polyak, K., et al. 1993. Negative regulation of G1 in mammalian cells: inhibition of cyclin E-dependent kinase by TGF-beta. *Science*, 260: 536-539.

Kretzschmar, M., Liu, F., & Hata, A., et al. 1997. The TGF-beta family mediator Smad1 is phosphorylated directly and activated functionally by the BMP receptor kinase. *Genes Dev,* 11: 984-995.

Kulkarni, A.B., Huh, C-G., & Becker, D., et al. 1993. Transforming growth factor β_1 null mutation in mice causes excessive inflammatory response and early death. *Proc Natl Acad Sci USA*, 90: 770-774.

Laiho, M., Weis, F.M., & Boyd, F.T., et al. 1991. Responsiveness to transforming growth factor-beta (TGF-beta) restored by genetic complementation between cells defective in TGF-beta receptors I and II. *J Biol Chem*, 266: 9108-9112.

Lee, S-J. 1990. Identification of a novel member (GDF-1) of the transforming growth factor-β superfamily. *Mol endocrinol*, 4: 1034-1040.

Lee, S-J. 1991. Expression of growth/differentiation factor 1 in the nervous system: Conservation of a bicistronic structure. *Proc Natl Acad Sci USA*, 88: 4520-4254.

Lee, S.C., Shea, M., & Battle, M.A., et al. 1994. Healing of large segmental defects in rat femurs is aided by rhBMP-2 in PLGA matrix. *J Biomed Mater Res*, 28: 1149.

Liu, F., Ventura, F., & Doody, J., et al. 1995. Human type II receptor for bone morphogenic proteins (BMPs): extension of the two-kinase receptor model to the BMPs. *Mol Cell Biol*, 15: 3479-3486.

Liu, F., Hata, A., & Baker, J.C., et al. 1996. A human Mad protein as a BMP-regulated transcriptional activator. *Nature*, 381: 620-623.

Loewe, S., & Muischnek, H. 1926. Effect of combinations: mathematical basis of problem. *Arch Exp Pathol Pharmakol.*

Loewe, S. 1928. Die Quantitation Probleme der Pharmakologie. *Ergeb Physiol Biol Chem Exp Pharmakol*, 27: 47-187.

Loewe, S. 1953. The problem of synergism and antagonism of combined drugs. *Arzneim Forsch*, 3: 285-290.

Loewe, S. 1957. Antagonism and antagonists. *Pharmacol Rev*, 9: 237-242.

Lowry, O.H., Rosebrough, N.J., & Farr, A.L., et al. 1951. Protein measurement with the Folin phenol reagent. *J Biol Chem*, 193: 265-275.

Luo, G., Hofmann, C., & Bronckers, A.L.J.J., et al. 1995. BMP-7 is an inducer of nephrogenesis, and is also required for eye development and skeletal patterning. *Genes & Dev*, 9: 2808-2820.

Luo, K., Zhou, P., & Lodish, H.F. 1995. The specificity of the transforming growth factor β receptor kinases determined by a spatially addressable peptide library. *Proc Natl Acad Sci USA*, 92: 11761-11765.

Luyten, F.P., Cunningham, N.S., & Ma, S., et al. 1989. Purification and partial amino acid sequence of osteogenin, a protein initiating bone differentiation. *J Biol Chem*, 264: 13377-13380.

Luyten, F.P., Chen, P., & Paralkar, V., et al. 1994. Recombinant bone morphogenetic protein-4, transforming growth factor-beta 1, and activin A enhance the cartilage phenotype of articular chondrocytes in vitro. *Exp Cell Res*, 210: 224-229.

Lyons, K.M., Graycar, J.L., & Lee, A., et al. 1989. Vgr-1, a mammalian gene related to Xenopus Vg-1 and a new member of the transforming growth factor β superfamily.

Proc Natl Acad Sci USA, 86: 4554-4558.

Lyons, K.M., Pelton, R.W., & Hogan, B.L . 1990. Organogenesis and pattern formation in the mouse: RNA distribution patterns suggest a role for bone morphogenetic protein-2A (BMP-2A). *Development*, 109: 833-844.

Lyons, K.M., Hogan, B.L., & Robertson, E.J. 1995. Colocalization of BMP 7 and BMP 2 RNAs suggests that these factors cooperatively mediate tissue interactions during murine development. *Mech Dev*, 50: 71-83.

Machado, S.G., & Robinson, G.A. 1994. A direct, general approach based on isobolograms for assessing the joint action of drugs in pre-clinical experiments. *Statistics in Medicine*, 13: 2289-2309.

Machwate, M., Zerath, E,. & Holy, X., et al. 1995. Systemic administration of transforming growth factor-β2 prevents the impaired bone formation and osteopenia induced by unloading in rats. *J Clin Invest*, 96: 1245-1253.

Maéno, M., Ong, R.C., & Suzuki, A., et al. 1994. A truncated bone morphogenetic protein 4 receptor alters the fate of ventral mesoderm to dorsal mesoderm: roles of animal pole tissue in the development of ventral mesoderm. *Proc Natl Acad Sci USA*, 91: 10260-10264.

Marcelli, C., Yates, A.J., & Mundy, G.R. 1990. In vivo effects of human recombinant transforming growth factor beta on bone turnover in normal mice. *J Bone Miner Res*, 5: 1087-1096.

Massagué, J., Cheifetz, S., & Endo. T., et al. 1986. Type beta transforming growth

factor is an inhibitor of myogenic differentiation. *Proc Natl Acad Sci USA*, 83: 8206-8210.

Massagué, J. 1990. The transforming growth factor-beta family. *Annu Rev Cell Biol*, 6: 597-641.

Massagué, J. 1992. Receptors for the TGF-β family. *Cell*, 69: 1067-1070.

Massagué, J., Andres, J., & Attisano, L., et al. 1992. TGF-β receptors. *Mol Rep Dev*, 32: 99-104.

Matthews, J.L. 1980. Bone structure and ultrastructure. In: Fundamental and clinical bone physiology, Urist, M.R., ed. J.B. Lippincott Company, Philadelphia. 4-44.

Mayer, H., Scutt, A.M., & Ankenbauer, T. 1996. Subtle differences in the mitogenic effects of recombinant human bone morphogenetic protein -2 to -7 on DNA synthesis on primary bone-forming cells and identification of BMP-2/4 receptor. *Calcif Tissue Int*, 58: 249-255.

McDonald, N.Q., Lapatto, R., & Murray-Rust, J., et al. 1991. New protein fold revealed by a 2.3-A resolution crystal structure of nerve growth factor. *Nature*, 354: 411-414.

McDonald, N.Q., & Hendrickson, W.A. 1993. A structural superfamily of growth factors containing a cystine knot motif. *Cell*, 73: 421-424.

McPherron, A.C., Lee, S-J. 1993. Two new members of the transforming growth factor-β superfamily containing a novel pattern of cysteines. *J Biol Chem*, 268: 3444-3449.

Meno, C., Saijoh, Y., & Fujii, H., et al. 1996. Left-right asymmetric expression of the TGF beta-family member lefty in mouse embryos. *Nature*, 381: 151-155.

Miettinen, P.J., Ebner, R., & Lopez, A.R. 1994. TFG-β induced transdifferentiation of mammary epithelial cells to mesenchymal cells: Involvement of type I receptors. *J Cell Biol*, 127: 2021-2036.

Millan, F.A., Denhez, F., & Kondaiah, P., et al. 1991. Embryonic gene expression patterns of TGF-β_1, β_2 and β_3. Growth Factors and Their Receptors. Berlin, Springer-Verlag, 419-472.

Miura, Y., Fitzsimmons, J.S., & Commisso, C.N., et al. 1994. Enhancement of periosteal chondrogenesis in vitro. Dose-response for transforming growth factor-beta 1 (TGF-beta 1). *Clin Orthop*, 301:271-280.

Moses, H.L., Coffey, R.J. Jr, & Leof, E.B., et al. 1987 Transforming growth factor beta regulation of cell proliferation. *J Cell Physiol Suppl*, 5: 1-7.

Moses, H.L., Yang, E.Y., & Pietenpol, J.A. 1990. TGF-beta stimulation and inhibition of cell proliferation: new mechanistic insights. *Cell*, 63: 245-247.

Muschler, G.F., Hyodo, A., & Manning, T., et al. 1994. Evaluation of human bone morphogenetic protein 2 in a canine spinal fusion model. *Clin Orthop*, 308: 229-240.

Mustoe, T.A., Pierce, G.F., & Thomason, .A, et al. 1987. Accelerated healing of incisional wounds in rats induced by transforming growth factor-beta. *Science*, 11,237: 1333-1336.

Muthukumaran, N., Ma, S., & Reddi, A.H. 1988. Dose-dependence of and threshold

for optimal bone induction by collagenous bone matrix and osteogenin-enriched fraction. *Coll Relat Res*, 8: 433-441.

Nakao, A., Afrakhte, M., & Moren, A., et al. 1997. Identification of Smad7, a TGFbeta-inducible antagonist of TGF-beta signalling. *Nature*, 389: 631-635.

Nemeth, G.G., Heydemann, A., & Bolander, M.E. 1989. Isolation and analysis of ribonucleic acids from skeletal tissues. *Anal Biochem*, 183: 301-304.

Nevins, M., Kirker-Head, C., & Nevins, M., et al. 1996. Bone formation in the goat maxillary sinus induced by absorbable collagen sponge implants impregnated with recombinant human bone morphogenetic protein-2. *Int J Periodontics Restorative Dent*, 16: 8-19.

Noda, M., & Rodan, G.A. 1986.Type-beta transforming growth factor inhibits proliferation and expression of alkaline phosphatase in murine osteoblast-like cells. *Biochem Biophys Res Commun*, 140: 56-65.

Noda, M., & Camilliere, J.J. 1989. In vivo stimulation of bone formation by transforming growth factor-β. *Endocrinology*, 124: 2991-2994.

Nohno, T., Ishikawa, T., & Saito, T., et al. 1995. Identification of a human type II receptor for bone morphogenetic protein-4 that forms differential heteromeric complexes with bone morphogenetic protein type I receptors. *J Biol Chem*, 270: 22522-22526.

Oefner, C., D'Arcy, A., & Winkler, F.K., et al. 1992. Crystal structure of human platelet-derived growth factor BB. *EMBO J*, 11: 3921-3926.

Ogawa, Y., Schmidt, D.K., & Nathan, R.M., et al. 1992. Bovine bone activin enhances bone morphogenetic protein-induced ectopic bone formation. *J Biol Chem*, 267:

14233-14237.

Ogawa, Y., Schmidt, D.K., & Dasch, J.R., et al. 1992. Purification and characterization of transforming growth factor-ß2.3 and –ß1.2 heterodimers from bovine bone. *J Bio Chem,* 267: 2325-2328.

Okazaki, Y.M., Shirai T, & Pan, H., et al. 1996. Recombinant human growth/differentiation factor 5 stimulates mesenchyme aggregation and chondrogenesis responsible for the skeletal development of limbs. *Growth Factors*, 13: 65-74.

Ono, I., Gunji, H., & Kaneko, F., et al. 1995. Efficacy of hydroxyapatite ceramic as a carrier for recombinant human bone morphogenetic protein. *J Craniofac Surg*, 6: 238-244.

Özkaynak, E., Rueger, D.C., & Drier, E.A., et al. 1990. OP-1 cDNA encodes an osteogenic protein in the TGF-ß family. *EMBO J (Eur Mol Biol Organ)*, 9: 2085-2093.

Özkaynak, E., Schnegelsberg, P.N.J., & Jin, D.F. et al. 1992. Osteogenic protein-2. A new member of the transforming growth factor-ß superfamily expressed early in embryogenesis. *J Biol Chem*, 267: 25220-25227.

Padget, R.W., St Johnston, R.D., & Gelbart, W.M. 1987. A transcript from a Drosophila pattern gene predicts a protein homologous to the transforming growth factor-beta family. *Nature*, 325: 81-84.

Paralkar, V.M., Vukicevic, S., & Reddi, A.H. 1991. Transforming growth factor ß type 1 binds to collagen IV of basement membrane matrix: Implications for development. *Dev Biol*, 143: 303-314.

Parfit, A.M. 1983. Stereologic basis of bone histomorphometry: Theory of quantitative microscopy and reconstruction of the third dimension. In: Bone histomorphometry: Techniques and interpretation. Recker RR, ed. Boca Raton: *CRC Press*, 53-87.

Parfitt, A.M., Drezner, M.K., & Glorieux, F.H., et al. 1987. Bone histomorphometry: Standardization of nomenclature, symbols, and units. *J Bone Min Res*, 2: 595-610.

Pelton, R.W., Nomura, S., & Moses, H.L., et al. 1989. Expression of transforming growth factor beta 2 RNA during murine embryogenesis. *Development*, 106: 759-767.

Pelton, R.W., Saxena B. & Jones, M., et al. 1990. Immunohistochemical localization of TGF-β_1, TGF-β_2, and TGF-β_3 in mouse embryo: Expression patterns suggest multiple rolls during embryonic development. *J Cell Biol*, 115: 1091-1105.

Pfeilschifter, J., Wolf, O., & Naumann, A., et al.1990. Chemotactic response of osteoblast-like cells to transforming growth factor beta. *J Bone Miner Res*, 5: 825-830.

Polyak, K., Kato, J.Y., & Solomon, M.J., et al. 1994. p27Kip1, a cyclin-Cdk inhibitor, links transforming growth factor-beta and contact inhibition to cell cycle arrest. *Genes Dev*, 8: 9-22.

Postlethwaite, A.E., Keski-Oja, J., & Moses, H.L., et al. 1987. Stimulation of the chemotactic migration of human fibroblasts by transforming growth factor beta. *J Exp Med*, 165: 251-256.

Postlethwaite, A.E., Raghow, R., & Stricklin, G., et al. 1994. Osteogenic protein-1, a bone morphogenetic protein member of the TGF-β superfamiily, shares chemotactic but not fibrogenic properties with TGF-β. *J Cell Physiol*, 161: 562-570.

Qian, S.W., Burmester, J.K., & Merwin, J.R., et al. 1992. Identification of a structural

domain that distinguishes the actions of the type 1 and 2 isoforms of transforming growth factor beta on endothelial cells. *Proc Natl Acad Sci USA*, 89: 6290-6294.

Reddi, A.H., & Huggins, C.B. 1972. Biochemical sequence in the transformation of normal fibroblasts in adolescent rats. *Proc Natl Acad Sci USA*, 69: 1601-1605.

Reddi, A.H., & Huggins, C.B. 1975. The formation of bone marrow in fibroblast-transformation ossicles. *Proc Natl Acad Sci USA*, 72: 2212-2221.

Reddi, A.H. 1992. Regulation of cartilage and bone differentiation by bone morphogenetic proteins. *Curr Opin Cell Biol*, 4: 850-855.

Reddi, A.H., & Cunningham, N.S. 1993. Initiation and promotion of bone differentiation by bone morphogenetic proteins. *J Bone Min Res*, 8: 499-502.

Reddi, A.H. 1994. Bone and cartilage differentiation. *Curr Opin Gen Dev*, 4: 737-744.

Reddi, A.H. 1996. BMP-1: resurrection as procollagen C-proteinase. *Science*, 71: 463.

Reddi, A.H., Muthukumaran, N., & Ma, S., et al. Initiation of bone development by osteogenin and promotion by growth factors. *Connect Tissue Res*, 20: 303-319.

Ripamonti, U. 1991. Bone induction in nonhuman primates. An experimental study on the baboon (Papio ursinus). *Clin Orthop*, 269: 284-294.

Ripamonti, U., Magan, A., & Ma. S., et al. 1991. Xenogeneic osteogenin, a bone morphogenetic protein, and demineralized bone matrices, including human, induce bone differentiation in athymic rats and baboons. *Matrix*, 11: 404-411.

Ripamonti, U. 1992. Molecules initiating bone differentiation: osteogenin and related

bone morphogenetic proteins. *SA J Sci*, 88: 354-355.

Ripamonti, U., Ma, S., & Cunningham, N., et al. 1992. Initiation of bone regeneration in adult baboons by osteogenin, a bone morphogenetic protein. *Matrix*, 12: 369-380.

Ripamonti, U., Ma, S., & Reddi, A.H. 1992. Induction of bone in composites of osteogenin and porous hydroxyapatite in the baboons. *Plast Reconstr Surg*, 89: 731-739.

Ripamonti, U., Ma, S., & Reddi, A.H. 1992. The critical role of geometry of porous hydro yapatite delivery system in introduction of bone by osteogenin, a bone morphogenetic protein. *Matrix*, 12: 202-212.

Ripamonti, U., Ma, S., & van den Heever, B., et al. 1992. Osteogenin, a bone morphogenetic protein, adsorbed on porous hydroxyapatite substrata induces rapid bone differentiation in calvarial defects of adult primates. *Plast Reconstr Surg*, 90: 382-393.

Ripamonti, U., van der Heever, B., & van Wyk, J. 1993. Expression of the osteogenic phenotype in porous hydroxyapatite implanted extraskeletally in baboons. *Matrix*, 13: 491-502.

Ripamonti, U., Yeates, L., & van den Heever, B. 1993. Initiation of heterotopic osteogenesis after chromatographic adsorption of osteogenin, a bone morphogenetic protein, onto porous hydroxyapatite. *Biochem Biophys Res Commun*, 193: 509-517.

Ripamonti, U., Ma, S., & Cunningham, N., et al. 1993. Reconstruction of the bone-bone marrow organ by osteogenin, a bone morphogenetic protein, and demineralized bone matrix in calvarial defects of adult primates. *Plast Reconstr Surg*, 91: 27-36.

Ripamonti, U., & Reddi, A.H. 1994. Periodontal regeneration: potential role of bone morphogenetic proteins. *J Periodont Res*, 29: 225-235.

Ripamonti, U., & Reddi, A.H. 1995. Bone morphogenetic proteins: Applications in plastic and reconstructive surgery. *Adv Plast Reconstr Surg*, 11: 47-74.

Ripamonti, U., Bosch, C., & van den Heever, B., et al. 1996a. Limited chondro-osteogenesis by recombinant human transforming growth factor-ß1 in calvarial defects of adult baboons (Papio ursinus). *J Bone Min Res*, 11: 938-945.

Ripamonti, U., van den Heever, B., & Sampath, T.K., et al. 1996b. Complete regeneration of bone in the baboon by recombinant human osteogenic protein-1 (hOP-1, bone morphogenetic protein-7). *Growth Factors*, 13: 273-289.

Ripamonti, U., Heliotis, M., & Rueger, D.C., et al. 1996. Induction of cementogenesis by recombinant human osteogenic protein-1 (hOP-1/BMP-7) in the baboon (Papio ursinus). *Arch Oral Biol*, 41: 121-126.

Ripamonti, U., Heliotis, M., & van den Heever, B., et al. 1996. Bone morphogenetic proteins induce periodontal regeneration in the baboon (Papio ursinus). *J Periodont Res*, 29: 439-445.

Roberts, A.B., Sporn, M.B., & Assoian, R.K. et al. 1986. Transforming growth factor type ß: Rapid induction of fibrosis and angiogenesis in vivo and stimulation of collagen formation in vitro. *Proc Natl Acad Sci USA*, 83: 4169-4171.

Roberts, A.B., & Sporn, M.B. 1990. The transforming growth factors-ß. In: Sporn MB, Roberts AB (eds.) Handbook of Experimental Pharmacology, 95: Part I. Springer-Verlag, Heidelberg, 419-472.

Roberts, A.B., Kim, S.J., & Noma, T., et al. 1991. Multiple forms of TGF-beta: distinct promoters and differential expression. *Ciba Found Symp*, 157: 7-15.

Robey, P.G., Young, M.F., & Flanders, K.C., et al. 1987. Osteoblasts synthesize and respond to TGF-β in vitro. *J Cell Biol*, 105: 457-463.

Rodriguez, C., Chen, F., & Weinberg, R.A., et al. 1995. Cooperative binding of transforming growth factor (TGF)-β2 to the types I and II TGF-β receptors. *J Biol Chem*, 270: 15919-15922.

Rosen, D.M., Nathan, R., & Armstrong, R., *et al.* 1990. Bone induction and transforming growth factor-β. *Ann NY Acad Sci*, 593: 98-106.

Rosenzweig, B.L., Imanura, T., & Okadome, T., et al. 1995. Cloning and characterization of a human type II receptor for bone morphogenetic proteins. *Proc Natl Acad Sci USA*, 92: 7632-7636.

Rupert, R., Hoffmann, E., & Sebald, W. 1996. Human bone morphogenetic protein 2 contains a heparin-binding site which modifies its biological activity. *Eur J Biochem*, 237: 295-302.

Rutherford, R.B., Wahle, J., & Tucker, M., et al. 1993. Induction of reparative dentine formation in monkeys by recombinant human osteogenic protein-1. *Arch Oral Biol*, 38: 571-576.

Sambrook, J., Fritsch, E. F., & Maniatis, T. 1989. Molecular cloning, a laboratory manual. Cold Spring Harbor Laboratory Press

Sampath, T.K., & Reddi, A.H. 1981. Dissociative extraction and reconstitution of extracellular matrix components involved in local bone differentiation. *Proc Natl Acad*

Sci USA, 78: 7599-7603.

Sampath, T.K., & Reddi, A.H. 1983. Homology of bone-inductive proteins from human, monkey, bovine and rat extracellular matrix. *Proc Natl Acad Sci USA*, 80: 6591-6602.

Sampath, T.K., & Reddi, A.H. 1984a. Distribution of bone inductive proteins in mineralized and demineralized extracellular matrix. *Biochem Biophys Res Commun*, 119: 949-961.

Sampath, T.K., & Reddi, A.H. 1984b. Importance of geometry of the extracellular matrix in endocondral bone differentiation. *J Cell Biol*, 98: 2192.

Sampath, T.K., Muthukumaran, N., & Reddi, A.H. 1987. Isolation of osteogenin, an extracellular matrix-associated, bone inductive protein, by heparin affinity chromatography. *Proc Natl Acad Sci USA*, 84: 7109-7113.

Sampath, T.K., Coughlin, J.E., & Whetstone, R.M. et al. 1990. Bovine osteogenic protein is composed of dimers of OP-1 and BMP-2A, two members of the transforming growth factor ß superfamily. *J Biol Chem*, 265: 13198-13205.

Sampath, T.K., Maliakal, J.C., & Hauschka, P.V., et al. 1992. Recombinant human osteogenic protein-1 (hOP-1) induces new bone formation in vivo with a specific activity comparable with natural bovine osteogenic protein and stimulates osteoblast proliferation and differentiation in vivo. *J Biol Chem*, 267: 20352-20362.

Sampath, T.K., Rashka, K.E., & Doctor, J.S., et al. 1993. Drosophila TGF-ß superfamily proteins induce endochondral bone formation in mammals. *Proc Natl Acad Sci USA*, 90: 6004-6008.

Sandhu, H.S., Kanim, L.E., & Kabo, J.M., et al. 1995. Evaluation of rhBMP-2 with an OPLA carrier in a canine posterolateral (transverse process) spinal fusion model. *Spine*, 20: 2669-2682.

Sasai, Y., Lu, B., & Steinbeisser, H., et al. 1995. Regulation of neural induction by the Chd and Bmp-4 antagonistic patterning signals in Xenopus. *Nature*, 377: 757.

Savage, C., Das, P., & Finelli, A.L., et al. 1996. Caenorhabditis elegans genes sma-2, sma-3, and sma-4 define a conserved family of transforming growth factor beta pathway components. *Proc Natl Acad Sci USA*, 93: 790-794.

Schimandle, J.H., Boden, S.D., & Hutton, W.C. 1995. Experimental spinal fusion with recombinant human bone morphogenetic protein-2. *Spine*, 20: 1326-1334.

Schlunegger, M.P., & Grutter, M.G. 1992. An unusual feature revealed by the crystal structure at 2.2 A resolution of human transforming growth factor-beta 2. *Nature*, 358: 430-434.

Schnitzler, C.M., Pettifor, J.M., & Mesquita J.M., et al. 1990. Histomorphometry of iliac crest bone in 346 normal black and white South African adults. *J Bone Miner Res*, 10: 183-199.

Schnitzler, C.M., Ripamonti, U., & Mesquita, J.M. 1993. Histomorphometry of iliac crest trabecular bone in adult male baboons in captivity. *Calcif Tiss Int*, 52: 447-454.

Schwall, R.H., Nikolic, K., & Szonyi, E., et al. 1988. Recombinant expression and characterization of human activin A. *Mol Endocrinol*, 3: 1237-1241.

Sekelsky, J.J., Newfeld, S.J., & Raftery, L.A., et al. 1995. Genetic characterization and cloning of mothers against dpp, a gene required for decapentaplegic function in

Drosophila melanogaster. *Genetics*, 139: 1347-1358.

Seyedin, S.M., Thomas, T.C., & Thompson, A.Y., et al. 1985. Purification and characterization of two cartilage-inducing factors from bovine demineralized bone. *Proc Natl Acad Sci USA*, 82: 2267-2271.

Solursh, M., Langile R.M., & Wood, J., et al. 1996. Osteogenic protein-1 is required for mammalian eye development. *Biochem Biophys Res Common*, 218: 438-443.

Sporn, M.B., & Roberts, A.B. 1988. Peptide growth factors are multifunctional. *Nature*, 332: 217-219.

Sporn, M.B., & Roberts, A.B. 1990. The transforming growth factor-βs, in Sporn MB, Roberts AB (eds): Peptide Growth Factors and Their Receptors. Berlin, Springer-Verlag, 419-472.

Sporn, M.B., & Roberts, A.B. 1992. Transforming growth factor-ß: Recent progress and new challenges. *J Cell Biol*, 119: 1017-1021.

Sporn, M.B., & Roberts, A.B. 1992. Transforming growth factor ß regulates the metabolism of proteoglycans in bovine cartilage organ cultures. *J Biol Chem*, 263: 12828-12831.

Statistical Analysis System 1989 SAS/STATS User's Guide, Version 6, 4th ed, Vol 1. SAS Institute Inc: Cary, NC: pp. 209-244.

Strong, D.D., Beachler, A.L., & Wergedal, J.E., et al. 1991. Insulinlike growth factor II and transforming growth factor β regulate collagen expression in human osteoblastlike cells in vitro. *J Bone Min Res*, 6: 15-23.

Sumner, D.R., Turner, T.M., & Purchio, A.F., et al. 1995. Enhancement of bone ingrowth by transforming growth factor-β. *J Bone Joint Surg*, 77-A: 1135-1147.

Suzuki, A., Thies, R.S., & Yamaji, N., et al. 1994. A truncated bone morphogenetic protein receptor affects dorsal-ventral patterning in the early Xenopus embryo. *Proc Natl Acad Sci USA*, 91: 10255-10259.

Tanaka, T., Taniguchi, Y., & Gotoh, K., et al. 1993. Morphological study of recombinant human transforming growth factor beta 1-induced intramembranous ossification in neonatal rat parietal bo[illegible]. *Bone*, 14. 117-123.

Taniguchi, Y., Tanaka, T., & Gotoh, K., et al. 1993. Transforming growth factor beta 1-induced cellular heterogeneity in the periosteum of rat parietal bones. *Calcif Tissue Int*, 53: 122-126.

ten Dijke, P., Hansen, P., & Iwata, K.K., et al. 1988. Identification of another member of the transforming growth factor type beta gene family. *Proc Natl Acad Sci USA*, 85: 4715-4719.

ten Dijke, P., Yamashita, H., & Sampath, T.K., et al. 1994. Identification of type I receptors for osteogenic protein-1 and bone morphogenetic protein-4. *J Biol Chem*, 269: 16985-16988.

Thesleff, I & Nieminen, P. 1996. Tooth morphogenesis and cell differentiation. *Curr Opin Cell Biol*, 8(6):844-850.

Toriumi, D.M., Kotler, H.S., & Luxenberg, D.P., et al. 1991. Mandibular reconstruction with a recombinant bone-inducing factor. Functional, histologic, and biomechanical evaluation. *Arch Otolaryngol Head Neck Surg*, 117: 1101-1112.

Tsuneizumi, K., Nakayama, T., & Kamoshida, Y., et al. 1997. Daughters against dpp modulates dpp organizing activity in Drosophila wing development. *Nature*, 389: 627-631.

Urase, K., Mukasa, T., & Igarashi, H., et al. 1996. Spatial expression of sonic hedgehog in the lung epithelium during branching morphogenesis. *Biochem Biophys Res Comm USA*. 225: 161-166.

Urist, M.R. 1980. Heterotopic bone formation. In: Fundamental and clinical bone physiology. Urist, M.R. ed. J.B. Lippincott Company, Philadelphia. 369-393.

Urist, M.R. 1965. Bone: Formation by induction. *Science (Wash. DC)*, 159: 893-899.

Urist, M.R., DeLange, R.J., &. Finerman, G.A. 1983. Bone cell differentiation and growth factors. *Science (Wash. DC)*, 220: 680-686.

Vainio, S., Karavanova, I., & Jowett, A., et al. 1993. Identification of BMP-4 as a signal mediating secondary induction between epithelial and mesenchymal tissues during early tooth development. *Cell*, 75: 45-58.

Van den Eijnden-van Raaij, A.K., Koornneef, I., & van Zoelen, E.J. 1988. A new method for high yield purification of type beta transforming growth factor from human platelets. *Biochem Biophys Res Commun*, 157: 16-23.

Van Obberghen-Schilling, E., Roche, N.S., & Flanders, K.C., et al. 1988. Transforming growth factor beta 1 positively regulates its own expression in normal and transformed cells. *J Biol Chem*, 263: 7741-7746.

Van Vlasselaer, P.V., Borremans, B., & van Gorp, U., et al. 1994. Interleukin 10 inhibits transforming growth factor-beta (TGF-beta) synthesis required for osteogenic

commitment of mouse bone row cells. *J Cell Biol*, 124: 569-577.

Vukicevic, S., Luyten, P., & Kleinman, H.K. 1990. Differentiation of canalicular cell processes in bone cells by basement membrane matrix components: Regulation by discrete domains of laminin. *Cell*, 63: 437-445.

Vukicevic, S., Helder, M.N., & Luyten, F.P. 1994. Developing human lung and kidney are major sites for synthesis of bone morphogenetic protein-3 (osteogenin). *J Histochem Cytochem*, 42: 869-875.

Vukicevic, S., Latin, V., & Chen, P., et al. 1994. Localization of osteogenic protein-1, a bone morphogenetic protein, during human embryonic development. *Biochem Biophys Res Commun*, 198: 693-700.

Vukicevic, S., Kopp, J.B., & Luyten, F.P., et al. 1996. Induction of nephrogenic mesenchyme by osteogenic protein 1 (bone morphogenetic protein 7). *Proc Natl Acad Sci USA*, 93: 9021-9026.

Wahl, S.M., Hunt, D.A., & Wakefield, L.M., et al. 1987. Transforming growth factor type beta induces monocyte chemotaxis and growth factor production. *Proc Natl Acad Sci USA*, 84: 5788-5792.

Wahl, S.M., Allen, J.B., & Weeks, B.S., et al. 1993. Transforming growth factor beta enhances integrin expression and type IV collagenase secretion in human monocytes. *Proc Natl Acad Sci USA*, 90: 4577-4581.

Wall, N.A., & Hogan, B.L. 1995. Expression of bone morphogenetic protein-4 (BMP-4), bone morphogenetic protein-7 (BMP-7), fibroblast growth factor-8 (FGF-8) and sonic hedgehog (SHH) during branchial arch development in the chick. *Mech Dev*, 53: 383-392.

Wang, E.A., Rosen, V., & Cordes, P., et al. 1988. Purification and characterization of other distinct bone-inducing factors. *Proc Natl Acad Sci USA*, 85: 9484-9488.

Wang, E.A., Rosen, V., & D'Alessandro, J.S., et al. 1990. Recombinant human bone morphogenetic protein induces bone formation. *Proc Natl Acad Sci USA*, 87: 2220-2224.

Weeks, D.L., & Melton, D.A. 1987. A material mRNA localized to the vegetal hemisphere in Xenopus eggs codes for a growth factor related to TGF-ß. *Cell*, 51: 861-867.

Wharton, K.A., Thomsen, G.H., & Gelbart, W.M. 1991. Drosophila 60A gene, another transforming growth factor β family member, is closely related to human bone morphogenetic proteins. *Proc Natl Acad Sci USA*, 88: 9241-9218.

Whitman, M. 1997. Signal transduction. Feedback from inhibitory SMADs. *Nature*, 389: 549-551.

Wieser, R., Wrana, J.L., & Massagué, J. 1995. GS domain mutations that constitutively activate T□R-1, the downstream signalling component in the TGF-β receptor complex. *EMBO J*, 14: 2199-2208.

Wozney, J.M., Rosen, V., & Celeste, A.J., et al. 1988. Novel regulators of bone formation: Molecular clones and activities. *Science*, 242: 1528-1534.

Wozney, J.M. 1992. The bone morphogenetic protein family and osteogenesis. *Molec Rep Dev*, 32: 160-167.

Wrana, J.L., Attisano, L., & Cárcamo, J., et al. 1992. TGFβ signals through

heteromeric protein kinase receptor complex. *Cell*, 71: 1003-1014.

Wrana, J.L., Attisano, L., & Wieser, R., et al. 1994. Mechanism of activation of the TGF-beta receptor. *Nature*, 370: 341-347.

Yasko, A.W., Lane, J.M., & Fellinger, E.J., et al. 1992. The healing of segmental bone defects, induced by recombinant human bone morphogenetic protein (rhBMP-2). A radiographic, histological, and biomechanical study in rats. *J Bone Joint Surg Am*, 74: 659-670.

Yu, Y.M., Becvar, R., & Yamada, Y., et al. 1991. Changes in the gene expression of collagens, fibronectin, integrin and proteoglycans during matrix-induced bone morphogenesis. *Biochem Biophys Res Commun*, 177: 427-432.

Zhao, G.Q., Deng, K., & Labosky, P.A., et al. 1996. The gene encoding bone morphogenetic protein 8B is required for the initiation and maintenance of spermatogenesis in the mouse. *Genes Dev*, 10: 1657-1669.